Neurosurgery Research Group, Biomedicum Helsinki, Finland
Department of Neurosurgery, University of Helsinki, Finland

Cerebrovascular Research Laboratory of the Department of Intensive Care Medicine, University Hospital and University Bern, Switzerland

Pathobiology of healing response after endovascular treatment of intracranial aneurysms – Paradigm shift from lumen to wall oriented therapy

Serge Marbacher

ACADEMIC DISSERTATION

To be publicly discussed with the permission of the Medical Faculty of the University of Helsinki in the lecture hall of Töölö Hospital on 5 December 2014 at 12 o` clock noon.

Helsinki, 2014

Supervised by
Associate Professor **Mika Niemelä**
Department of Neurosurgery
Helsinki University Central Hospital
Helsinki, Finland

Associate Professor **Juhana Frösén**
Department of Neurosurgery
Helsinki University Central Hospital
Helsinki, Finland

Professor **Javier Fandino**
Department of Neurosurgery
Kantonsspital Aarau
Aarau, Switzerland

Reviewed by
Associate Professor **Pauli Helén**
Department of Neurosurgery
Tampere University Hospital
Tampere, Finland

Professor **Hannu Manninen**
Department of Clinical Radiology
Kuopio, Finland

Opponent
Professor **Jacques Morcos**
Department of Neurosurgery
University of Miami
Miami, FL, USA

ISBN 978-951-51-0476-2 (paperback)
ISBN 978-951-51-0477-9 (pdf)
http://ethesis.helsinki.fi/
Helsinki University Press
Helsinki, 2014

For Predrag Dragutinović

Author’s contact information:

Serge Marbacher
Department of Neurosurgery
Kantonsspital Aarau
Tellstrasse 1
5000 Aarau
Switzerland
tel: +41 62 838 66 97
fax: +41 62 838 66 29
email: serge.marbacher@ksa.ch

Abbreviations

2D-DSA	Two-dimensional intra-arterial digital subtraction angiography
3D-DSA	Three-dimensional intra-arterial digital subtraction angiography
3D-FLASH	Three-dimensional fast low-angle shot sequence
3D-MRA	Three dimensional magnetic resonance angiography
AA	abdominal aorta
AAA	Abdominal aortic aneurysms
ACA	Anterior cerebral artery
AChA	Anterior choroidal artery
ACOM	Anterior communicating artery
α-SMA	α-smooth muscle actin
ATENA	Analysis of treatment by endovascular approach of non-ruptured aneurysms
BA	Basilar artery
BAC	Balloon assisted coiling
BAPN	Beta-aminopropionitrile
BMI	Body mass index
BRAT	Barrow rupture aneurysm trial
CAMEO	Cerebral aneurysm multicentre european onix
CAP	Cellulose acetate polymer
CARAT	Cerebral aneurysm rerupture after treatment
CCA	Common carotid artery
CDKN	Cyclin-dependent kinase inhibitor
CE	Contrast enhanced
CFD	Computational fluid dynamics
CI	Confidence interval
CLARITY	Clinical and anatomical results in the treatment of ruptured intracranial aneurysms
CM-Dil	1,1'-dioctadecyl-3,3,3'3'-tetramethylindocarbocyanine perchlorate with a thiol-reactive chloromethyl group
CONSCIOUS	Clazosentan to overcome neurological ischemia and infarct occurring after subarachnoid hemorrhage
CSF	Cerebrospinal fluid
CT	Computed tomography
CTA	Computed tomography angiography
DACA	Distal anterior cerebral artery
DAPI	4',6-diamindino-2-phenylindole
DCI	Delayed cerebral ischemia

DCVS	Delayed cerebral vasospasm
DMEM	Dulbeco's modified Eagle's medium
DSA	Digital subtraction angiography
ECM	Extracellular matrix
EJV	External jugular vein
eNOS	Endothelial nitric oxide synthase
EDNRA	Endothelin type A receptor gene
EVG	Elastica van Gieson
EVT	Endovascular treatment
FBS	Fetal bovine serum
FDA	United states food and drug administration
$FE2^{+}$	Ferrous
FG	Fibrin glue biopolymer
FITC-lectin	Fluorescein isothiocyanate conjugated lycopersicon esculentum (tomato) lectin
FLASH-MRI	Fast low angle shot MRI
FRED	Flow re-direction endoluminal device
GCS	Glasgow coma scale
GDC	Guglielmi detachable coil
GFP	Green fluorescent protein
GWAS	Genome-wide association studies
HE	Hematoxylin & eosin
IA	Saccular intracranial aneurysm
ICA	Internal carotid artery
IEL	Internal elastic lamina
IL-1β	Interleukin 1beta
IMASH	Intravenous magnesium sulfate for aneurysmal subarachnoid
ISAT	International subarachnoid aneurysm trial
ISUA	International study of unruptured intracranial aneurysms
LCCA	Left common carotid artery
LOX	Lysine oxidase
MCA	Middle cerebral artery
MCP	Monocyte chemotactic protein
MMP	Matrix metalloproteinases
MRI	Magnetic resonance imaging
MT	Masson's trichrome staining
NF-κβ	Nuclear factor-kappa beta
nNOS	Neuronal nitric oxide synthase
NO	Nitric oxide
OA	Ophthalmic artery
OPT	Optical projection tomography

OSI	Oscillatory shear index
PComA	Posterior communicating artery
PBS	Phosphate buffered saline
PFA	Paraformaldehyde
PMN	Polymorphonuclear leukocytes
RA	Renal artery
RCCA	Right common carotid artery
ROI	Regions of interest
ROS	Reactive oxygen species
RT	Room temperature
SAC	Stent assisted coiling
SAH	Subarachnoid hemorrhage
SD	Standard deviation
SDS	Sodium dodecyl sulfate
SMC	Smooth muscle cell
SNPs	Single-nucleotide polymorphisms
STASH	Simvastatin in aneurysmal subarachnoid hemorrhage
TdT	Terminal transferase
TLR	Toll-like receptor
TNF-α	Tumor necrosis factor-alpha
TOF-MRI	Time-of-flight MRI
TUNEL	TdT-mediated dUTP biotin nick end labeling technique
TXR	Standard Texas Red
UCAS	Unruptured cerebral aneurysm study of Japan
WEB	Woven EndoBridge
WFNS	World Federation of Neurological Surgeons
WL	White light
WSS	Wall shear stress

Contents

Original publications

I **Complex bilobular, bisaccular, and broad-neck microsurgical aneurysm formation in the rabbit bifurcation model for the study of upcoming endovascular techniques.**
Marbacher S, Erhardt S, Schläpp JA, Coluccia D, Remonda L, Fandino J, Sherif C. AJNR Am J Neuroradiol. 2011 Apr;32(4):772-7.

II **Long-term patency of complex bilobular, bisaccular, and broad-neck aneurysms in the rabbit microsurgical venous pouch bifurcation model.**
Marbacher S, Tastan I, Neuschmelting V, Erhadt S, Collucia D, Sherif C, Remonda L, Fandino J. Neurol Res. 2012 Jul;34(6):538-46.

III **The Helsinki rat microsurgical sidewall aneurysm model.**
Marbacher S, Marjamaa J, Abdelhameed E, Hernesniemi J, Niemelä M, Frösen J. J Vis Exp. 2014 Oct 12;(92).

IV **Loss of mural cells leads to wall degeneration, aneurysm growth, and eventual rupture in a rat aneurysm model.**
Marbacher S, Marjamaa J, Bradacova K, von Gunten M, Honkanen P, Abo-Ramadan U, Hernesniemi J, Niemelä M, Frösen J. Stroke. 2014 Jan;45(1):248-54.

V **Intraluminal cell transplantation prevents growth and rupture in a model of rupture-prone aneurysms.**
Marbacher S, Frösen J, Marjamaa J, Anisimov A, Honkanen P, von Gunten M, Abo-Ramadan U, Hernesniemi J, Niemelä M. Stroke. Nov 4. [Epub ahead of print]

The original publications are reproduced with the permission of the copyright holders. In the thesis, the publications are referenced by their Roman numerals.

Abstract

Background and Purpose: Subarachnoid hemorrhage attributable to saccular intracranial aneurysm (IA) rupture is a devastating disease leading to stroke, permanent neurological damage and death. Despite rapid advances in the development of endovascular treatment (EVT), complete and long lasting IA occlusion remains a challenge, especially in complexly shaped and large-sized aneurysms. Intraluminal thrombus induced by EVT may recanalize. The biological mechanisms predisposing IA to recanalize and grow are not yet fully understood, and the role of mural cell loss in these processes remains unclear. To elucidate these processes, animal models featuring complex aneurysm architecture and aneurysm models with different wall conditions (such as mural cell loss) are needed.

Materials and Methods: Complex bilobular, bisaccular and broad-neck venous pouch aneurysms were microsurgically formed at artificially created bifurcations of both common carotid arteries in New Zealand rabbits. Sidewall aneurysms were microsurgically created on the abdominal aorta in Wistar rats. Some sidewall aneurysms were decellularized with sodium dodecyl sulfate. Thrombosis was induced using direct injection of a fibrin polymer into the aneurysm. CM-Dil-labeled syngeneic smooth muscle cells were injected into fibrin embolized aneurysms. The procedures were followed up with two-dimensional intra-arterial digital subtraction angiography, contrast-enhanced serial magnetic resonance angiographies, endoscopy, optical projection tomography, histology and immunohistochemistry.

Results: Aneurysm and parent vessel patency of large aneurysms with complex angioarchitecture was 90% at one month and 86% at one year follow-up in the bifurcation rabbit model. Perioperative and one month postoperative mortality and morbidity were 0% and 9%. Mean operation time in the rat model was less than one hour and aneurysm dimensions proved to be highly standardized. Significant growth, dilatation or rupture of the experimental aneurysms was not observed, with a high overall patency rate of 86% at three week follow-up. Combined surgery-related mortality and morbidity was 9%. Decellularized aneurysms demonstrated a heterogeneous pattern of thrombosis, thrombus recanalization and growth, with ruptures in the sidewall rat model. Aneurysms with intraluminal local cell replacement at the time of thrombosis developed better neointima, showed less recurrence or growth and no ruptures. Growing and ruptured aneurysms demonstrated marked adventitial fibrosis and inflammation, complete wall disruption and increased neutrophil accumulation in unorganized luminal thrombus.

Conclusions: Creation of complex venous pouch bifurcation aneurysms in the rabbit is feasible, with low morbidity, mortality and high short-term and long-term aneurysm patency. They represent a promising approach for in vivo animal testing of novel endovascular therapies. The sidewall aneurysm rat model is a quick and consistent method to create standardized aneurysms. Aneurysms missing mural cells are incapable of organizing a luminal thrombus, leading to aneurysm recanalization and increased inflammatory reactions. These, in turn, result in severe wall degeneration, aneurysm growth and eventual rupture. The results of the presented studies suggest that the biologically active luminal thrombus drives the healing process towards destructive wall remodeling and aneurysm rupture. Local smooth muscle cell transplantation compensates for mural cell loss and reduces recurrence, growth and rupture rate in a sidewall aneurysm rat model.

1 Introduction

Rupture of an intracranial aneurysm (IA) causes subarachnoid hemorrhage (SAH), a life-threatening condition leading to stroke, permanent neurological damage and death. In Finland and Switzerland, an estimated 170, 000 Finns and 250, 000 Swiss are harboring IAs and about 1000 Finnish and 700 Swiss patients suffer from SAH every year.[1, 2] The disease has significant socioeconomic impact as SAH often affects relatively young patients. The number of years of potential life lost is comparable with that of ischemic stroke and intracranial hemorrhage.[3] Thanks to major improvements in surgical techniques, diagnosis and interventional treatment, the average case fatality rates for SAH have decreased by 17% over the last three decades.[4, 5] The overall case fatality rate shows regional differences and remains around 40-50%.[5, 6]

Due to the increased use of computed tomography (CT) and magnetic resonance imaging (MRI), an increasing number of incidental unruptured IAs are being diagnosed. Many of these IAs never rupture during the person’s lifetime, and specific indicators to identify aneurysms that could rupture are lacking. Since prophylactic treatment to prevent rupture is associated with significant risks[7, 8] the decision to treat represents a dilemma for the surgeon: do the risks of preventive treatment outweigh the risk of death or severe disability through spontaneous IA rupture. Size and location of the IA, patient’s age and gender, environmental and genetic factors, hemodynamics and morphological parameters of the IA are included in an educated guess about the risk of rupture.

The rupture of an IA and subsequent SAH can be prevented with either microsurgical clipping of the IA neck or endovascular occlusion of the IA lumen. The less invasive endovascular treatment (coiling) of small narrow-necked cerebral aneurysms has been shown to be associated with slightly lower morbidity than neurosurgical clipping, especially in the posterior circulation.[9, 10] However, disappointing long-term results with persisting neck remnants, unacceptably high rates of aneurysm recanalization and late aneurysm rerupture have been observed following endovascular treatment in large clinical trials.[11, 12] Aneurysm recurrence is a significant clinical problem that occurs in approximately 20-35% of patients and necessitates retreatment in half of reopened IA.[10, 12-17] The mechanisms underlying reopening are poorly understood. Most of the proposed concepts for IA reopening and elaborate EVT approaches are focused on the visible IA lumen.

Far too little attention has been paid to the condition of the IA wall or the biological mechanisms involved in IA wall remodeling, intraluminal thrombus formation and tissue response to EVT materials. This is not least attributable to the lack of animal models that allow both assessment of biological responses induced by embolization devices and evaluation of mechanisms of IA growth and rupture.

Today's animal models can only be used to evaluate either induction, growth, and rupture of IA, or to test the technical proficiency of endovascular devices. Standardized aneurysm models for multicenter preclinical trials are needed. Most of the current EVT modalities focus on the visible IA lumen.

There is a growing body of evidence suggesting that the IA wall itself holds the balance between "rupture prone" and "stable" IA conditions. A key event believed to lead to wall degeneration and eventual rupture of the IA wall is the loss of mural cells, which reduces the capacity of the IA wall for maintenance and repair of the wall matrix.[18] Extensive studies are needed to unravel the underlying mechanisms leading to particular IA wall conditions and the chronological sequences from "repair and maintenance" to ''degradation and destruction''. Insights into these mechanisms may then lead to the development of highly specific imaging modalities that could identify the aneurysm wall condition, enable the estimation of individual IA's rupture risk, predict long-term success of EVT and help establish new therapeutic approaches.

2 Review of the literature

2.1 Intracranial aneurysm

2.1.1 Epidemiology

The prevalence of saccular intracranial aneurysms (IA) is estimated to be 2.3% in adults without risk factors for aneurysms.[19] When adjusted for sex (50% men) and age (50 years), the overall prevalence is estimated to be 3.2% in a population without comorbidity.[20] Based on this data, an estimated 170, 000 Finns and 250, 000 Swiss are living with IAs. In retrospective and prospective postmortem, angiographic and magnetic resonance studies, prevalence ranges between 0.1% and 8.4%[19, 21-25], with the highest rate found in imaging studies using improved detection modalities (3-Tesla magnetic resonance angiography [MRA]).[24]

The percentage of IA, which are acquired lesions, is lower in men and increases steadily after the third decade of life.[19, 20] Most intracranial aneurysms are saccular in shape (>95%) and located in the anterior circulation (>80%), predominantly on the circle of Willis.[26-29] Multiple intracranial aneurysms (most often two or three; in one rare case, 13 aneurysms were found arising from one main branch[30]) are frequently (30%) found in adult patients harboring IA.[31-34]

2.1.2 Formation and rupture

The exact pathogenesis of IA formation and rupture is unknown. There is a large body of evidence suggesting that both genetic and acquired factors play an important role in IA formation and rupture. Most ruptured aneurysms are attributed to modifiable risk factors.[35, 36] However, many of these IAs never rupture during the person's lifetime and specific indicators to identify aneurysms that will rupture are lacking. In some ways, risk factors for aneurysm formation differ from risk factors for rupture.

2.1.2.1 Size and location

IA size is an independent predictor for rupture. In the prospective arm of the International study of unruptured intracranial aneurysms (ISUA), a five-year cumulative rupture rate of 0% for patients without prior subarachnoid hemorrhage in anterior circulation aneurysms of less than 7 mm in size was demonstrated. The risk of rupture for aneurysms smaller than 5 mm presented in the Unruptured cerebral aneurysm study of Japan (UCAS) was 0.36% per year[37], which was in line with another Japanese prospective study on Small unruptured intracranial aneurysms (SUAVe study; 0.34% per year). Based on these figures, preventive treatment is rarely justified. However, the ISUA and UCAS data stands in contrast with other series[34, 38-41] as well as clinical experience that shows many aneurysms do rupture more frequently below this threshold. The incidence of de-novo IA found in routine follow up screening is low (4.4%), but the rupture risk (14.5% over five years) is much higher than the risk of small-sized IA reported in ISUA.[39, 42] A proposed future multicenter clinical trial may provide evidence in favor of, or against the preventive treatment of unruptured aneurysms.[43]

Location seems to be an independent risk factor for aneurysm rupture. Significant association with the risk of rupture was found in aneurysms in the anterior [37] or posterior[37, 42] circulation and seems to be linked to aneurysm size (anterior circulation IA tend to rupture at a smaller size).[37, 38]

2.1.2.2 Morphological parameters

The study of IA morphology may allow conclusion on inner wall remodeling processes and has been linked to aneurysm rupture. Higher IA fundus/neck aspect ratio (with positive correlation of high ratios[44]), shape[37], and secondary pouches[45] were found to be associated with rupture. Multiloculated aneurysms are common, with 57% ruptured and 27% unruptured aneurysms found in an autopsy study.[34] Factors such as the development of unbalanced contact constraints between the IA and its periadventitial environment have been proposed as additional predictors of IA rupture risk.[46] Based on retrospective data, it has been postulated that shape is more indicative of increased risk than size.[47, 48]

Hemodynamic parameters[49-51] and the configuration of the aneurysm in relation to its parent arteries[52] are other known factors that may influence IA rupture risk assessment. In a retrospective and prospective study, the IA size-ratio (IA size divided by parent artery diameter) correlated strongly with IA rupture status.[53] Evaluation of six morphological and seven hemodynamic parameters for significance with respect to rupture, revealed that hemodynamics is as important as morphology.[51] It has been reported that ruptured aneurysms have a lower wall shear stress (WSS) and higher oscillatory shear index (OSI)[50], and that in vivo thin-walled regions of unruptured cerebral aneurysms colocalize with low WSS.[49] Univariate analyses in middle cerebral artery IA showed that the aspect ratio, WSS, normalized WSS, OSI and WSS gradient are significant parameters. In multivariate analyses, however, only lower WSS was significantly associated with rupture status.[51] Computational fluid dynamics (CFD) may have great future potential for individual IA rupture risk assessment. However, the assumptions of boundary conditions for computational simulations might make results questionable, and data derived from CFD studies must be interpreted with extreme caution.[54]

In light of this nonambiguous relationship between morphological factors and risk of IA rupture, these parameters should be considered in addition to aneurysm size in IA rupture risk assessment. Patients with documented growth[55], prior history of SAH[56], and multiple IA[34, 57] (with the largest and more proximal IA most often rupturing first), have a higher risk for IA rupture, but only when confounding factors are not taken into account.[42, 57] Growth of IAs of all sizes are associated with a higher risk of rupture.[40] Multiple small aneurysms have a higher risk of growth when compared to single aneurysms, but single IAs demonstrated higher growth rates.[58]

2.1.2.3 Age, gender, and environmental factors

Female sex, patient's age, cigarette smoking, history of hypertension and alcohol consumption are robust risk factors associated with IA rupture. Together, the modifiable influences of smoking, hypertension and heavy alcohol consumption account for > 80% of all IA ruptures.[35, 36] These three variables may change throughout the life span, and represent potential confounding factors for less common risk factors[59]. The proposed protective effects of hormone replacement therapy, oral contraceptives, white ethnicity, lean body mass index (BMI), hypercholesterolemia and diabetes remain uncertain.[35, 36, 60]

Estrogen play a central role in vascular biology. Studies have long indicated that hormone replacement therapies are associated with reduced risk of IA rupture[61], that prevalence of IA is higher in older women[20], and that earlier age at menopause tends to be associated with the presence of IA.[62] Furthermore, estrogen deficiency increased the susceptibility of rats to IA formation.[63, 64] Estrogen has therefore been implicated in aneurysm formation and rupture but the exact role of female hormone levels in the pathogenesis remains unclear. Pregnancy and delivery do not seem to increase the risk of IA rupture.[65]

In case-control (but not in longitudinal) studies, hypercholesterolemia was demonstrated to lower the risk of IA rupture.[60, 66, 67]This data is in line with findings for intracerebral hemorrhage[68], but contradict studies that demonstrated increased risk[69], and studies demonstrating no effect on risk of IA rupture.[37] Whether the effect of hypercholesterolemia is influenced by associated use of statins remains unknown.[66, 70] Data for IA rupture in association with lean BMI and rigorous physical activity is inconsistent.[60] Regular physical exercise seems to decrease the risk of harboring an IA.[71]

Several case-control studies demonstrated a significant risk reduction of IA rupture for patients with diabetes mellitus.[60, 67, 69, 70] The biological basis for these findings is unknown. It has been hypothesized that patients with diabetes may die of other reasons before developing SAH or that altered lifestyle factors and continuous medical care reduce the risk of SAH.[60, 70]

2.1.2.4 Family history of ruptured IA

Familial predisposition is an important nonmodifiable risk factor. Approximately 10% of patients suffering from ruptured IA have a positive family history.[72] The prevalence of IA in individuals with a first-degree relative[73] (4%) is just above that of the general population, but is doubled for patients with two or more affected family members[74]. Patients with familial predisposition are more likely to have multiple aneurysms; most likely in the middle cerebral artery territory.[42, 75] The proportion of larger aneurysms (>10mm), younger age at the time of rupture and female gender tends to be higher than in sporadic IA rupture.[73, 76]

2.1.2.5 Associated conditions and genetics

IA associated disorders including autosomal dominant polycystic kidney disease, fibromuscular dysplasia, Ehlers–Danlos syndrome type IV, and arteriovenous malformations are rare risk factors for IA rupture. Whether Marfan's syndrome is associate with increased prevalence of IA is highly controversial.[77, 78] The most common disease associated with IA (0.3% of all IA patients) is autosomal dominant polycystic kidney disease, with an estimated 4% to 40% harboring intracranial aneurysm (10% to 30% multiple aneurysms).[29]

Low estimates of SAH heritability (41%) in an extensive twin study led to the conclusion that SAH is mainly of nongenetic origin, and familial SAHs can be attributed largely to environmental risk factors.[79] The significant role of environmental influences on IA rupture can be partly explained by confounding risk factors such as smoking, high blood pressure, and heavy alcohol consumption. Familial clustering of these circumstances may contribute to the high percentages of SAH risk reported in patients with one affected first-degree relative. Environmental factors, however, are possibly related to lifestyle practices such as alcohol consumption or smoking.[59] Screening of patients with two first-degree relatives is still recommended.[20]

Despite the finding that familial SAH is more strongly determined by modifiable risk factors than genetic background[79] there is a large body of evidence for significant genetic contribution to IA pathogenesis. There is no single specific gene but rather several genetic loci associated with IA formation. Candidate gene association studies (linkage studies of familial cases or candidate genes examination in case-control studies) and more recently Genome-wide association studies (GWAS) revealed genetic loci with multiple pathophysiological mechanisms mainly involved in vascular endothelial and smooth muscle cell (SMC) homeostasis and extracellular matrix (ECM) maintenance.[80-82] Linkage studies in families and sib pairs with IA revealed several loci with association to IA formation but only few have been replicated in different populations and thus far have not produced robustly replicable loci.[80, 83] GWAS is a most promising approach that allows to focus on genetic single-nuecleotide polymorphisms (SNPs) in a large population cohort from different populations to find variants associated with IA formation. To date the strongest association with IA are found for SNPs on chromosome 9 within the cyclin-dependent kinase gene, chromosome 8 near the SOX17 transcriptor gene, and chromosome 4 near the endothelin type A receptor gene (EDNRA).[82]

The first GWAS of IA found common associated SNPs on chromosome 2q, 8q, and 9p.[84] In this GWAS of Finnish, Dutch and Japanese cohorts, the authors found that the genes on 9p with the strongest association encode for cyclin-dependent kinase inhibitors that regulate SMC proliferation and apoptosis.[85, 86] The locus 9p21.3 has a strong association to both IA and abdominal aoartic aneurysm (AAA) formation.[85] The Associated SNPs on 8q most likely act via SOX17, a box transcription factor family, which is required for both endothelial formation and maintenance.[87, 88] A second GWAS, with nearly three times as many subjects (European and Japanese cohorts) as the initial study, confirmed the two loci on 8q and 9p and identified three new risk loci on chromosome 10q, 13q, and 18q[89]. The strongest of the newly identified loci was found on 18q and the gene identified within the region is involved the in cell cycle progression. Further analysis using the two Japanese replication cohorts from the second GWAS revealed SNPs on chromosome 4q coding for the EDNRA.[90] SNPs near the EDNRA gene, which is involve in endothelin signalling and is activated at the site of vascular injury and modulates vasoconstriction and vasodilatation, was confirmed in another GWAS in a Japanese population.[91] Despite the importance of genetic association with IA for future clinical risk profiling, identification of new biological pathways, and drug development one need to keep in mind that all identified loci explain only a few percentages of the overall risk of IA formation.[89]

2.1.3 Pathobiology of IA rupture

2.1.3.1 Aneurysm wall

Normal cerebral arteries are composed of three distinct layers, the intima, media and adventitia. The intima consists of a small amount of collagenous connective tissue and is covered by a layer of endothelial cells. An internal elastic lamina (IEL) composed of tropoelastin molecules cross-linked by lysyl oxidase[92] provides mechanical strength[93] and separates the intima from the media. The media is comprised of closely packed layers of SMC, embedded in collagenous bundles and a few elastic fibers.[94] In comparison with extracranial arteries, the external elastic lamina is absent and the adventitia much thinner. The wall thickness of intracranial arteries of the Circle of Willis is 0.5 to 0.6 mm[95] and endothelial lined channels (vaso vasorum) are present in proximal segments of cerebral arteries.[96] The so-called “medial defects of Forbs” or medial gaps[97] (lacking the tunica media and frequently found at the lateral angle or the apex of arterial bifurcation), were thought to be congenital defects and sites of locus minoris resistentiae and therefore predisposed to aneurysm formation. However, it soon became obvious that these defects cannot be the major etiologic factor for saccular IA. Animal and autopsy studies revealed that IA develop close to, rather than in the medial defects.[98] The collagen fibers at the medial defects are believed to act as an anchor for the adjacent smooth muscle of the media[93] and actually provide more stability to the vessel wall than causing weakness.[99]

In contrast to the normal cerebral artery wall, the IA lacks clearly defined histological layers. The endothelial cell layer is often disrupted with smaller intercellular gaps or is complete absent, leaving the inner surface of the aneurysm covered with blood cells and fibrin clot.[100] The IEL disappears at the level of the neck[101] and SMC migrate into the intima, proliferate and cause intimal thickening (myointimal hyperplasia). The muscular layer is either composed of a thick myointima hyperplasia-like layer with many disorganized SMC or an almost decellularized, very thin and hyalinized wall.[100, 102] The muscular layer demonstrates various degrees of connective tissue deposits, intramural bleeding, hemosiderin deposits and inflammatory cell infiltration.[100, 102, 103] The adventitia mostly remains unaltered.[101]

Comparison of ruptured and unruptured aneurysms harvested during aneurysm surgery revealed that disruption of the endothelial cell layer, inflammatory cell infiltration, degeneration of the wall matrix (breakdown of collagen), partial hyalinization of the wall and loss of mural cells are characteristics associated with rupture.[100, 102] However, degeneration and inflammation of the IA wall are also present in unruptured IA suggesting that the aneurysm wall is in a constant process of remodeling (maintenance and repair).

Frösen et al. identified four different wall types (type A to D) that most likely reflect consecutive stages of wall remodeling or wall degeneration that eventually lead to aneurysm rupture.[102] Type A aneurysms occur more frequently in younger patients and consist of an organized endothelialized wall with linearly arranged layers of SMC. Type B aneurysms are composed of a thickened wall with disorganized SMC. Aneurysms with a hypocellular wall with either myointimal hyperplasia or organizing thrombus (Type C) has a higher likelihood of rupture than Type A or B. Type D aneurysms demonstrate extremely thin thrombosis-lined hypocellular walls and reveal a 100% positive rupture status. Noninvasive identification of the aneurysm wall type would not only allow a precise prediction of rupture risk, but also aid in tailoring (based on the stage of wall degeneration) future therapeutic interventions.

2.1.3.2 Mural cell loss and the role of oxidative stress

Injury to the arterial wall induces SMC to proliferate, migrate to the intima and to synthesize new matrix.[104] This "repair process" of damaged artery walls also seems to play an important role in the IA wall homeostatic balance.[105] SMC undergo phenotypic modulation, from differentiated spindle-like cells expressing mainly contractile proteins (smooth muscle α-actin) to proliferative pro-matrix-remodeling cells that dissociate from each other (spiderlike cells) and express inflammatory factors and matrix metalloproteinases (MMP).[106, 107] This phenotypic modulation from contractile to proliferative phenotype is an early event in IA formation and appears to be strongly related to the wall remodeling process.[105, 107] The exact mechanisms that eventually trigger morphological wall changes producing a rupture-prone wall condition remain unknown. A key event believed to lead to wall degeneration and eventual rupture of the IA wall is the loss of mural cells, which is synonymous with loss of repair processes.[18] In support of the theory that SMC loss leads to decreased capacity for IA wall adaption and repair, gene expression analysis studies demonstrated ruptured IA to be associated with disturbance in cell homeostasis[108] and pathways involved in wounding and defense response (intima formation mediated by SMC[104]).

Inflammation plays a pivotal role in aneurysm formation, growth and rupture. Loss of mural cell is a histological hallmark of ruptured IA but the cause of cell death remains unexplained.[100, 102] Proinflammatory mediators[109, 110], humoral immune responses[111-114], proteolytic enzymes, oxidative stress[115-117] and local hypoxia[118] are all contribute to the loss of SMCs. Both programmed (apoptosis), and uncontrolled cell death (necrosis) have been proposed as potential mechanisms of cell death.[102, 115, 118-121] Three smaller series reported apoptotic cell death by means of terminal transferase (TdT)-mediated dUTP biotin nick end labeling technique (TUNEL) that was associated with IA wall rupture.[115, 119, 120] These series stand in contrast with two larger series showing an insignificant difference in the number of TUNEL-positive IA wall cells in ruptured and unruptured IA.[102, 112] TUNEL staining is not a method designed specifically for apoptosis, but it detects DNA fragmentation resulting from apoptotic cascade and may also label cells that have suffered severe DNA damage (cells undergoing necrosis). Cysteine-dependent aspartate-directed proteases (caspases) are a family of cysteine proteases that play an essential role in apoptosis and are considered important in detecting programmed cell death. Caspases are found in the IA wall in addition to TUNEL staining.[115, 121] Given the large amount of cell loss in comparison with the amount of cells with positive staining for apoptosis, it seems likely that uncontrolled cell death also plays an important role in mural cell loss. Notably, areas resembling fibrinoid necrosis are often seen in IA wall regions with few remaining cells.[18]

The apoptotic pathways can be divided into “extrinsic” (death-receptor pathway, activation of caspase-8) and “intrinsic” (Cytochrome c pathway, activation of caspase-9). Both pathways lead to activation of caspase-3 which initiates cell apoptosis. Laaksamo et al. found that cell death in IA walls is mainly activated via the intrinsic pathway.[115] Furthermore, they demonstrated that expression of heme-oxygenase-1 (detoxification enzyme and marker for oxidative stress) is associated with IA wall degeneration and rupture, suggesting that high oxidative stress is most likely responsible for activation of the intrinsic apoptotic pathway. In the later study hemeoxygenase-1 expression was associated with inflammatory cells. However, the source of oxidative stress is not only from inflammatory cells but is believed to be multifactorial, including luminal thrombus[122], remnants of apoptotic and necrotic cells[123], inducible nitric oxide synthase (produces reactive oxygen species)[116, 117], oxidized low-density protein (can additionally trigger both apoptosis and necrosis)[124] and local hypoxia (occlusion of vasa vasorum).[118]

Activated gene expression profiles of the intima and media of cerebral arterial walls in rats using laser-microdissection techniques revealed close relation of inflammation, oxidative stress and apotosis with aneurysm formation and progression.[125] Apoptotic changes of SMC were found in pre and early stages of IA formation indicating an association between apoptosis of medial SMC and formation of IA.[126] Inflammatory cytokines have been shown to induce SMC death during IA formation.[127] However, at a later stage of IA degeneration and rupture inflammatory cell-derived cytokines do not seem to play a significant role in programmed cell death.[115]

Study of cultured SMC from human IA walls revealed great variability in growth capacity among different patients.[128] This may indicate genotype differences in SMC growth, apoptosis, and survival characteristics. Loci with genetic polymorphism that associates with IA formation or IA rupture has been investigated using large genome-wide association studies (GWAS).[80-82, 85, 89, 91] Among the identified loci there is one with a strong association signal originating from tumor suppressor genes (encode for cyclin-dependent kinase inhibitor [CDKN]) regulating SMC proliferation and apoptosis.[85, 86] In a vascular injury model CDKN2B knock-out mice demonstrated reduced neointimal lesions and larger aortic aneurysms due to increased SMC apoptosis.[86] These findings corroborate the hypothesis that genetic polymorphisms affect survival and function of SMCs and may predispose to sIA formation.

2.1.3.3 The role of inflammation

Inflammatory cells including macrophages, T-cells, polymorphonuclear leukocytes (PMN), natural killer cells, and mast cells have been detected in the IA wall. Macrophages are a major source of MMP and are believed to play a key role in vascular remodeling.[129, 130] In mice models of intracranial aneurysm, it has been shown that the majority of leukocytes are macrophages, and mice with clodronate liposome-induced macrophage depletion or mice lacking monocyte chemotactic protein-1 (MCP-1; chemotactic factor for macrophages) have significantly fewer aneurysms.[129, 130] Transcription factors Ets-1 and nuclear factor-kappa beta (NF-κβ) were found to modulate expression of MMP and MCP-1 (among many others), and experimental aneurysm formation can be reduced by inhibiting these factors.[131] The largest genome-wide gene expression study comparing the transcriptome of ruptured and unruptured IAs in the same anatomical location found that NF-κβ and Ets transcription factor binding sites were significantly enriched among the upregulated genes in ruptured IA walls.[108] Simultaneous inhibition of Ets and NF-κβ, with the use of chimeric decoy oligodeoxynucleotides, reduced expression of MCP-1 and macrophage infiltration, decreased IA size, thickened IA wall and restored decreased collagen biosynthesis of pre-existing IAs.[132] The majority of macrophages in human IA walls are CD163-positive.[102] CD163 is a hemoglobin scavenger receptor that is expressed in macrophages involved in anti-oxidative defense which dampens and resolves inflammation. Recently, mast cells have been implicated in the pathogenesis of IA wall inflammation. Inhibition of mast cell degranulation reduced the inflammatory response and inhibited the size and medial thinning of experimental IA walls.[133]

Antibodies and complement are found in most human IA wall matrix and are bound to mural cells.[111-114] Tulamo et al. demonstrated that complement activation (studied by immunostaining for the membrane attack complex) is associated with IA wall degeneration and rupture.[112] Furthermore, the complement system was found to be activated via the classical pathway with an alternative pathway amplification.[113, 114] Based on the elucidated profile of complement components and the association of C5b-9 with lipids in the extracellular matrix, they hypothesized that the inflammatory process is a chronic rather than an acute targeted inflammatory reaction.[114] Complement activation was found mainly in the outer media-representing regions (mostly in the matrix and cellular debris in decellularized areas), which suggests that complement activation may be a reaction and not a mediator of mural cell loss processes.

Interleukin 1beta (IL-1β), interleukin 6 and tumor necrosis factor-alpha (TNF-α) are important cytokines involved in aneurysm wall inflammation.[110, 134] Moriwaki et al. demonstrated that IL-1β deficient mice exhibit delayed aneurysm progression compared with wild-type mice.[110] The data further indicates that IL-1β promotes SMC apoptosis which may further enhance aneurysm formation. TNF-α has both proapoptotic and proinflammatory action in IA wall. It has been reported that higher levels of TNF-α correlate with the expression of intracellular calcium release channels, Toll-like receptors and reduction of tissue inhibitor of metalloproteinase-1 result in higher MMP activity in the IA wall.[109] Frösen et al. demonstrated that the expression of receptors for transforming growth factor beta (mediates matrix synthesis[135]), vascular endothelial growth factor (mediates SMC migration[136]), and basic fibroblast growth factor (stimulates myointimal hyperplasia[137]) are involved in IA wall remodeling.[138] It has been hypothesized that endothelial nitric oxide synthase (eNOS) protects arterial walls from inflammation through reduction of hemodynamic stress. Aoki et al. demonstrated that deficiency of eNOS can be compensated by neuronal nitric oxide synthase (nNOS).[139] Hence, IA formation was similar in eNOS and wild-type mice. However, eNOS and nNOS-deficient mice exhibited increased incidence of IA formation with increased macrophage infiltration.[139]

2.1.3.4 The role of luminal thrombosis

Luminal thrombosis is frequently seen in histopathological series of IA walls.[100, 102, 103] Endothelial injury is believed to be one of the earliest events in aneurysm formation and increased damage of the endothelial layer is associated with rupture.[100, 102] The endothelial cells provide a nonthrombogenic surface. There is an increase in reactive oxygen species (ROS) in dysfunctional endothelial cells, which (among other mechanisms) impair synthesis of nitric oxide (NO) and is where pathologic quantities of von Willebrand factor are expressed. Extensive damage leads to loss of endothelial cells and exposition of the underlying thrombogenic surface.

Ideally, the intraluminal thrombus is organized by SMC, myofibroblasts or fibroblasts that synthesize collagen and finally transform the thrombus into stable fibrotic scar tissue. In an experimental aneurysm model it has been shown that the cells organizing the thrombus mainly originate from the aneurysm wall.[140] Although luminal thrombus can serve as a scaffold for SMC migration, proliferation, and growth of intimal hyperplasia, the thrombus may also affect the aneurysm wall detrimentally which can shift the balance from “healing” towards “destruction”.

It has been shown in aortic aneurysms that leukocytes, platelets and erythrocytes get trapped in the fibrin network of a fresh thrombus. Breakdown of red blood cells releases free oxidant hemoglobin and heme-iron which increases the toxicity of ROS derived from platelets and leukocytes.[122] Red blood cell hemagglutination is further responsible for tissue-plasminogen activator and plasminogen retention involved in the postponed progressive fibrinolysis.[141] The cytotoxic compounds (including iron) released from the thrombus can diffuse in the nearby IA wall. Accumulation of heme deposits and iron might induce inflammatory cell infiltration into the IA wall.[18] In AAA, release of matrix-degrading proteases (MMP-8 and MMP-9) and highly active peroxidases by neutrophils leads to increased oxidative stress and chronic proteolytic injury that degrades the wall.[141, 142] Furthermore, PMNs store and release leukocyte elastase which impairs anchorage of mesenchymal cells to the fibrin matrix and therefore prevents cellular re-colonization[142]. Similar to these findings in AAA, it seems likely that neutrophils cause chronic proteolytic injury and damage to mural cells due to increased oxidative stress, as outlined above (2.1.4.2 Mural cell loss and the role of oxidative stress). Degranulation of thrombocytes leads to release of thrombocyte-derived growth factor that modulates mural cells (cell survival, proliferation and matrix synthesis).[138] In addition, angiogenic growth factors increase permeability of the endothelium and subsequent transendothelial diffusion of lipids, immunoglobulin and other plasma proteins to the IA wall. These processes are likely to enhance damage to mural cells and increase inflammation.[18] In addition, the luminal thrombus may induce local hypoxia and reduce diffusion of nutrients to the IA wall.[118]

Acute thrombus induction has been linked to mural destabilization not only in experimental aneurysms[143, 144] but also in clinical settings after application of flow diverters for IA occlusion.[145, 146] These studies consistently found large numbers of inflammatory cells and loss of mural cells in destabilized aneurysm wall segments after rapid thrombosis.[143, 144, 146] In a swine sidewall aneurysm model it has been shown that 50% of small-neck aneurysm undergo fast thrombosis and aneurysm rupture (n = 4), while wide-neck aneurysm undergo stepwise thrombosis which results in stable aneurysms (n = 6).[144]

In flow-diverter treatment, 100% of the aneurysm volume is filled with thrombus. In a Guglielmi detachable coil embolization, approximately 70% of the aneurysm volume is filled with thrombus.[147-149] A recent meta-analysis found IA recurrence rates of 21% after coil embolization.[150] The risk of growth and rupture of recurrent aneurysms after coil embolization makes retreatment necessary in approximately 10% of cases. Recanalization has been linked to a packing volume with higher recurrence rates in aneurysms, with over 80% of intraluminal thrombus.[147, 151-153] In large and giant aneurysms, coil packing density is particularly poor, resulting in >95% of intraluminal thrombus and recurrence rates of >50%.[154-160] Partial coil occlusion of the aneurysm lumen not only contributes to a higher rate of aneurysm recurrence, but also re-rupture.[158] Presence of intraluminal thrombosis itself is a possible risk factor for reopening of a coiled IA.[160, 161]

Taken together, it seems likely that the thrombolytic processes and failed thrombus organization are responsible for IA recurrence after endovascular treatment. We hypothesize that the effect of the luminal thrombus on the IA wall and the IA wall condition at the time of thrombosis are the determining points for thrombus organization into scar tissue (neointima formation by infiltration of SMC or myofibroblasts) or continuous remodeling (driven by inflammatory processes) of the wall which is primarily destructive.

2.1.4 Subarachnoid hemorrhage

Subarachnoid hemorrhage (SAH) due to intracranial aneurysm rupture is a life-threatening condition leading to stroke, permanent neurological damage and death. SAH accounts for 5% to 10% of all strokes, with an incidence of 6-11 per 100,000 (range 2 in China to 22.5 in Finland)[2, 162, 163] in most populations. Incidence increases with age and for the female sex (1.2 times[162]). Blacks and Hispanics also seem to have a higher proportion (2.1 times) than men and Whites.[164-166] For unknown reasons, (and not explained by a higher prevalence of unruptured IA), the incidence in Finland, Northern Sweden and Japan is as high as 16 to 22.5 per 100,000, indicating a higher risk for rupture.[1, 163, 167] In Finland approximately 1000, and in Switzerland approximately 700 patients suffer from SAH every year.[1, 2] The disease has a significant socioeconomic impact. SAH often affects relatively young patients (mean age 55 years[165]), and the number of years of potential life lost is comparable with ischemic stroke and intracranial hemorrhage.[3] Every second patient suffers permanent disability and the estimated lifetime cost is more than double that of an ischemic stroke.[168] The minimal decreases in SAH incidence (virtually no change in high income countries between 1970 and 2008[169]) between 1950 and 2005, and stable prevalence of IA might be explained by changes in lifestyle and/or increased preventive treatment.[20, 162] The proportional frequency in low to middle-income countries (7 per 100,000) is almost twice that of high-income countries (4 per 100,000).[169]

2.1.4.1 Presentation, diagnosis, and grading

Characteristically, patients report "the worst headache of their life" and may syncope during SAH. Other frequent presenting signs include neck pain (meningismus), drowsiness, coma, cranial nerve and other focal neurological deficits, vomiting, increased blood pressure, seizure, ocular hemorrhage and history of sentinel headache. Patients presenting with sentinel headaches have a high risk of early rebleeding and must be treated with particular care.[170]

The common practice for diagnostic evaluation of SAH including IA visualization is thin-cut non contrast enhanced CT scan (with potential subsequent computed tomography angiography [CT angiography [CTA]) and conventional digital subtraction angiography (DSA). A new-generation CT scan will reveal SAH in 100% and 93% of cases within 12 and 24 hours after onset of symptoms.[171] However, due to fast clearance of cerebrospinal fluid (CSF), sensitivity drops to 50% within one week. MRI is not sensitive in the first two days but may accurately identify the rupture site in case of multiple IA.[172] Patients with clinical suspicion and negative CT scan require lumbar puncture for cerebrospinal fluid analysis. Xanthochromia occurs twelve hours after SAH and persists up to two weeks.[173] Recent studies suggest that a lumbar puncture is not needed if the CT scan is performed within six hours after onset of acute headache without atypical presentation.[174, 175] Misdiagnosed patients may feel less ill at the time of presentation but are at higher risk of death and disability.[173]

In patients with a negative CT scan but positive lumbar puncture, the chance of harboring IAs is high (>40%).[176] In cryptogenic SAH (initial DSA negative but lumbar puncture positive SAH; 10-20% of all SAH[177]), perimesencephalic SAH may need no additional imaging. It is recommended to follow-up non-perimesencephalic SAH more aggressively (DSA one and six week after index SAH).[177]

Several grading systems are used to assess the patient's clinical condition at the time of SAH and to predict outcome. The most widely used Hunt and Hess scale[178] (based on the Botterell classification[179]) was originally meant to support decision-making regarding the timing of aneurysm treatment after SAH. An expert committee proposed the World Federation of Neurological Surgeons (WFNS) scale[180] which is currently preferred as it is based on the Glasgow Coma Score (GCS) and the presence of focal neurological deficits.[181] However, the Hunt and Hess scale has strong predictive power for outcome (compared to GCS and WFNS); and scores on the day of surgery have better prognostic values than those at admission.[182]

In 1980, Fisher et al. proposed a SAH bleeding scale based on CT characteristics to predict the patient's risk of developing delayed cerebral vasospasm. A simple alternative scale was proposed and has demonstrated superior inter- and intraobserver agreement in predicting symptomatic vasospasm.[183]

2.1.4.2 Complications and outcome

The most feared complication of SAH is rebleeding. The frequency of rebleeding is about 10%[170] (range 1.7%[184] to 17.3%[185]), and a clear association with poor prognosis has been documented.[186] Risk factors are advanced age, larger aneurysm (>10 mm), premorbid hypertension, poor clinical grade at the time of admission and active bleeding demonstrated in CTA.[187] The risk of rebleeding is highest within the first six hours.[170, 185] This time frame provides a window for beneficial short-course antifibrinolytic therapy.[188] The estimated risk of rebleeding of ruptured aneurysms is 4% in the first day, decreasing to 1% to 2% in the following weeks, and increasing up to 30% to 50% for the first three months.[170]

Delayed cerebral vasospasm (DCVS) is another devastating complication associated with high mortality and morbidity. Cerebral artery vasoconstriction occurs in 50% to 70% of patients between three and 12 days after SAH.[189-191] Despite half a century of research, no effective treatment for DCVS has been found. Promising results from single center Phase 2a[192] and multicenter dose-finding Phase 2b studies[191] with Clazosentan (a selective endothlin A receptor antagonist) demonstrated significant reduction of angiographic vasospasm. However, they failed to demonstrate an effect on vasospasm-related morbidity, mortality or functional outcome.[190] The paradigm asserting that attenuation of vasospasm improves patient outcome was not supported, leading to increased attention for the early pathophysiological consequences of aneurysmal SAH. Although lower incidence of angiographic vasospasm does not correspond with better functional outcomes, angiographic vasospasm is not an epiphenomenon that does not contribute to poor outcome. Exploratory post-hoc analysis of the Phase 2b data revealed a strong association between angiographic vasospasm and cerebral infarction.[193] Efforts at reducing vasospasm are still warranted and substances reducing vasospasm with fewer drug-related adverse events may lead to improved patient outcome in the future.

Other frequently encountered complications include seizures, acute or chronic hydrocephalus, intraparenchymal or subdural hematoma and non-vasospasm related early and delayed cerebral infarction. Most patients experience additional medical complications (40% severe complications resulting in increased morbidity and mortalityand prolonged hospital stay) as follows: fever, hyperglycemia, hypertension, anemia, cardiac dysfunction, pulmonary edema (cardiogenic or neurogenic), pneumonia, sepsis, renal and hepatic dysfunction, gastrointestinal bleeding, cardiac dysfunction, thrombocytopenia, deep venous thrombosis and electrolyte disturbances.[194]

Average case fatality rates for SAH have been declining slightly[4, 5] and outcomes have improved during the past few decades, but overall case fatality is still almost 50%.[5, 6] Early (21 days to one month) fatality due to SAH is higher in low to middle-income countries as compared to high-income countries[169], presumably due to differences in patient management. Initial SAH contributes in most part to overall mortality (10% to 15% die before reaching the hospital and 25% within the first 24 hours after onset of SAH[195]) and partly explains the slow decrease despite improve management strategies. One third of survivors require lifelong care.[6] One third of "good outcome" patients also suffer from cognitive deficits.[196]

Aneurysmal SAH patients have a shortened life expectancy even if they recover well from the initial SAH and IA occlusion.[197] The increased risk of death (especially in younger age groups) that remains after the first three months is explained by increased risk for vascular diseases[198] and cerebrovascular events.[197] Interestingly, patients with untreated unruptured IA have also above-average long-term mortality (50%) compared with the general population. Men with treated unruptured IA enjoy normal life expectancy while women show higher mortality (28% after clipping and 23% after coiling) as compared to a matched general population.[199] After SAH, patients need long-term care not only to screen for de-novo aneurysms and to prevent further cardiovascular events, but also to provide support for physical and neuropsychological impairment.

2.1.4.3 Treatment options

The ultimate goal of treatment is to prevent rebleeding and to prevent and treat secondary complications caused by the initial SAH. Most recent updates on the management of aneurysmal subarachnoid hemorrhage can be found in the American Heart Association and European Stroke Organization guidelines for the management of Intracranial Aneurysms and Subarachnoid Haemorrhage.[200-202]

Teaching status, larger hospital size and higher SAH caseload were associated with better outcomes and lower mortality rates in patients (especially those being clipped) with acute SAH. Therefore, low-volume hospitals (<10 aneurysmal SAH cases per year) may consider early transfer of patients to high-volume centers (>30 aneurysmal SAH cases per year).[203] IA obliteration should be performed as early as possible to reduce the rate of rebleeding. The international cooperative study on the timing of aneurysm surgery suggested that poor grade and elderly patients should not be operated on before day ten and good grade patients have improved outcome if treated within the first three days after SAH.[26, 204] Outcome was worse if surgery was performed in the 7 to 10-day post-bleed interval. A randomized trial confirmed that patients undergoing early surgery have the best chances, and patients with surgery on day four to seven, the worst.[205] However, the best timing of

IA repair remains controversial. Today's coil era makes timing of IA repair less of an issue (timing of endovascular occlusion seems not to affect procedural complications or 6-month outcomes).[206] Current practices still support early treatment but also include IA occlusion (for patients eligible for treatment) between day four to ten after initial ictus.

Determining whether clipping or coiling is performed should be a multidisciplinary decision. The multicenter International subarachnoid aneurysm trial (ISAT) of neurosurgical clipping versus endovascular coiling in 2143 patients demonstrated better one-year clinical outcomes; defined as survival without dependency (absolute risk reduction of 7.4%).[184] The survival benefit continued for at least seven years. It is important to acknowledge that only patients suitable for both endovascular and surgical management (22.4% of all study patients) were enrolled in ISAT and most of them were good grade patients (Hunt and Hess grade 1 and 3; >90%) with mostly small (95%) aneurysms of the anterior circulation (93.7%). ISAT results have often been extrapolated to other patients not included in the study. The barrow ruptured aneurysm prospective mono-center "intend to treat" trial (BRAT) compared the two treatment modalities and found that at one year after treatment, coil embolization (62.3% of randomized patients actually received endovascular coil embolization) resulted in fewer poor outcomes than clip occlusion.[207] At three years, patients assigned to coiling still showed a 5.8% favorable difference, although it was not significant.[208] Both the BRAT and ISAT study demonstrated significantly lower rates of recurrence and retreatment after neurosurgical clipping and more common late rebleeding after endovascular coiling. ISAT demonstrated that the risk of epilepsy and significant cognitive decline was reduced in the endovascular group.[10] With the exception of verbal memory (significant decrease after clipping), the outcomes in terms of quality of life and cognitive deficits seem similar in the two treatment modalities.[209] A systematic review of endovascular versus surgical IA repair confirmed better clinical outcome but greater risk of rebleeding after coiling. The risk of vasospasm is higher after clipping, whereas the ischemic infarct, shunt-dependent hydrocephalus and procedural complication rate of the two treatments is without significant difference.[210]

There is a growing body of evidence that patient subgroups may benefit from one of the two treatment modalities. Middle cerebral artery aneurysms (often superficially located at the bi/trifurcation [>80%], and with unfavorable neck diameter and dome size ratio for coiling[211]), and patients presenting with a significant intraparenchymal hematoma[212] (>50 mL) or acute subdural hematoma[213], are believed to be ideal candidates for surgery.[214] On the other hand, older individuals[215, 216], poor grade patients and those with confirmed DCVS[217], and posterior circulation aneurysms (especially basilar apex[218]) seem to be better candidates for coiling. Numerous publications and editorials regarding ISAT and BRAT point to the ongoing controversy concerning the best aneurysm treatment. Hopefully ISAT II will provide robust evidence and shed more light on the issue.[219]

Immediate imaging is recommended after IA occlusion to identify remnants or recurrence that may require treatment (in the Cerebral aneurysm rerupture after treatment [CARAT] study, rerupture occurred at a median of 3 days following IA repair[220]). Acute hydrocephalus must be treated by placing an external ventricular or lumbar drainage. Lumbar drainage placement seems to reduce shunt-dependent chronic hydrocephalus[221], but rapid or gradually weaning seems not to influence the course of hydrocephalus.[222] Oral nimodipine is the only calcium antagonist showing strong evidence of reducing cerebral infarction and improving outcome after SAH, and should be administered to all patients.[223, 224] Reduction of DCVS and delayed cerebral ischemia (DCI) by lumbar drainage and intrathecal thrombolytic infusion remains controversial. Trials using phosphodiesterase 3 inhibitor (Cilostazol)[225] and statins[226] (Simvastatin in aneurysmal subarachnoid hemorrhage [STASH])[227] are still in progress, while large trials of endothelin-1 antagonists[228] (Clazosentan to overcome neurological ischemia and infarct occurring after subarachnoid hemorrhage [CONSCIOUS 1-3])[190, 229, 230] and magnesium sulfate (intravenous magnesium sulfate for aneurysmal subarachnoid hemorrhage [IMASH])[231] have not demonstrated any clinical benefit. Euvolemia and normal circulating blood volume is recommended to prevent DCI. Hypopvolemia and hypotension in the acute phase of SAH is associated with an increased risk of DCI. Prophylactic hypertension and hypervolemia do not influence the clinical course but are, in turn, associated with significant complications (pulmonary edema, myocardial infarction, electrolyte abnormalities).[232, 233] Noninvasive monitoring of DCVS development is performed using transcranial Doppler ultrasound recording of flow velocities in basal cerebral arteries.[234] CT and MRI perfusion imaging may be useful to determine specific regions at risk for DCI.

Historically, treatment of ischemic deficits was performed using volume expansion and induced arterial hypertension. The primary current treatment is augmentation of hemodynamics to improve cerebral perfusion by maintenance of euvolemia and induced hypertension.[235] Rescue therapies include cerebral angioplasty for large basal arteries and/or intraarterial vasodilator infusion for more distal arteries. Important critical care strategies include maintaining normothermia, normoglycemia and prevention of anemia, as these measures are associated with improved outcome. After discharge, it is reasonable to refer patients for neuropsychological evaluation.

2.2 Endovascular treatment of IA

2.2.1 Evolution of endovascular treatment

2.2.1.1 Pre balloon, balloon, and coil era

Early IA treatment was performed by ligation of the common carotid artery. In 1885, Sir Victor Horsley ligated the right common carotid artery after finding a pulsating mass in the middle cranial fossa.[236] Direct treatment of an IA was first described in 1931 by wrapping it with a piece of autologous muscle.[237] It was Walter E. Dandy who clipped the first aneurysm in 1937[238], using a silver clip developed by Harvey Cushing.[239] Although this rational and safe treatment option for IA was established the invasiveness of the extravascular approach (craniotomy and brain retraction) led to the desire to find more gentle physiological procedures for IA occlusion. Technological advances at that time facilitated the search for less invasive alternatives using the intravascular space as natural route to approach IAs.

The development of cerebral angiography eventually paved the road for less invasive extravascular-intravascular and endovascular approaches. Neurologist Antonio E. Moniz, who won the Nobel Prize in Physiology and Medicine in 1949, found a contrast agent tolerable to humans and introduced cerebral angiography in 1927.[240] In 1941, neurosurgeon Sidney C. Werner inserted a silver wire into a paraclinoid giant aneurysm via transorbital approach and heated the wire to 80°C for one minute.[241] Neurosurgeon Sean F. Mullan introduced sharp electrodes through a burr hole under biplane radiographic control into the aneurysm. He applied 200 to 2,000 milliamps for 1 to 2 hours, and arteriograms every 30 minutes documented the thrombus formation within the fundus. 61 patients were treated, with adequate occlusion of the IA in 49 patients.[242] Yasargil believed that aneurysm occlusion could be achieved using magnetic particles directed into the IA, causing thrombosis.[243] Yasargil was unable to test the hypothesis himself but shared his ideas with Robert Rand.[244] John Alksne, a fellow of Rand, started clinical experimentation and successfully induced thrombosis using magnetic embolization material.[245, 246] They reported stereotactic occlusion of 22 anterior communicating artery aneurysms after placement of a magnet on the aneurysm wall and injection of an iron and methyl methacrylate suspension.[247] At that time, thrombus induction had also been attempted through the use of highly experimental pilojections.[248]

Neurosurgeon Alfred J. Luessenhop and Velasquez facilitated a shift from the extravascular approach to a more physiological endovascular approach. For the first time in 1964, these pioneers reported the catheterization of an intracranial artery and an attempt to treat IA by advancing a silicon balloon into a supraclinoid carotid lesion. This was carried out by connecting a glass chamber to a stump of the external carotid artery and introducing a tube into the internal carotid artery.[249] More selective catheterization was achieved by attachment of a micromagnet to the tip of the catheter and guiding it via external magnetic field.[250] Already in 1963, T.J. Fogarty et al. developed a balloon-tipped microcatheter tor extraction of arterial emboli and thrombi.[251] It was a Russian neurosurgeon who demonstrated endovascular IA occlusion for the first time while preserving the parent artery, using detachable and non-detachable inflatable balloons. Fedor A. Serbinenko was inspired by watching children manipulating helium-filled balloons through the tether lines at a May Day celebration in Moscow`s Red Square.[252] He treated more than 300 patients with his handmade manufactured silicone and latex balloons, with and without scarifying the parent artery.[253] Many neuroendovascular centers around the world started to apply Serbinenko's concept and published mortality rates of approximately 20%.[254] The high incidence of immediate complications (uncontrolled delivery of the balloon), delayed rupture and recanalization proved that balloon embolization was not safe.

In 1988 and 1989, Hilal et al. ushered in the age of coils by reporting the use of short nonretrievable (and hence noncontrollable) stiff pliable pushable coils for endosacular treatment of IA.[255] These coils were able to achieve more complete occlusion also in irregularly shaped aneurysms. In 1991, the Italian neurosurgeon Guido Guglielmi presented the clinical application of electrolytically detachable platinum coils and solved most of the problems associated with pushable coils or balloons: The coils presented were soft (gently adopted to the shape of the aneurysm, causing less deforming pressure on the fragile wall), retrievable (less migration in parent arteries), variable in length, controllable, circular helical in shape (memory allows for denser packing) and most importantly, detachable at will. Although the idea of catheterizing an aneurysm via the endovascular route by a stainless steel wire electrode and applying electronic current was not new and had already been tested in the early 1980's (with marginal success).[256] The mechanism of detachment was discovered almost a decade later. In January 1989, Guglielmi continued his research efforts, not with electrothrombosis, but with small magnets and metallic particles at the University of California in Los Angeles. The magnet was mounted on the tip of a stainless steel wire and introduced "endovascularly" into the aneurysm followed by iron microsphere injection into the circulation. Frustrated by the incomplete occlusion with the ferromagnetic technique, he thought of adding electrothrombosis. The electrical current did not increase thrombosis but induced erosion of the wire at the site of the magnet. The magnet fell off the wire (by electrolysis) and the detachment mechanism was born. As the magnet failed to induce enough thrombosis, radiopaque and biocompatible platinum coils were soldered to the tip of the stainless steel delivery wire. The Guglielmi detachable coil (GDC) had been developed. Since the United States Food and Drug Administration (FDA) approved GDCs to treat IA, endovascular technology has evolved rapidly. A timeline with most important key events in the evolution of endovascular treatment is given in **Figure 1**.

2.2.1.2 Guglielmi detachable coil

The controlled deployment of coils using the GDC system paved the way for widespread use of endovascular approaches as therapy for IA occlusion. The high rate of morbidity and mortality associated with detachable balloons and pushable coils was reduced to an acceptable level of mortality (1.4% and 1.7% in ruptured and unruptured IA) and morbidity (8.6% and 7.7% in ruptured and unruptured IA).[257, 258] Although parent artery occlusion is hardly seen with controlled GDC placement, complications such as thromboembolism and intraoperative rupture have remained and are more common in ruptured than unruptured aneurysm.[259] Despite the promising results of >90% of adequately occluded IA at the time of initial treatment, several drawbacks soon became evident. First, persisting neck remnants and high rates of aneurysm recanalization place the patient at risk for retreatment and aneurysm re-rupture. A review of >8,000 coiled IA revealed that reopening occurs in 21%, necessitating retreatment in 11%.[13] Second, not all IA can be treated with an endovascular approach using GDC alone.

In order to improve incomplete IA occlusion and IA recanalization, two main concepts were developed: increase in device filling volume, and increase in device bioactivity and thrombogenicity. It became evident that even in aneurysms with highly packing density of coil loops, approximately 70% to 80% of the aneurysm volume is filled with thrombus which, may remain unorganized long-term, especially in large aneurysms.[147-149, 260] Hydrogel coils to enhance aneurysm volume filling and reduce clefts of unorganized thrombus between the coil loops were therefore developed.[261] These coils consist of synthetic polymeric hydrogel attached to the surface of a platinum coil. After submersion in blood, the hydrogel hydrates and swells to its maximum volume in approximately 20 minutes, the hybrid device increases the radial thickness of the coil by a factor of three and expands to nine-fold its volume.[262] Although greater aneurysm volume filling, reduced amounts of unorganized thrombus and high rates of delayed, progressive aneurysm occlusion were observed, hydrogel coils failed to improve IA recurrence and retreatment in large clinical series[262] and were suspected of inducing increased perianeurysmal edema and hydrocephalus. Modification of coil shape and softness allow increases in packing density of coils. Spherical coils that deploy into a three dimensional configuration (3D-coils) were developed to improve coil and volume density even in aneurysms with wider necks and unfavorable sac-to-neck ratio.[263] After early clinical experience with first[264] and second generation the 3D-coils appear to be safe and may improve initial angiographic IA occlusion. Fibered coils were proposed to be more thrombogenic and to lead to significantly improved occlusion rates compared to bare platinum coils.[265]

The other concept to improve long-term durability of aneurysm occlusion was aimed at accelerating thrombus remodeling and enhancing fibrosis and scar formation. Biologically inert bare platinum coils were covered with bioabsorbable material. In experimental settings, polyglycolic/polylactic acid-coated (Matrix) and bioabsorbable polymeric coils successfully showed enhanced thrombus organization, accelerated aneurysm fibrosis, reduced angiographic recurrence rate and improved neointima formation[260, 266, 267] However, large long-term clinical trials failed to demonstrate decreased rates of recurrences when compared to standard GDC embolization, even after controlling for factors influencing recanalization.[268] Next generation Matrix-2 coils demonstrated improved mechanical performance and anatomic outcome as compared to Matrix-1 coils but one-year outcomes were similar to those of bare platinum coils.[269] Cerecyte coils consist of a regular bare platinum coil with polyglycolic acid running through the lumen of the primary platinum wind and therefore does not differ in terms of stiffness or handling from bare platinum coils.[270] Despite promising preliminary experiences using Cerecyte coils, twelve-month follow up data on angiographic results did not differ significantly when compared to bare platinum coils. The Cerecyte coil trial with 23 participating centers revealed that there was no significant difference in the angiographic outcomes between Cerecyte coils and bare platinum coils at 6 months.[271]

A systemic review of initial occlusion, and reopening and retreatment rates revealed that studies with IA treated with modified coils demonstrated worse initial occlusion rates when compared with studies using standard platinum coils.[13] It has been hypothesized that the less favorable initial occlusion rate may be due to inferior handling of the devices or potential bias of using modified coils in more complex IA configurations. At follow-up, reopening and retreatment rates were comparable to standard platinum coils. However, this data also needs to be interpreted with caution because the review grouped the different kind of coils and therefore might have missed a certain subtype with a positive effect. Lack of firm conclusion is further compounded by the scarcity of studies on different coiling materials containing high quality evidence.[272] In a systematic review of 82 studies using bare platinum, hydrogel, Matrix and Cerecyte coils, the rate of unfavorable angiographic outcome at follow-up (defined as either recanalization, <90% occlusion or incomplete occlusion) did not differ significantly between coil types.[273] In this review, however, the quality of the evidence remains low due to high heterogeneity, small sample size and potential publication bias.

The exact reason for the high rate of recanalization after IA coil occlusion, independent of coil type, remains obscure. It is interesting to note that IA size is not only a significant risk factor for IA rupture, but also for the reopening of coiled IA.[12, 13, 274, 275] The risk is particularly high (>50%) in large (>10mm) and giant aneurysms (>25mm).[154-158] In these aneurysms (most of them are already partially thrombosed at the time of initial coiling), the packing density is extremely poor and large amounts of thrombus is generated.[14, 158] Another significant predictor of IA recurrence after coiling is IA rupture status.[12, 275, 276] The difference in recurrence rate between unruptured and ruptured lesions was found not to be associated with aneurysm size, neck width or initial angiographic success of occlusion, which lead to the assumption that some biological difference between the two entities exist.[12] Size and rupture status are probably interrelated risk factors; as soon as an IA increases in size, the aneurysm may change its biological behavior and may become more prone to rupture.

Low coil packing density, large neck-dome ratio and initial incomplete IA occlusion all result in increased proportion of intra aneurysmal thrombus formation and represent a risk factor for aneurysm reopening. IA location in posterior circulation has been proposed as an important risk factor for IA recurrence after endovascular treatment.[16, 277] A comparison of studies between exclusively posterior circulation IA studies and studies representing predominantly anterior circulation IA confirmed the higher risk of coiled IA reopening in the posterior circulation.[13] A possible explanation may be the selection bias between favored surgical treatments of anterior circulation in comparison with posterior circulation IAs.

2.2.1.3 Stents, flow diverters and liquid embolic agents

In order to overcome the limitation of the GDC system in terms of recurrence, and to extend the indication of EVT to IA presenting with more complex angioarchitecture, various approaches and devices have been developed. Balloon assisted coiling (BAC) was introduced to remodel the anatomy of the aneurysm orifice, especially in wide-neck aneurysm.[278] Single or double lumen non detachable balloons are temporarily inflated to bridge the aneurysm neck and to provide counter bearing for an increased number of coils that are deployed into the aneurysm lumen. The balloons are deflated and removed at the completion of IA coiling. BAC was reported to be associated with increased procedural complications.[279] However, large multicenter prospective studies (Analysis of treatment by endovascular approach of nonruptured aneurysms [ATENA][280] and Clinical and anatomical results in the treatment of ruptured intracranial aneurysms [CLARITY][281]) and more recent single-center studies[282, 283] did not confirm these concerns. The immediate and long term anatomical outcome (adequate IA occlusion) seems to be favorable following balloon-assisted coil remodeling. In addition, the deflated balloon across the neck serves as a precautionary measure ready to be inflated in case of intraoperative rupture. According to these results, the wide use of the balloon-assisted remodeling technique has been proposed, especially for the treatment of wide-necked aneurysms.

Intracranial stents serve as scaffold to prevent coil herniation, to protect the parent artery, to serve as scaffold for neo-endothelization, and to improve intraluminal IA thrombosis caused by reduction of blood inflow. The first stenting of an IA was reported in 1997 by Higashida using a ballon expandable coronary stent in combination of a GDC.[284] In 2002 the first stent specifically designed for wide-necked IA received FDA approval. The Neuroform stent had an open-cell design and its application was initially associated with technical problems while the performance and handling of the latest (fourth) version of the Neuroform stent has significantly improved. In 2007 the FDA approved the Enterprise stent. This stent was self-expanding, had a closed-cell design that can be recaptured if it is only partially deployed. The Solitaire AB was the first fully deployable and retrievable stent that allowed temporary stenting during IA remodeling.

Stent assisted coiling (SAC) is particularly useful in cases of wide-necked IA or unfavorable anatomy to bridge the IA neck if the neck is not fully respected by the coil mass or to protect against coil migration. SAC refers to several different techniques such as "crossing stent" (stent deployment first, then coiling via microcatheter trough the stent struts which is more difficult if a closed-cell device is used), "jailing" (the microcatheter for coil deployment is placed in the IA sac first, then stent deployment), "semi-jailing" (partial deployment of the stent, coiling followed by retrieval of the stent), and "temporary stenting" (full stent deployment, coiling followed by retrieval of the stent). A stent may also be used as a "finishing stent" (coiling first without sent, then stent deployment for example to push protruding coil loops back into the IA sac).

Despite the potential benefits SAC has repeatedly shown higher rates of complications as compared to coiling; with and without remodeling. A large retrospective single center series revealed higher permanent neurological complications (7.4% vs 3.8%) and significant higher mortality (4.6% vs 1.2%) after SAC when compared to nonstented EVT.[285] However, angiographic recurrence was significantly reduced in IA with stented (14.9) versus nonstented (33.5%) EVT.[285] A review of 39 articles confirmed a high overall complication incidence associated with SAC of 19%, with periprocedural mortality of 2.1%.[286] These finding are consistent with a recently published larger series[287, 288]. Comparison of the two pioneer stents, approved by the FDA (Neuroform stent in 2002 and Enterprise stent in 2007) for EVT of wide-necked IA, did not show a difference in complication rates or patient outcome.[289] However, the Neuroform stent was found to be an independent predictor of recanalization. This is in line with increased retreatment rates in series using the Neuroform stent[290, 291] when compared with a multicenter study using closed-cell Enterprise stents.[292] One direct comparison revealed that the Enterprise stent offers better handling than the Neuroform stent, but both devices result in similar immediate and mid-term angiographic results.[293] Although the rate of recanalization and retreatment seems lower after SAC as compared to nonstent EVT, the higher periprocedural risk (especially in ruptured aneurysms)[289], led to the assumption that wide use of stents is not recommended.[294] This issue remains controversial. A most recent series comparing SAC and BAC found that SAC may yield lower rates of retreatment and higher rates of aneurysm obliteration than BAC, with a similar morbidity rate.[295] In addition, one need to keep in mind that the rapid technical development of stents and delivery catheters makes it difficult, if not impossible, to compare in large patient series various types of stents and SAC procedures.

All available flow diverters on the market (Pipeline, Silk, Surpass and Flow re-direction endoluminal device [FRED]) are designed with a mesh that redirects the blood from the aneurysm and allows tissue ingrowth to seal the IA orifice.[296] Although indications are not clearly established, flow diverters are mainly applied to large and giant aneurysms, wide-neck and complex IA morphologies, locations untreatable with standard coiling techniques, segmental diseased arteries with either multiple or fusiform aneurysms and IA with history of failed EVT. A meta-analysis has confirmed that flow-diverter devices are feasible and effective with a high rate of complete IA occlusion.[297] However, associated morbidity and mortality is significant and potential complications not observed with other EVT, have become evident. In a meta-analysis of 29 studies, Brinjikji et al. reported a 5% morbidity rate, 4% mortality rate, 3% risk of delayed IA rupture, 3% intraparenchymal hemorrhage, and a delayed perforator infarction of 3% (with significantly lower odds among patients with anterior circulation aneurysm).[297]

Postprocedural SAH is a devastating complication that is more frequently observed in symptomatic aneurysms, aneurysms with large aspect ratio and aneurysms of large and giant size.[146, 298] The mechanisms of delayed rupture are unclear but a growing body of evidence points towards reverse/destructive remodeling of the IA wall due to thrombus formation. Although the phenomenon of post-procedural SAH is more frequent after abrupt induction of thrombus by flow diversion, it has also been documented after complete IA occlusion using GDC. Not only experimental studies[III, IV, 143, 144], but also clinical studies have indicated the important role of sudden large thrombus formation in the pathological mechanism of disease.[145, 146, 299, 300] This hypothesis supports the fact that increased aneurysm size leads to larger amounts of thrombus. Furthermore, delayed rupture is frequently seen in symptomatic aneurysm showing intramural enhancement (suggesting hemorrhage or inflammation), indicating another link to the aneurysm wall[301]. Microscopic pathology demonstrates aneurysm walls consisting of collagen infiltrated with neutrophils but with an almost absent aneurysm wall.[146, 302] IA become symptomatic if they grow or expand through intramural thrombosis. Both mechanisms indicate disturbance in aneurysm wall homeostasis. The wall probably loses its mechanisms to counterbalance inflammatory stress induced by abrupt stagnation of blood flow, formation of an instable thrombus, full lytic enzymes generated by the captured leucocytes and breakdown of blood products. In addition, intraluminal thrombus formation increases oxidative stress and prevents diffusion of oxygen and nutrients to the IA wall. The large thrombus induces inflammatory reactions that overwhelm the IA wall defense mechanism (depending on the IA wall condition). This leads to wall destruction and eventual rupture, prior to thrombus stabilization/organization and scar formation through cell ingrowth.

Perianeurysmal changes through inflammation caused by EVT-induced intraaneurysmal thrombosis has been described many times.[300, 301, 303, 304] It is not known whether the proposed measures of adding coils in combination with flow diverters or use of steroids results in reduced incidence of delayed rupture in large and giant aneurysms after flow diverter placement.[297, 300, 301, 304] Different degrees of inflammation may exist depending on both the volume of induced thrombus and the IA wall condition. The importance of intraluminal thrombosis as an important factor for inflammation is indicated by reports of aneurysm wall and peri-aneurysmal inflammation in partially thrombosed aneurysms.[300, 305] Aneurysm wall enhancement can be found in almost 20% after EVT using GDC and may not be pathological, rather part of a normal healing response.[300] Bearing in mind the existing association between postprocedural SAH and increased aneurysm size, it is of great interest that larger aneurysm size is an independent predictor of wall enhancement.[303] Other proposed mechanisms that flow-diversion devices can cause intra-aneurysmal pressure increase, possibly leading to aneurysm rupture, are highly speculative.[306]

Another potentially severe complication associated with the use of flow diverters is delayed ipsilateral parenchymal hemorrhage. Although the number of reported cases are small, it seems unrelated to the size or morphology of the treated lesion[307]. Putative mechanisms include dual antiplatelet therapy, transformation of ischemic stroke, loss of autoregulation of distal arteries, and the "Windkessel effect", with increased blood pressure waveform to the distal vessel territories.[296, 297, 307] In one meta-analysis, occlusion of perforators and subsequent ischemic stroke was 6%, with higher rates in posterior circulation (likely because of lack of collaterals) and large/giant aneurysms.[297, 308, 309] Potential mechanisms are stent wall thrombosis, distal thromboembolism or parent artery occlusion. Finally, late thrombosis and in-construct stenosis has been reported.[310-312]

Intravascular flow disrupters were designed in order to overcome limitations associated with flow diverters (perforator occlusion, in-construct stenosis, ipsilateral parenchymal hemorrhage and need for antiplatelet therapy). After successful preclinical testing, the feasibility of woven EndoBridge (WEB) devices, especially for wide-neck bifurcation aneurysms, has been confirmed in preliminary clinical series.[313, 314]

Results of a prospective observational study in 20 European centers using the liquid embolique agent onyx revealed good preliminary results in selected patients with aneurysms that were considered unsuitable for coil treatment, or in whom previous treatment had failed.[315] Despite the promising results from the Cerebral aneurysm multicentre european onix (CAMEO) trial, complications including mass effect and parent vessel stenosis emerged following further clinical experience and have damped enthusiasm for its widespread use.[316]

The use of covered stents (endovascular grafting, complete covering of IA neck) emerged as promising treatment option for complicated IA.[317, 318] However, only limited data about this technique has been reported up to now. A prospective, multicenter-based study examined 45 aneurysms in 41 patients treated with Willis stent-grafts revealed its feasibility and an acceptable long-term (mean 43.5 months) occlusion rate of 87%.[319] Despite their restricted application in intracranial vascular segments without critical side-branches, stent-grafts may add a useful option in selected cases.

Figure 1. Evolution of endovascular treatment.

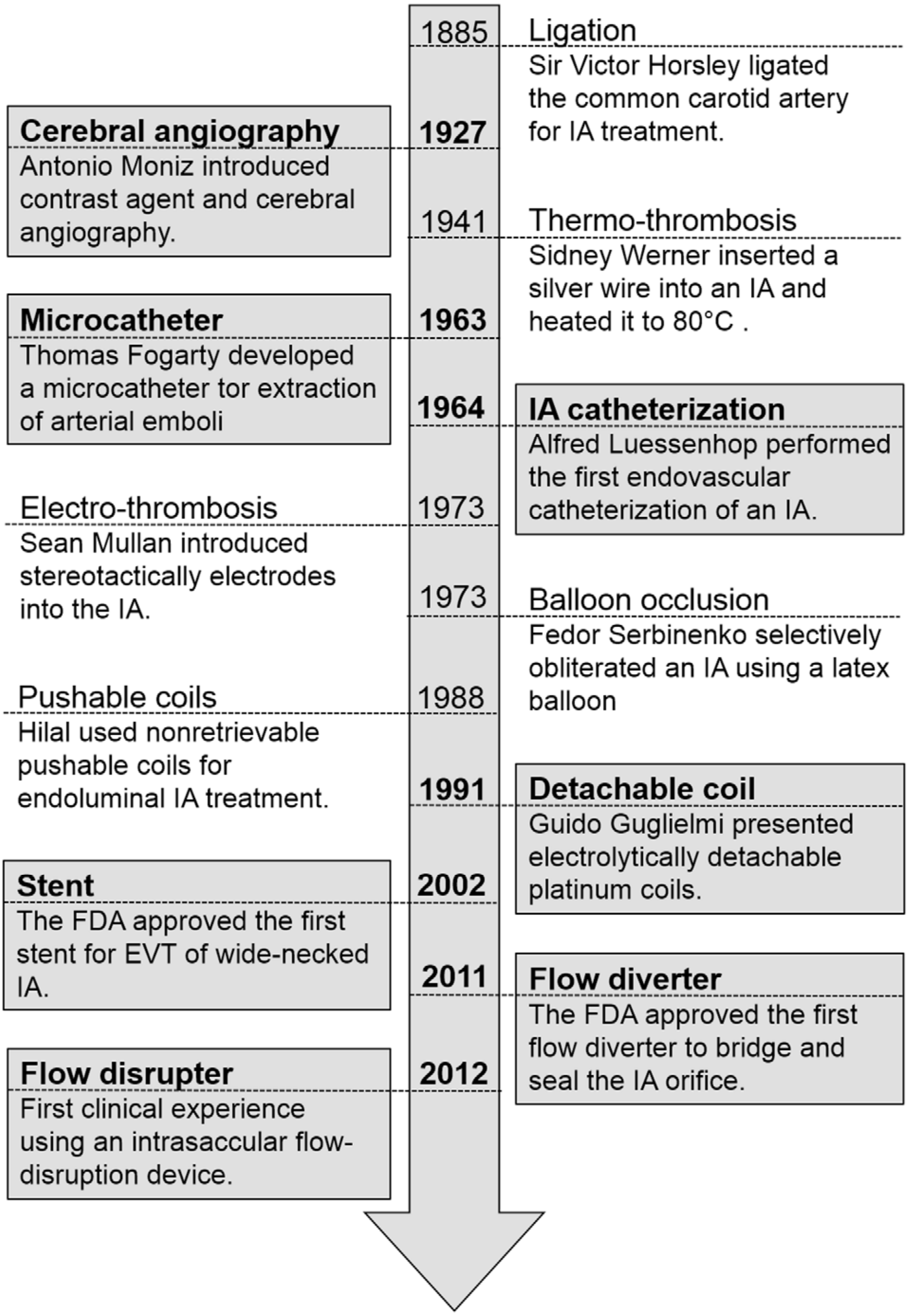

The timeline presents key events in the evolution of EVT. The techniques and devices still used today are printed in bold, highlighted and framed.

2.2.2 Aneurysm recurrence after EVT

2.2.2.1 The role of the aneurysm wall

Aneurysm recurrence is a distressing and significant clinical problem that occurs in approximately 20-30% of patients and necessitates retreatment in half of reopened IA.[12-15] The mechanisms underlying reopening are poorly understood. Most of the hypothesized concepts are based on subjective interpretation of morphological IA changes. These volume-oriented mechanisms include coil compaction, coil migration into intraluminal thrombus and resorption of pre-existing intraluminal thrombus.[161, 320, 321] Under the presumption that the aneurysm is a simple expansion of the parent artery lumen, it seems compelling to suspect coil compaction after total occlusion as the likely cause of aneurysm neck recanalization.

Histological studies after plain platinum coil embolization revealed that the unorganized intraluminal thrombus organizes by growing granulation tissue, first at the aneurysm wall, and finally by the expansion of endothelial cell lining over the granulation tissue at the aneurysm neck.[322] Drawing upon these findings and confirmation of these healing processes in experimental settings, deficient fibrosis, insufficient neointima and lack of endothelization after GDC embolization tentatively seem to be mechanisms of IA recurrence.[321, 323, 324] However, based on extensive experience with canine carotid bifurcation aneurysm models, Raymond et al. found thrombus organization, endothelialization and neointima formation occur concurrently with IA recurrence following plain platinum coil occlusion.[325] Based on these findings, they suggested an alternative concept and proposed that contraction of connective tissue leads to shrinkage of the fibrosed cavity resulting in a displacement towards the fundus, opening of recurring space, progressive enlargement and coil compaction.[325] The same group emphasized the role of the endothelial lining in residual lesions, recurrences and growth of recurrences after EVT of canine sidewall venous pouch aneurysms.[326, 327]

Cognard et al. found regrowth after subtotal occlusion to be more frequent than true recurrences and emphasized that aneurysm growth might be an important factor for IA recurrence.[275] They hypothesized that IA growth is interrelated with coil compaction in that regrowth may produce changes in the coil mesh, or conversely, that round coil compaction could lead to recanalization of the neck and restart the process of IA growth. Rigorous 3D image processing of IA reopening revealed that not coil compaction, but also aneurysm growth is an important mechanism for recurrence of initially complete or near-complete obliteration.[328] However, the study population of this single center evaluation was rather small (eight major IA recurrences out of 175; three unruptured and five ruptured cases) with a limited follow-up period of seven months and use of different coil types (bare platinum coils and hydrocoils). It also remains unclear whether different mechanisms of recurrence may be present in ruptured and unruptured aneurysms. A most recent publication confirms that true IA growth plays a major role in IA recurrence after

EVT.[329] Comparison of the areas of the coil mass and aneurysm sac in 29 patient with significant IA recurrence revealed IA growth as leading cause of recurrence in more than half of the cases (18 patients).

Ruptured and unruptured aneurysms represent a different biological entity. Histopathological series clearly demonstrate underlying differences in aneurysm morphology between ruptured and unruptured aneurysms. Ruptured aneurysms are associated with wall degeneration, and exhibit extremely thin thrombosis-lined hypo to acellular walls with degenerated extracellular matrix and loss of endothelial cells.[100, 102] Although risk factors for IA recurrence have been identified, it remains difficult to determine which aneurysm will reopen and which will not.

A growing body of evidence emphasizes the paramount importance of the aneurysm wall in IA growth and IA recurrence after EVT. The triggers of IA wall remodeling after EVT are associated with inflammation which is regularly seen after embolization.[300, 301, 303, 304] Intraluminal thrombus induction (which is the ultimate goal of all endovascular approaches) causes inflammation in the IA wall (2.1.4.4). The role of luminal thrombosis). It is likely that "healthy" IA walls can better withstand stress caused by sudden thrombosis than degenerated IA walls. Ruptured IA, partially thrombosed, large and giant IA often demonstrate more pronounced wall degeneration and seem to be more susceptible to inflammatory reactions. This leads to destructive remodeling that causes IA wall growth, recurrence and eventually rupture. Multiple retreatments after EVT using coil embolization are more likely in ruptured than unruptured IA[330] and aneurysm with previous recurrence are associated with almost 50% of major recurrences[12] which also points to mechanisms other than lumen-oriented causes of IA recurrence. Further evidence comes from studies demonstrating that factors (smoking) suspected to increase inflammation in the IA increase IA recurrence after EVT[331], whereas factors (acetylsalicylic acid) assumed to reduce mural IA inflammation seem to prevent from IA recurrence or re-intervention.[332] The finding that recurrences in patients with multiple aneurysm is higher when compared to the subpopulation of patients with single IA corroborate the notion of biological causes for IA recurrence after EVT using standard coils.[333]

It has been shown in experimental aneurysms that the major source of thrombus organizing neointima cells are derived from the aneurysm wall, with perhaps a negligible contribution from circulating bone marrow cells.[140] The finding that intraluminal unorganized thrombus is mainly organized by IA wall cells is in line with human histological studies after plain platinum coil embolization. Bavinski et al. found that granulation tissue response starts at the periphery of the luminal clot adjacent to the aneurysm wall within the first two weeks after coil embolization.[322] Degenerated IA walls cannot recruit SMC to ingrow and organize the thrombus which leads to blood clot lysis, recanalization and new thrombus formation. This continues in a disastrous cycle of ongoing IA wall inflammation and destruction.

The presumably better wall condition in unruptured IA could serve to explain why unruptured IA demonstrate lower rebleeding rates[334], necessitate less retreatment[330], and present more stably after coil embolization than ruptured IA with a more degenerated wall type.[12, 275, 276, 329, 333, 335-337] EVT of IA with an almost decellularized thin wall seems not be able to organize the thrombus, and intraluminal scar formation is likely to fail. Raymond et al. could not explain the change in recurrence after treatment of unruptured and ruptured IA based on factors, such as aneurysm size, neck width, or quality of initial angiographic result.[12] They therefore made the assumption that some biological difference must exist. A systemic review (January 1999 – September 2008) on recurrence rates after EVT found lower IA recurrence rates in studies with exclusively rupture IA.[13] This differ from previous studies directly comparing recurrence rates of ruptured and unruptured IA.[12, 275, 276, 329, 333, 337] The authors hypothesized that this contradictory finding is likely due to higher proportions of large and posterior localization in unruptured aneurysms which is explains the relatively higher rate of reopening in unruptured aneurysms.[13] Analysis of a matched (aneurysm location, diameter, and neck size) cohort of ruptured and unruptured IA demonstrated that not only increased risk of recanalization in ruptured IA but also more significant degrees of recanalization and a higher percentage of ruptured IA requiring retreatment[337]. Furthermore, time to recanalization is significantly shorter in ruptured IA compared to unruptured IA.[337] IA recurrence rates after EVT using standard coils in relation to rupture status, size, and location are given in **Table 1**.

The capacity of the IA wall to organize an intraluminal thrombus must be viewed in relation to the amount of thrombus. The quantity in relation to recurrence rate is reflected in the percentage associated with IA size increase. Overall recurrence rates for small aneurysms (4-10 mm) are reported to be 5%-20%, depending on neck size.[14] This increases to 35%-50% in large (10-25 mm), and 60%-90% in giant aneurysms.[12, 14, 338, 339] These findings correspond with clinical series reporting that low packing density is linked to higher recurrence rates in aneurysms with over 80% of intraluminal thrombus.[147, 151-153, 161, 340] Poor packing results in many empty spaces (clefts) filled with thrombus needing to be organized and even in “highly/tightly packed” aneurysms 75% of the aneurysm sac is filled with thrombus.[340] Presence of acute intra-aneurysmal and/or perianeurysmal soft thrombus was suspected to be responsible for the finding that aneurysms treated within 14 days of SAH demonstrate lower rate of resolution of contrast filling between coil interstices, higher recanalization rates and reduced stability of small neck remnants when compared to delayed EVT after SAH (>14 days).[341]

In stable non-progressing IA remnants after EVT (on 6 month follow-up angiography) re-rupture rate is low (0.4%)[320] and single endovascular retreatment likely to be successful if retreatment is needed.[15] On the other hand in unstable IA with documented regrowth after EVT rupture rate is higher (7.9%)[320] and necessity of multiple endovascular retreatments rather the rule than the exception.[15]

These findings are in line with the observation that stable IA (during 12 month interval) show a low risk for future morphological loss (4.8%) compared with unstable IA which show a high risk for additional late loss of morphology (38.3%; P<0.001, odds ratio=12.4).[330]
In general the reopening rate is lower in clipped than in coiled IA[9, 10, 208] which also indicates that recurrence originates from the IA wall. In a large series long-term angiographic follow-up (mean of 4.4 years) of clipped IA without residua recurrence was found to be 1.5% (2/135).[342] The factors underlying regrowth of perfectly clipped aneurysms remains controversial and include break or slippage of the clip, fragility of the wall along the clip edge, small rests of IA neck not detected by 2D-DSA, or inappropriate clip application.[342, 343] Recurrence in IA with known "dog-ear" and "broad-based" residua recurrence is as high as 25% (2/8) and 75% (3/4).[342] Multiple clips are often necessary for surgical treatment of broad-based IA with the result that portions of the aneurysm wall are included in the reconstructed vessel segment.

The notable difference between IA clip ligation and IA coiling is the fact that clipping removes the diseased vessel segment and realigns healthy arterial walls. Conventional histological and electron microscopy findings following experimental clipping confirm that the normal vessel wall is completely reconstructed directly underneath the blades of the clip.[321] If the parent artery segment is not diseased (fusiform enlarge, dysplastic or arteriosclerotic, broad necked aneurysm) the clip blades pull the opposing healthy vessel walls towards each other, excluding the diseased vessel segment. Luminal coil placement does not exclude the pathology from the blood circulation but increases thrombus-induced stress to the IA wall. Failed healing, exposure to hemodynamic stress or continuous wall remodeling/growth may all contribute to IA reopening after coil embolization. IA devices such as stents and flow diverters exclude the aneurysm from the blood circulation by bridging the pathological wall segment. As long as the lumen is not recanalized and remains excluded from the circulation, healing is more likely than after coil embolization. Consequently, there is a better chance for long-lasting occlusion, as confirmed by higher rates of complete occlusion.[297]

One must keep in mind that angiographic healing is not biological healing.[322, 325, 344] Histopathological studies revealed that 50% (n = 6/12) of IA (two small, three large and one giant) that had been deemed 100% occluded on angiography, showed tiny open spaces between the coils at the neck on gross examination.[322] Animal studies confirmed the discrepancy between angiographic and histological findings with overrated radiologic occlusion after coil treated bifurcation aneurysms in rabbits.[344] Molyneux et al. reported histological findings in two patients 2 and 6 months after GDC embolization of giant partially thrombosed IA.[157] They found the coils embedded in unorganized thrombus with no sign of endothelialization of the luminal surface. It must be noted that not only thrombus in large or giant aneurysm remain largely unorganized[157] but also small ruptured IA (<6mm) demonstrate remnants of unorganized thrombus, fresh blood clot, and void spaces three years after plain platinum coil embolization.[260]

True understanding of IA reopening after EVT requires comprehensive knowledge of the biological mechanisms involved in aneurysm wall remodeling, intraluminal thrombosis formation and resorption, tissue response to EVT materials and the effects that these factors have on each other. Insights into pathological processes might help address the root cause of the problem; namely the diseased arterial vessel segment (or aneurysm wall), rather than the arterial outpouch consequence of the disease. One must remember that an angiographic complete IA occlusion cannot be equated with clinical cure of the diseased vessel segment.

Follow-up of initially adequate coiled IA <10mm is recommended at six months post coiling. Later follow-up, within the first 5-10 years, does not seem beneficial in detecting reopened IA. However, in case of IA growth, extended follow-up imaging may be considered for size >10 mm, location at the basilar tip, partial thrombosis, recurrent IA after EVT, presence of multiple IA or familiar predisposition.[274] Routine angiographic surveillance after endovascular treatment of aneurysms has a very low complication rate of 0.43% (0.04% permanent major morbidity, 0.07% temporary major morbidities, and 0.32% temporary minor morbidities – including two third of these representing access site complications).[345]

Table 1. Aneurysm recurrence after EVT using mainly standard coils.

1. Rupture status

Authors (year)	**Follow-up (months)**	**Unruptured % of recurrence (n/n)**	**Ruptured % of recurrence (n/n)**
Cognard et al.[275] (1999)	3-48	7 (4/54)	17 (16/94)
Raymond et al.[12] (2003)	12 (mean)	27 (52/190)	40 (76/191)
Ngyen et al.[276] (2007)	20 (mean)	22 (16/72)	52 (23/44)
Tan et al.[337] (2011)	20-25 (mean)	20 (10/49)	40 (19/47)
Vanzin et al.[333] (2012)	21 (mean)	22 (42/194)	31 (80/261)
Abdihalim et al.[329] (2014)	9 (mean)	5 (5/92)	20 (24/120)

2. Size

Authors (year)	**Follow-up (months)**	**Small <10mm % of recurrence (n/n)**	**Large >10 to ≤25mm % of recurrence (n/n)**	**Giant >25mm % of recurrence (n/n)**
Byrne et al.[320] (1999)	6-12	14 (24/176)	15 (12/81)	100 (2/2)
Tateshima et al.[159] (2000)	19 (mean)	8 (2/24)	40 (4/10)	50 (4/8)
Raymond et al.[12] (2003)	12 (mean)	21 (47/221)	51 (81/160)	-
Murayama et al[14] (2003)	6-12	21 (66/579)	35 (70/198)	59 (43/73)
Standhardt et al.[346] (2008) *	35 (mean)	14 (22/163)	25 (5/20)	45 (9/19)
Plowman et al.[347] (2011)	6	26 (88/345)	28 (27/97)	40 (4/10)
Gao et al.[339] (2012) †	38 (mean)	-	11 (6/53)	36 (10/28)
Dorfer et al.[15] (2012)	6-18	15 (61/403)	38 (66/173)	-
Chalouhi et al.[348] (2014) §	6-60	35 (62/177)	47 (29/62)	52 (11/21)

3. Location

Location and authors (year)	**Follow-up (months)**	**% of recurrence (n/n)**
BA tip		
Bavinski et al.[349] (1999)	2-72	39 (12/31)
Tateshima et al.[159] (2000)	19 (mean)	24 (10/41)
Raymond et al.[12] (2003)	12 (mean)	39 (43/109)
Henkes et al.[277] (2005)	19 (mean)	35 (62/178)
Peluso et al.[350] (2008)	34 (mean)	18 (27/138)

Posterior circulation		
Lempert et al.[351] (2000)	7 (mean)	22 (17/76)
Pandey et al.[352] (2007)	31 (mean)	25 (55/225)
Carotid-ophtalmic artery		
Raymond et al.[12] (2003)	12 (mean)	29 (19/73)
Yadla et al.[353] (2011)	28 (mean)	18 (21/118)
Acom		
Raymond et al.[12] (2003)	12 (mean)	25 (11/44)
Guglielmi et al.[354] (2009)	-	16 (23/144)
Finitsis et al.[335] (2010)	36 (mean)	22 (51/234)
Corns et al.[355] (2013)	6	19 (18/97)
PComA		
Raymond et al.[12] (2003)	12 (mean)	37 (16/43)
Corns et al.[355] (2013)	6	57 (35/61)
Paraclinoid		
Park et al. (2003)	14 (mean)	25 (12/49)
AChA		
Kang et al.[336] (2009)	19 (mean)	15 (10/67)
ICA bifurcation		
van Rooij et al.[356] (2008)	16 (mean)	18 (7/40)
Oishi et al.[357] (2013)	24 (mean)	14 (3/22)
DACA		
Oishi et al.[358] (2013)	9 (mean)	35 (6/17)
Park et al.[359] (2013)	20 (mean)	38 (6/16)
MCA		
Raymond et al.[12] (2003)	12 (mean)	32 (9/28)
Iijima et al.[360] (2005)	15 (mean)	20 (21/105)
Quadros et al.[361] (2007)	13 (mean)	15 (8/55)
Vendrell et al.[362] (2009)	50 (mean)	27 (31/114)
Brinjikji et al.[363] (2011)	>3	32 (9/28)
Corns et al.[355] (2013)	6	34 (12/35)
Mortimer et al.[364] (2014)	6	19 (42/219)

AChA = anterior choroidal artery; Acom = anterior communicating artery; BA = basilar artery; DACA = distal anterior cerebral artery; ICA = internal carotid artery; MCA = middle cerebral artery PComA = posterior communicating artery; * = small (<12 mm), large (13-24 mm), angiographic FU was available for 76% of all aneurysms; † = large (15–25 mm), § = small (10-14 mm), large (15-24 mm).

2.2.3 Experimental aneurysm models

Increased understanding of the complex pathobiology of IA growth, rupture and the effects of EVT depends on epidemiological data analysis, clinical findings, histopathology of IA samples obtained during surgery, and gene linkage analysis.[18, 82, 140, 144, 297] Experimental work using animal models of IA are needed to delineate the biological mechanisms of IA formation and growth, and to establish new endovascular and medical therapies to prevent IA rupture. Today's models can be divided in two main groups according to the subject under examination: first, models to evaluate induction, growth and rupture of IA and second, aneurysm models as tools for testing novel endovascular devices (biological interaction of EVT), evaluation of basic biological concepts and hemodynamics of IA and training for neurointerventional radiologists and endovascular neurosurgeons.

The models developed by Hashimoto et al. are the most physiological IA models to-date in terms of representing human morphology, histology, hemodynamics and IA vessel surroundings.[365] In all other models, aneurysms are created by direct vessel manipulation on intra- and extracranial arteries. Those working with extracranial models must be aware of differences in hemodynamic characteristics and vascular biology between the extra- and intracranial arteries. Furthermore, the perianeurysmal space of the extracranial models differ greatly from that of human IA. With the exception of autogenous vein graft aneurysm production on the wall of the basilar artery and middle cerebral artery, aneurysms are not created in the subarachnoid space, but in the soft tissue of the neck[325, 366], leg, retroperitonal space, or within the abdominal cavity using either venous or arterial auto or allografts.

Smaller animals (mice and rat) are more often used for the study of IA biology while larger animals (rabbit, dog, and swine) are mainly used for testing endovascular devices (**Figure 2A**). The number of studies performed in swine and dogs remains stable, while the number of experiments in mice, rats and rabbits is steadily increasing (**Figure 2B**). Animal models in sheep and monkey have been described but have never undergone detailed methodological analysis and are rarely used today.

2.2.3.1 Aneurysm models for the study of endovascular therapies

None of the preclinical aneurysm models for testing endovascular devices currently available combine all the ideal characteristics. The basic requirements include: 1) stable parent vessel and aneurysm size without growth or shrinkage over time; 2) size of aneurysm and parent artery similar to larger cerebral arteries (enables realistic micro catheter interventions); 3) long-term patency without spontaneous thrombosis and no need for anticoagulation or anti-aggregation therapy; 3) standardized method with good reproducibility; 4) hemodynamics (high shear stress at the neck of the aneurysm), coagulation profiles (clotting and thrombolytic system) and tissue and immunologic reactions similar to those of humans IA; 5) aneurysmal environment similar to the subarachnoid space in humans; 6) wide availability of the animal and easy handling; 7) low costs.

Histopathological analysis of microsurgically created swine venous pouch sidewall aneurysms revealed robust healing (exuberant thrombosis and thick neo-intimal formation) beyond that expected in humans. Untreated sidewall swine aneurysms have a tendency for spontaneous thrombosis[367, 368], making immediate EVT necessary. However, embolization performed at the time of creation is unfavorable as tissue reaction to surgery and the embolic device overlap. Unlike in swine, the canine sidewall venous pouch aneurysm model exhibits excellent long-term patency without need for an antithrombotic regimenand shows modest progressive increases in size during the first month after creation.[369] However, extensive healing (less than that in swine), is also seen in the canine model, with complete intra-aneurysmal fibrosis after GDC embolization.[370] Microsurgically created aneurysms have been criticized due to the unknown biological effect of artery wall disruption at the site of anastomosis, suture line healing, trauma induced by the surgical procedure itself, and presence of suture material in the aneurysm neck and use of venous, rather than arterial walls.

Comparison of histopathologic and immunohistochemical analysis of human, rabbit and swine aneurysms embolized with GDC revealed that the rabbit model (elastase-induced) offers superior similarity to human IA tissue reactions when compared to tissue reactions in swine.[323] In contrast to the fast and complete healing process in the canine and swine sidewall model, the rabbit elastase model produced cases with persistence of unorganized thrombus after GDC.[371] Thanks to these findings and additional potential advantages (aneurysm and parent artery size and hemodynamics similar to human IA[372], coagulation system similar to humans[373], neck subjected to high shear stress[374], easy microsurgical technique, low morbidity, low costs, easy handling and excellent long-term patency[375]), elastase-induced aneurysms created in the common carotid arteries along the brachiocephalic artery of rabbits, became a useful widespread preclinical tool for neuroendovascular device development.[366] Technical modification made the model easier to perform with improved reproducibility.[376] Since more evidence has been collected, complications such as stroke, laryngeal hemiplegia and hemorrhagic tracheal necrosis have also been reported.[377]

The multiple elastic membranes destructed by the intraluminal elastase perfusion may cause long lasting inflammatory repair processes in the entire aneurysm wall which despite the increased neck shear stress, do not represent true bifurcation aneurysm but rather, sidewall aneurysms. It has been shown that true bifurcational hemodynamics are essential to determine the device effectiveness.[378] Major shortcomings of microsurgical creation of venous pouch arterial bifurcation aneurysms in rabbits (requires very good microsurgical skills, low aneurysm patency rates and high morbidity rates) were overcome by modifying microsurgical techniques, aggressive anticoagulation treatment and anesthesia (resulting in aneurysm patency rates and mortality rates comparable with those of the rabbit elastase model).[379] It remains a matter of debate if the morphologic and histologic characteristics of human cerebral aneurysms is more accurately modeled by elastase-digested arterial sacs or by surgically created vein pouch aneurysms.[380, 381]

The standardization of aneurysm creation is not the only potential advantage of surgical models. Others include the opportunity to vary aneurysm angioarchitecture to study the influence of the angle between the aneurysm axis and parent artery, to examine various hemodynamic conditions and fundus to neck ratios and to test new endovascular devices in complex aneurysm formations.[382, 383] To a certain degree, neck size and aneurysm volume can also be controlled and adjusted in elastase-induced aneurysms and modified techniques result in more consistent aneurysm diameters.[384]

Standardized and reproducible aneurysm creation is of utmost importance to improve preclinical assessment of novel endovascular devices and enhance comparability of results between laboratories. To date, the most standardized aneurysm model in terms of graft origin, aneurysm shape and dimensions, volume-to-orifice ratio and parent vessel to aneurysm long axis angle is the rat arterial sidewall aneurysm model developed by Frösen and colleagues.[140] Although standard catheter systems cannot be used when embolizing the aneurysms, the relatively low costs make the model a suitable tool to test and refine embolization devices that will be tested later in other more complicated and expensive models. In a recent review of in vivo experimental IA models, the most appropriate models to test for recurrences after endovascular occlusion were found to be surgical bifurcation model in dogs and the elastase-induced aneurysm model in rabbits.[382] There has been no standardized multicenter preclinical study of any device or model to date.

None of the available aneurysm models that can be embolized represent a human saccular cerebral artery aneurysm properly. All artificial aneurysm constructions cannot recreate the complex phenomenon involved in human IA pathobiology. Nevertheless, taking the potential confounding effects of the chosen model and species into consideration, basic biological concepts of novel EVT approaches can be tested in the models available today. Investigators must choose the most appropriate one from a wide range of different techniques that suits the experimental goals, practical considerations and laboratory environment.

2.2.3.2 Aneurysm models for the study of grow and rupture

IA models have been developed to systematically investigate the mechanisms of IA formation and growth.[385] After pioneer work of aneurysm creation by direct vessel manipulation on extra- and intracranial arteries by McCune et al.[386], German and Black[387], White et al.[388], Troupp and Rinne[389], Nishikawa et al.[390], and

Kerber et al.[391], it was Hashimoto and colleagues[365] who first reported successful indirect induction of saccular cerebral aneurysms using a combination of lathyrogen (beta-aminopropionitrile [BAPN]), deoxycorticosterone, salt hypertension and ligation of unilateral common carotid artery (CCA).

Despite the combined vessel wall stress by lathyrogens (decreased collagen and elastin cross-linking by inhibiting lysine oxidase [LOX]), and induction of systemic hypertension (unilateral nephrectomy, unilateral CCA, increased salt intake and doexycorticosterone results), the incidence of spontaneous IA creation was low.[365] Modifications of the model allowed for increased incidence of IA formation through induction of hypertension caused by renal infarction (ligation of the posterior branches of the bilateral renal arteries). Administering deoxycorticosterone to animals with renal infarction was not essential, but feeding with a diet high in salt containing 8% sodium chloride increased the incidence of lesions.[392] Unilateral CCA ligation facilitates comparison of the arterial bifurcation of the non-ligated side (frequent IA formation) with the ligated side (no IA formation). Aneurysms develop only in the posterior circulation when both of the CCA are ligated.[393] Disturbance of collagen synthesis by LOX inhibition with BAPN treatment increases the developmental rate of IA three months after induction. Aneurysms in BAPN-treated rats are larger in size and have a thinner media wall thickness than BAPN-untreated controls undergoing the same blood pressure augmentation.[127] It has been shown that the number of induced aneurysms and the number of ruptured IA is associated with increases in maximal blood pressure.[393] Induction of IA in female rats necessitates bilateral oophorectomy to compensate for the protective effect of estrogen.[63, 64] In addition to these important gender differences, one should be aware that genetic factors are involved in cerebral aneurysm formation in different rat strains.[394]

Cerebral aneurysms without direct vessel manipulation have also been developed in monkey[395], dog[396], rabbit[397] and mice[398] models. Although findings were in accordance with spontaneous lesions in humans[399], ethical concerns, long IA induction period, and high costs limit the widespread use of monkeys. In dogs, de novo bifurcations were surgically created using both native CCA. The canine model allows assessment of the extracranial arterial hemodynamic microenvironment and evaluation of triggers of molecular changes associated with aneurysmal vascular degradation.[400] The arteries are large enough to easily perform 3D-DSA and enable CFD characterization. In rabbits, nascent IA formation at the basilar terminus is successfully created by increased hemodynamics through bilateral CCA ligation without any additional manipulation.[397] These findings are in line with the original work by Hassler who reported considerable bulging of the artery and morphological changes (cushions in the intima, defects of the media and defective intraepithelial leukocytes) in the circle of Willis by CCA ligation in rabbits.[401] While unilateral CCA ligation seems insufficient to induce microaneurysms constantly[402], bilateral CCA ligation proved to be a reliable tool to evaluate molecular mechanisms involved in initial vascular remodeling induced by hemodynamic insult.[403, 404]

Induction of IA in mouse models provides an advantage for genetic analysis due to the wide availability of genetically modified mice. However, induction of IA in mice requires more time and the number of induced IA is lower than in rats, caused by resistance to induced hypertension and vascular inflammation.[385] The first mouse model was established through ligations of left common carotid arteries and posterior branches of bilateral renal arteries with high salt diet.[398] In subsequent publications, BAPN was added to the feeding regimen.[110, 129] In this mouse model, IA developed at the right anterior cerebral artery–olfactory artery bifurcations in approximately 80%, four to five months after the induction. Nuki and colleagues reported a mouse model which induces large IA formations at 60–80% incidence within three to four weeks by single stereotaxic injection of elastase into the CSF at the right basal cistern, and hypertension by continuous angiotensin II infusion through an implanted osmotic pump.[405, 406] Although a case of spontaneous SAH from a large aneurysm 12 days after IA induction was reported in this elastase-induced hypertensive mouse model, the precise incidence of IA rupture remains unknown.[406] Toll-like receptor (TLR)-4 and MMP-9 associated IA formation has been reported in Type 1 diabetes in rat.[407]

IA animal models reporting spontaneous rupture are rare. In the hypertension and BAPN-induced IA rat model, rupture rate is 3% during the three month period of IA maturation, and spontaneous rupture in mice has never been observed.[385] Recently, the elastase-induced hypertensive mouse model has been modified to increase the reproducibility of IA development and rupture.[408] Hosaka and colleagues induced chronic hypertension by ligation of the right renal artery and left CCA. One week later, various concentrations of elastase were injected into the right basal cistern (modified stereotactic coordinates with higher success rate of infusion into the CSF space of the circle of Willis compared with previous reported coordinates). Further vessel wall stress was induced through continuous angiotensin II infusion (1000ng/kg/min), hypertensive diet (8% sodium chloride) and feeding of BAPN (0.12%). Unless early neurological symptoms developed, animals were euthanized three weeks after elastase injection. Based on their elastase dose study, they recommended the use of 10 µL of 1.0 U/mL elastase to investigate IA formation without rupture and 10 µL of 10 U/mL elastase to study IA rupture. In mice given 10 µL of 1.0 U/mL elastase solution, 90% developed IA and 20% had ruptured IA. Intracranial aneurysm models are summarized in **Table 2**.

During aneurysm formation, wall remodeling processes either lead to stabilization of the wall or further degeneration and rupture. IA models of rupture are of great interest when exploring the differing pathobiological mechanisms between

IAs that never rupture and IAs that most likely will proceed to rupture. In the future, this may allow assessment of biomarkers or imaging modalities to detect rupture prone IAs and to develop therapeutic drugs for IA stabilization (prevention of rupture). The delivery route could either be systematic or locally, by EVT. In addition to the elastase-induced hypertensive mouse model of IA formation and rupture, it will be essential to produce animal models which will also allow the study of embolization device healing processes in growing and rupture-prone aneurysms.

Significant growth and reports of rupture in extracranial artery aneurysm models are rare. Moderate aneurysm growth within the first weeks after creation has been found in the rabbit elastase-induced[409, 410], in combined surgical and elastase/type I collagenase[411] in the surgical sidewall model[412] , and the dog surgical bifurcation model.[369] Regarding the swine surgical sidewall aneurysm model, multiple investigators revealed consistent aneurysm rupture in sudden thrombosed or only partially occluded aneurysms within four to five days after creation.[143, 144, 324, 413] Details of studies reporting aneurysm growth and rupture of models in extracranial arteries are presented in **Table 3**.

Figure 2. Experimental aneurysm studies.

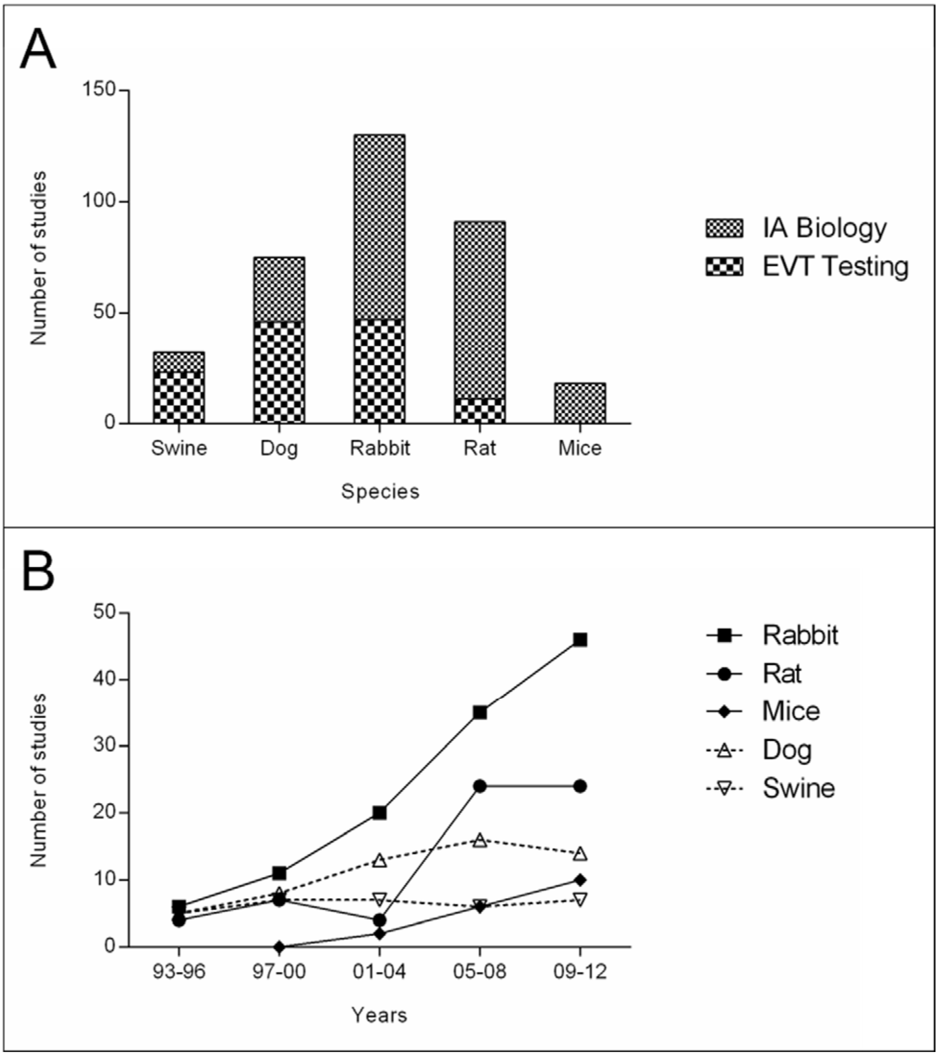

A, the percentage of studies testing endovascular devices decreases proportionally with the size of the animal. Inversely, the proportion of number of studies addressing the biology of IA increases in smaller species. **B**, since the early nineties, the number of animal studies performed (five four-year periods) has been increasing steadily in rabbit, rat and mice models. The number of publications using dog and swine has remained fairly stable over time. An online search of Medline/Pubmed database (1993-2012) was performed using the keywords ”swine”, ”dog”, ”rabbit”, ”rat”, and ”mice” in combination with ”intracranial aneurysm” using the Boolean operator “AND”.

Table 2. Intracranial aneurysm models of growth and rupture

Author (year)	Animal (location)	Methods and technique	Growth and time course	Rupture and time course	Histological findings
White et al.[388] (1961)	Dog / left ICA junction	Injection of hypertonic saline, plasmocid, hyaluronidase, and nitrogen mustard	Most consistent with injection of hypertonic saline 50% (n = 5/10) within three weeks	No rupture	The lesion resembled congenital berry aneurysms
Hashimoto et al.[365, 393] (1978)	Rat / Circle of Willis bifurcations (ACA and OA) of non-ligated side	Left CCA and posterior branches right RA ligation, one week later posterior branches left RA alone or plus 0,2% BAPN or/and plus 1% NaCl	12% (n = 2/17) 61% (+BAPN) (n = 11/18) 61% (+1% NaCl) (n = 11/18) 95% (+BAPN +1% NaCl) (n = 18/19) All groups within three or four months	0% (n = 0/17) 22% (+BAPN) (n = 4/18) 17% (+1% NaCl) (n = 3/18) 32% (+BAPN +1% NaCl) (n = 6/19) Time course not reported	Generally in accordance with lesions in man; IEL absent; walls composed of fibrous connective tissue/hyaline degeneration, areas cellular composed of SMC or fibroblasts; some blebs or daughter aneurysms; larger IA intraluminal thrombi, organized in some cases.
Hashimoto et al.[395] (1987)	Monkey / Circle of Willis bifurcations (ACA and OA) of non-ligated side	Left CCA and posterior branch right RA ligation, one week later posterior branch left RA and 1% NaCl drinking water, two weeks later 0,2% BAPN diet	29% (n = 2/7) / one year	No rupture	Similar to lesions in man; wall of first case very thin; second aneurysm thrombosed and organized, loss of IEL and medial muscle layer, wall composed of connective tissue.
Morimoto et al.[398] (2002)	Mouse / Circle of Willis bifurcations (ACA and OA) of non-ligated side	Unilateral left CCA and posterior branches right RA ligation, one week later posterior branches left RA plus 1% NaCl drinking water	78% (n = 14/18) within four months	No rupture	Similar to pathological changes in experimentally induced IAs in rats and monkeys, thinning of SMC layer and loss of IEL in early stages
Nuki et al.[406] (2009)	Mouse / major bifurcations of circle of Willis	Elastase injection (various doses) right basal cistern and hypertension by continuous angiotensin II	0% (PBS) (n = 0/10) 10% (3.5 mU) (n = 1/10) 30% (17.5 mU)	Rupture reported but incidence unknown	Thin wall intact endothelial and SMC layers, thick wall discontinued endothelial cell layers and scattered,

		infusion (1000ng/kg per minute)	(n = 6/20) 77% (35 mU) (n = 34/20) within two weeks		faint SMC staining, disorganized elastic lamina in both thin and thick portions, inflammatory cells throughout the wall
Hosaka et al.[408] (2013)	Mouse / major bifurcations of circle of Willis	Left CCA and right RA ligation, one week later elastase injection (various doses milliunits - mU) right basal cistern and angiotensin II infusion (1000ng/kg per minute) plus 0,12% BAPN plus 8% NaCl	90% (10µl 1U/ml) 100% (5µl 10U/ml) 100% (10µl 10U/ml) 100% (20µl 10U/ml) within three weeks (n =10 / group)	20% (10µl 1U/ml) 40% (5µl 10U/ml) 60% (10µl 10U/ml) 50% (20µl 10U/ml) Time course not reported	Destruction of the elastic lamina within the wall, consistent inflammatory cells infiltrating the wall, partial or complete absence of intimal endothelial cells, capillary formation and thickening of SMC layer.

ACA = anterior cerebral artery; BAPN = beta-aminopropionitrile; CCA = common carotid artery; ICA = internal chorotid artery; OA = ophthalmic artery; PBS = phosphate buffered saline; RA = renal artery.

Table 3. Extracranial aneurysm models reporting growth and rupture.

Author (year)	**Animal (location)**	**Methods and technique**	**Growth and time course**	**Rupture and time course**	**Histological findings**
Troupp and Rinne[389] (1964)	Rabbit (CCA)	Arteriotomy glued with Methyl-2-Cyanoacrylate	32% (n = 16/50) within 4-21 weeks	No rupture	Not reported
Byrne et al.[413] (1994)	Swine (CCA)	Surgical sidewall (arteriotomy 4 mm) EJV graft (15-20 mm length); left untreated or embolized using GDC	Tendency for growth in aneurysms with partial thrombosis	100% (n = 4/4) of untreated aneurysm after 4 ± 0.5 days 75% (n = 3/4) of partial occlusion (<90%) after 4 ± 1 days	Marked edema and acute inflammatory infiltration of the whole wall, wall dissection, and necrosis of smooth muscle fibers.
Raymond et al.[324] (1999)	Swine (CCA)	Surgical sidewall (arteriotomy 5 mm) EJV graft; embolized using collagen sponges (20 × 15 × 7 mm)	Not reported	80% (n = 4/5) of residual aneurysm after collagen sponge occlusion after 3-5 days	Not reported
Fujiwara et al.[410] (2001)	Rabbit (CCA)	Elastase induced; Baseline stump at day three (3.2 ± 0.6 mm width and 6 ± 1.3 mm height); left untreated	100% (n = 6/6) within the first month then remains stable (5 ± 0.9 mm width and 10 ± 2.2 mm height)	No rupture	Not reported
Yang et al.[414] (2001)	Dog (CCA)	Surgical sidewall (arteriotomy 3–4 mm) EJV graft (approximately 6–8 mm height); embolized using CAP	20% (n = 1/5) of partially thrombosed aneurysm between 4-8 weeks	40% (n = 2/5) of one total and one subtotal occlusion after 4 and 5 days	The wall structure was so badly damaged that no clear cell structure could be seen
Aassar et al.[409] (2003)	Rabbit (CCA)	Elastase induced; Baseline stump at day three (3.1 ± 0.6 mm width); left untreated	100% (n = 42/42) during the first two weeks (4.2 ± 0.7 mm width)	No rupture	Loss of the IEL and near complete loss of medial elastic lamellae
Murayama et al.[266] (2003)	Swine (CCA)	Surgical sidewall (arteriotomy 6-8 mm) EJV graft (7 mm width and 8-12 mm height); embolized using GDC	Not reported	23% (n = 3/10) of tight packed GDC aneurysm after 5 days (n = 2) and 12 days (n = 1)	Unorganized intraluminal clot (5 day) and large neck hematoma (day 12), rupture point at the dome of the venous pouch
Becker et al.[143] (2007)	Swine (CCA)	Surgical sidewall (arteriotomy 6-8 mm) EJV graft (7-10 mm width	50% (n = 1/2) of partial occlusion	100% (n = 2/2) of partial occlusion (<50%) after 6 and 8 days	Inflammatory cell infiltration in aneurysm sac and neutrophil

		and 8-10 mm height); left untreated or embolized using calcium alginate	(<50%) within 8 days		infiltration within unorganized thrombus
Yang et al.[411] (2007)	Rabbit (CCA)	Combined surgical and Elastase and type I collagenase infused; Baseline stump (2.0 ± 0.1 mm width); left untreated	100% (n = 10/10) during the first two weeks (3.2 ± 0.3 mm width)	33% (n = 3/9) one after one day, one after two weeks, and one after four weeks	Thinning of the wall composed of a thin layer of acellular fibrous tissue and loss of elastic lamellae and collagen
Tsumoto et al.[369] (2008)	Dog (CCA)	Surgical bifurcation (neck diameter 6.9 ± 1.5 mm) EJV graft (9.4 ± 1.1 mm width and 17.8 ± 1.1mm height) left untreated	100% (n = 5/5) continuous up to ten months (11.1 ± 1.9 mm width and 18.7 ± 1.3mm height)	No rupture	Not reported
Ding et al.[412] (2012)	Rabbit (CCA)	Surgical sidewall (arteriotomy 5 mm) EJV graft (4.3 ± 1.2 mm width and 4.3 ± 1.4 mm length); left untreated	100% (n = 6/6) within first three weeks (5.8 ±1.5 mm width and 6.1 ± 1.3 mm length)	No rupture	Not reported
Raymond et al.[144] (2012)	Swine (CCA)	Surgical sidewall (arteriotomy 4-6 mm and 5-7 mm) EJV graft (small: 7-8 mm x 11-17 mm and giant: 9 mm x 26mm); left untreated, lacking endothelium, or completely clipped	Not reported	100% (n = 7/7) of giant aneurysms 50% (n = 2/4) of small aneurysms with a small neck Fatal rupture day four, nonlethal within one week	Intraluminal unorganized thrombus in all ruptured aneurysm, many areas with loss of SMC and elastic fibers, inflammatory cells infiltrating the venous wall, hemorrhagic wall transformation
Marbacher et al.[IV] (2014)	Rat (AA)	Surgical sidewall (arteriotomy 2-2.5 mm) arterial thoracic graft (2.5 mm x 3.5-4 mm) left untreated or decellularized grafts	33% (n = 4/12) within the first week. Largest growth (43×38×24 mm) 10-fold size compared to baseline	25% (n =3/12) earliest rupture within eleven days after creation	strong adventitial inflammation, neutrophil infiltration and inflammatory cells in medial matrix, luminal thrombus with neutrophils

AA = abdominal aorta; CAP = coronary artery perforation; CCA = common carotid artery; EJV = external jugular vein; GDC = Guglielmi detachable coil; IEL = internal elastic lamina; SMC = smooth muscle cell.

3 Aims of the study

To develop animal models that more closely mimic human features of intracranial aneurysms:

I To demonstrate the feasibility of creating aneurysms with complex angioarchitecture by using the venous pouch bifurcation model in rabbits.

II To further evaluate the complex venous pouch bifurcation rabbit aneurysm model with regard to long-term patency rate.

III To present step-by-step procedural instructions of the Helsinki rat sidewall aneurysm model in order to provide a standardized model for different wall conditions.

To evaluate the influence of different aneurysm wall conditions on cicatrization and destructive wall remodeling:

IV To investigate the hypothesis that loss of mural cells leads to destructive remodeling, aneurysm growth and eventual rupture in a rat model.

V To determine the impact of mural cell loss on wall remodeling of thrombosed aneurysms and to assess the potential reversal of this process through transplantation of smooth muscle cells to the aneurysm lumen.

4 Material and methods

4.1 Microsurgical aneurysm models

4.1.1 Study designs, animals and anesthesia

4.1.1.1 Complex microsurgical aneurysm formation in rabbits

Adult female New Zealand rabbits were randomly assigned to three experimental groups. Complex angioarchitecture bilobular, bisaccular and broad-neck venous pouch aneurysms were microsurgically created at an artificially formed bifurcation of both CCA. Animals were followed up using 2D-DSA and CE-3D-MRA one week, one month and one year postoperative.

4.1.1.2 Microsurgical aneurysm formation in rats

After pilot series, three months old male Wistar rats were randomly allocated to experimental groups. Saccular aneurysms from syngeneic thoracic aortas were transplanted to the abdominal aorta. To study the natural course of sodium dodecyl sulfate (SDS) decellularized and non decellularized aneurysms, animals were followed up for one month using weekly CE-MRA. Endoscopy and histology of the aneurysms were used to assess the role of periadventitial environment, aneurysm wall and thrombus remodeling.

In the experiments aimed at studying the effect of thrombus formation on different wall conditions, animals were randomly assigned to three groups: Non-decellularized aneurysms, decellularized aneurysms, and decellularized but cell transplanted aneurysms. Thrombus induction was performed using fibrin glue (FG) biopolymer. Animals were followed up at a single time point at day three, week one and week three after creation. After interim analysis, a replication of experiments was performed for time point week one. Endoscopy, optical projection tomography, histology and immunohistochemistry were used to study the fate of transplanted cells, thrombus organization, collagen deposits and neointima formation.

4.1.2 Complex venous pouch bifurcation aneurysm model in rabbits

4.1.2.1 Perioperative and postoperative management

Prior to surgery, a single dose of amoxicillin (25mg/kg) is given intravenously. All surgical procedures are performed under sterile conditions and wounds are irrigated thoroughly with neomycin sulfate for infection prophylaxis. During microsurgical dissection of both CCAs, small arterial branches running medially as well as the superior laryngeal nerve are preserved. At the time of CCA clamping, animals receive 1000 IU heparin intravenously. The right CCA is cut as proximally as possible to obtain a long donor artery for a tensionless anastomosis. Thrombogenic adventitia is carefully removed from the anastomosis site. During the anastomosis procedure, the vessels are thoroughly and continuously rinsed with a mixture of heparinized and papaverinized saline. The suture lines at the aneurysm neck are covered with small pieces of fat tissue to enhance coagulation. Postoperatively, all animals received intravenous acetylsalicylic acid (10 mg/kg), intramuscular vitamin B12 and glucose infusion to compensate for dehydration during surgery. Low molecular weight heparin (250 IU/kg) is administered daily for 3 days. Oral acetylsalicylic acid is given daily, up to five weeks post-surgery.

4.1.2.2 Venous graft harvesting

Animals are fixed in supine position with their neck clipped and skin disinfected. A midline incision is made from the manubrium sterni to the angle of the jaw. The bifurcation or segments of the left external jugular vein serve as grafts for the creation of complex angioarchitecture aneurysms. All resected venous grafts are kept in a mixture of heparinized and papaverine saline. Before starting the anastomosis procedure, all vessels were extensively irrigated with heparinized saline and papaverine.

Venous graft preparation. For the creation of bilobular aneurysms, either the internal-external or transverse-external jugular vein bifurcation is ligated and then resected five millimeters proximal and distal to the bifurcation with 4-0 silk. For bisaccular aneurysms, two one-centimeter venous segments are resected and sutured together. Broad-necked aneurysms are formed using a one-centimeter long venous segment incised along the longitudinal axis, sutured together at both the proximal and distal ends and anatomized to the CCA bifurcation (**Figure 3**).

4.1.2.3 Surgical techniques of venous pouch aneurysm creation

CCA preparation. Approximately three to four centimeters of the left CCA is exposed just proximal to the carotid bifurcation. The right common carotid artery (RCCA) is isolated and mobilized as far distally and proximally as possible. The RCCA is temporarily clipped distally, ligated and cut as far proximally as possible. The exposed left common carotid artery (LCCA) segment is temporarily clipped using atraumatic clamps and elliptical arteriotomy is performed according to the size of the prepared complex venous pouch aneurysm.

Anastomosis procedure. The distal end of the right CCA is sutured to the back of the left CCA The venous pouch is then sutured to the back of the right CCA and anastomosed to the left CCA on the back side. The same procedures are performed on the front side. Before placement of the last frontal stitch, the right clip of the RCCA is removed to allow backflow into the aneurysm. After prompt filling and washout of trapped air and debris, the last suture is placed. The suture lines at the aneurysm neck are covered with small pieces of fat tissue to enhance coagulation

(**Video 1**). During the anastomosis procedure, the vessels were thoroughly and continuously rinsed with papaverine. The skin incision was closed with absorbable threads.

4.1.3 Saccular arterial sidewall aneurysm model in rats

4.1.3.1 Animal preparation and video recordings

All supplies are sterile and the procedure is performed in aseptic technique[198]. The rats are placed in a supine position with their front and hind paws immobilized with surgical tape without stretching or compressing the skin. The back is bent by placing a thick marker or cautery pen under the lumber region. It is important to obtain as much lumbar spine lordosis as possible in order to improve retroperitoneal exposure and access to the infrarenal aorta which facilitates microsurgical anastomosis.

A digital video camera attached to the was used to document preoperative aneurysm dimensions (width and length), microsurgical anastomosis procedures (total operating time, aortic clamping time, time for anastomosis creation, time to hemostasis, number of extra sutures, graft ischemia time and complications), patency and pulsation of the graft, patency of distal abdominal aorta and aneurysm harvest procedure including endoscopy at magnifications of 6x to 40x.

4.1.3.2 Arterial graft harvesting

The midventral abdominal wall is cut and the diaphragm identified just above the liver. The connective tissue is cut at the bottom of the diaphragm to access the rib cage. The thoracic cavity is opened by cuts through the ribs one centimeter left and right of the rib cage midline. The lungs are mobilized to the right side of the heart and the rats sacrificed by overdosing with intracardiac injection of ketamine hydrochloride.

The thoracic aorta is traced back from the dorsal wall of the thorax upwards to the aortic arch. A non-absorbable 6-0 silk ligature is placed just above the first intercostal artery leaving the aorta. The descending aorta is then cut just below the left subclavian artery and then below the ligature. The graft is trimmed to achieve perpendicular standardized aneurysm geometry and its width and length are measured. Untreated donor arterial grafts are immediately re-implanted to minimize potential ischemic damage to the vessel wall. Grafts to be decellularized are treated with SDS and stored at -4° Celsius until re-implantation.

Although it has been shown that spontaneous thrombosis in sidewall aneurysms can be significantly reduced using an “oblique cut of the aneurysm pouch”[415] and a minimized “volume-to-orifice area”[416], we decided to perform a standardized perpendicular long axis aneurysm creation in relation to the parent artery, and standardized aneurysm dimensions to avoid group differences in aneurysm hemodynamics and associated rate of thrombosis.

4.1.3.3 Surgical technique of saccular aneurysm formation

Dissection of the abdominal aorta. The abdominal cavity is opened via midventral cut just above the genitals and extended along the linea alba upwards to the xiphoid process. Small intestines and the prominent cecum are moved to the right or the left. The ligament in between the small intestine and the descending colon is cut in cranial direction to allow wider exposure of the dorsal body wall. A self-retractor is placed to hold the bowels apart. The abdominal aorta is dissected from adjacent large veins.

End to side anastomosis. Loose connective tissue and adventitia is removed at the level of the planed anastomosis site. The abdominal aorta is clamped to the anastomosis first distally, and then proximally. Eliptical arteriotomy, which had higher patency rate in both aortic and CCA sidewall aneurysm[417], is preferred over linear incision. The length of the arteriotomy is standardized to the width of the graft. Following arteriotomy, end to side suturing of the saccular graft is performed either with continuous or interrupted sutures. The first two sutures are placed at the proximal and distal end of the arteriotomy. If interrupted suturing is chosen then the back side nine o'clock suture is placed first. Subsequent sutures can be spaced starting adjacent to the very first suture. The same procedures are performed on the front side.

If continuous suturing is performed, dissection and pseudo aneurysm formation of the abdominal artery might be reduced by placing the first and final sutures at nine o'clock and three o'clock. Previous research suggested beginning and ending sutures along the lateral portion of the incision rather than the apices, avoiding having to place the final knots in a potentially weak area.[417]

Hemostasis and closure. After the end to side anastomosis, the site is rinsed with saline and the distal clamp removed first to allow for backflow. The proximal vascular clamp is then removed and patency confirmed by observation of volume increase of the aneurysm during peak arterial pulse wave and visual assessment of swirling blood within the aneurysm. Distal abdominal artery patency is assessed through the direct "milking test". Suture lines around the anastomosis can be covered with small pieces of adipose tissue or Spongostan for additional hemostasis if minor oozing is still present. A detailed description is provided in **Video 2**.

Figure 3. Complex venous pouch bifurcation aneurysm.

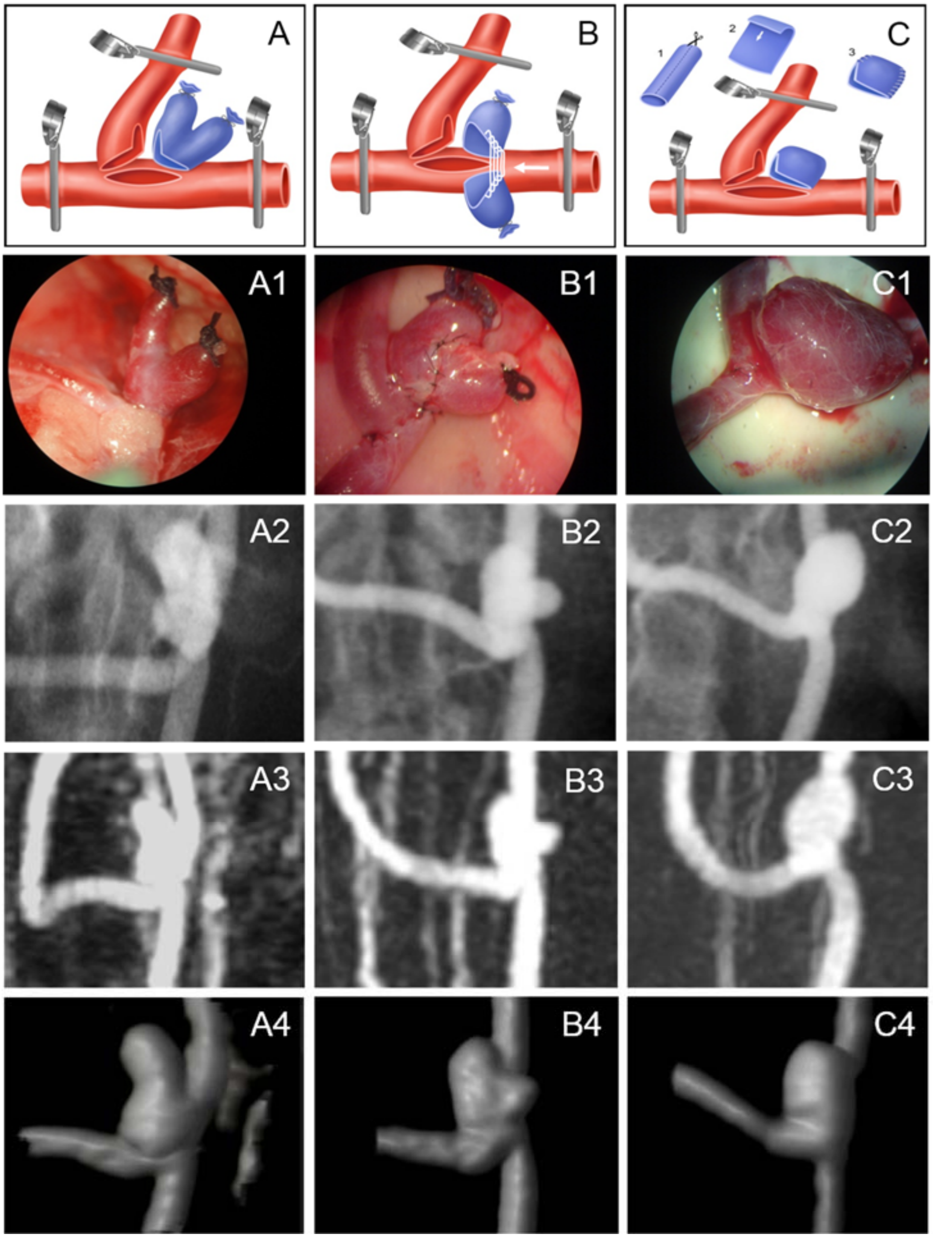

Surgical steps (**A-C**), intraoperative photographs (**A1-C1**), 2D-DSA (**A2-C2**), CE-3D-MRA (**A3-C3**), and surface rendered 3D-reconstructions (A4-C4). **A**, bilobular: vein bifurcation stump; **B**, bisaccular: two venous pouches sutured together (white arrow); **C**, broad-neck: vein incised longitudinally (1), folded along its transverse axis (2), and sutured together proximally and distally (3).

4.2 Imaging modalities

4.2.1 Macroscopic and endoscopic inspection

After final follow-up MRA, the animals underwent laparotomy and dissection of the aneurysm (**Video 3**). The tissues were perfusion-fixed with 4% paraformaldehyde (PFA) in phosphate buffered saline (PBS) and measured in all dimensions. The posterior wall of the aorta was opened and evaluated by macro- and endoscopic intraluminal aneurysm surface inspection. Neointima formation was graded as described previously with slight modification.[418] Analysis of neointima formation based on at least one macro- and endoscopic video screenshot was performed blinded, by two observers (**Video 4**).

4.2.2 Magnetic resonance imaging

4.2.2.1 CE-3D-MRA in rabbits

Animals underwent CE-3D-MRA using a 1.5 T scanner Magnetom Avanto Syngo B17 (Siemens Medical Solutions, Erlangen, Germany). T2-weighted fast spin-echo and 3D time-of-flight MRA (3D-TOF-MRA) gradient-echo sequences were performed. After manual bolus injection of Gadovist® (0.1 ml/kg) CE-3D-MRA was performed using T1-weighted 3D fast-spoiled gradient-echo. Three-dimensional aneurysm reconstructions were performed using the Philips ViewForum Workstation (**Video 5**).

4.2.2.2 MRI and CE-MRA in rats

MRA studies were performed with a 4.7 T scanner. Existing protocols for high resolution TOF-MRA[419] were combined with contrast enhanced angiography. All animals underwent high-resolution imaging postoperatively and at final follow-up as defined by the respective group, to evaluate contrast enhancement, flow characteristics, parent vessel integrity, perianeurysmal environment, changes in aneurysm volume, extent of spontaneous thrombosis and recanalization.

After shimming and scout images, a three-dimensional fast low-angle shot sequence (3D-FLASH) was acquired. Afterwards, a 3D-FLASH with short imaging time was performed. At that time, the animals received a bolus injection of Gd-DOTA (1 ml/kg body weight, intravenously, injection time < 3 s) and the 3D-FLASH with short imaging time (CE-MRA) was repeated twice without delay between the scans (late CE-MRA). In total, MR imaging took approximately 30 minutes **(Figure 4).**

4.2.3 Digital subtraction angiography

The rabbit's left or right femoral artery was microsurgically exposed and cannulated using a straight 5.5 French vascular sheath. The sheath was introduced in retrograde manner and fixed distally. Images were obtained by rapid sequential 2D-

DSA at two frames per second using a small focal spot at 66 kV and 125 mA. Anteroposterior and lateral views were obtained. Intra-arterial bolus injection of non-ionic iopamidol (0.6 ml/kg) as contrast agent was administered at a rate of approximately 3 ml/s.

4.2.4 Morphometric measurements

4.2.4.1 Aneurysm volume on 2D-DSA and CE-3D-MRA

Measurements on 2D-DSA images, including aneurysm dome (length and width) and aneurysm neck, were performed using standardized software installed in the DSA equipment and referencing an external sizing device.

The same aneurysm characteristics were measured in CE-3D-MRA's using the best three-dimensional projections which included parent vessel and all dimensions of the created aneurysm. To assess morphologic features, each aneurysm was measured three times in a blinded fashion using the automatic measurement tool of ImagePro Discovery® analysis software. The volume of the aneurysm was calculated approximately using a cylindrical volume formula: aneurysm volume = 3.14 x (width/2)2 x length[420]. Three-dimensional visualization of the direction of the orifice and aneurysm lobes was performed using the surface rendering mode of the Philips View Forum Workstation.

4.2.4.2 Aneurysm patency, recurrence and growth on CE-MRA

CE-MRA were analyzed and scored according to a schema previously used to evaluate spontaneous thrombosis of experimental sidewall aneurysms in dogs.[415] Aneurysm patency was categorized on contrast filling in the aneurysms axial dimension as patent (> 50%), partially thrombosed (< 50%), or completely thrombosed (no aneurysm filling).

Accordingly, aneurysm recurrence was categorized as: 0 = no recurrence (no filling); 1 = partial recurrence (< 50%); and 2 = complete recurrence (> 50%). Growing aneurysms were further analyzed using 3D active contour segmentation software itk-SNAP (**Figure 5**).[421]

4.2.5 Optical projection tomography

4.2.5.1 In vivo FITC-lectin perfusion and tissue processing

On day 0, 3, and 7 following cell transplantation, 200ul Fluorescein isothiocyanate (FITC)-conjugated Lycopersicon esculentum (tomato) lectin diluted in 200µl PBS was injected to the femoral vein and allowed to circulate for 5 min. Rats were kept on a warm heating block after injection prior to euthanization through a lethal dose of xylazine-ketamine. Intracardiac perfusion-fixation was carried out at room temperature with PBS followed by 4% PFA in PBS.

The specimens were removed from the abdominal cavity, immersed in 4% paraformaldehyde at 4°C overnight and embedded in 1% low-melt agarose. The samples were mounted on rotary stages, dehydrated in 75% methanol, and subsequently cleared using a 1:2 mixture of benzyl alcohol and benzyl benzoate over a 72-hour period.

4.2.5.2 Data acquisition and visualization

Optical projection tomography was applied to scan the aneurysms stepwise at 0.9 degrees, resulting in 400 images of projection data over one complete revolution. Images were taken with the following filters: WL (white light; visualization of suture material – assigned color white), green fluorescent protein (GFP)1; visualization of fibrin biopolymer – assigned color yellow, GFP+, FITC-lectin; visualization of vessel wall – assigned color blue and Standard Texas Red (TXR); CM-Dil; visualization of transplanted cells – assigned color red.

Post-alignment was carried out on a minimum of three levels through the specimen and image stacks were reconstructed and three-dimensional volumetric representations visualized in a Bioptonics viewer. Automated object detection (transplanted cells and vessel wall) and isosurface rendering in maximal intensity projections was performed to create 3D animations using Imaris 7 image processing software (**Videos 6-8**).

Figure 4. MRI studies in the rat.

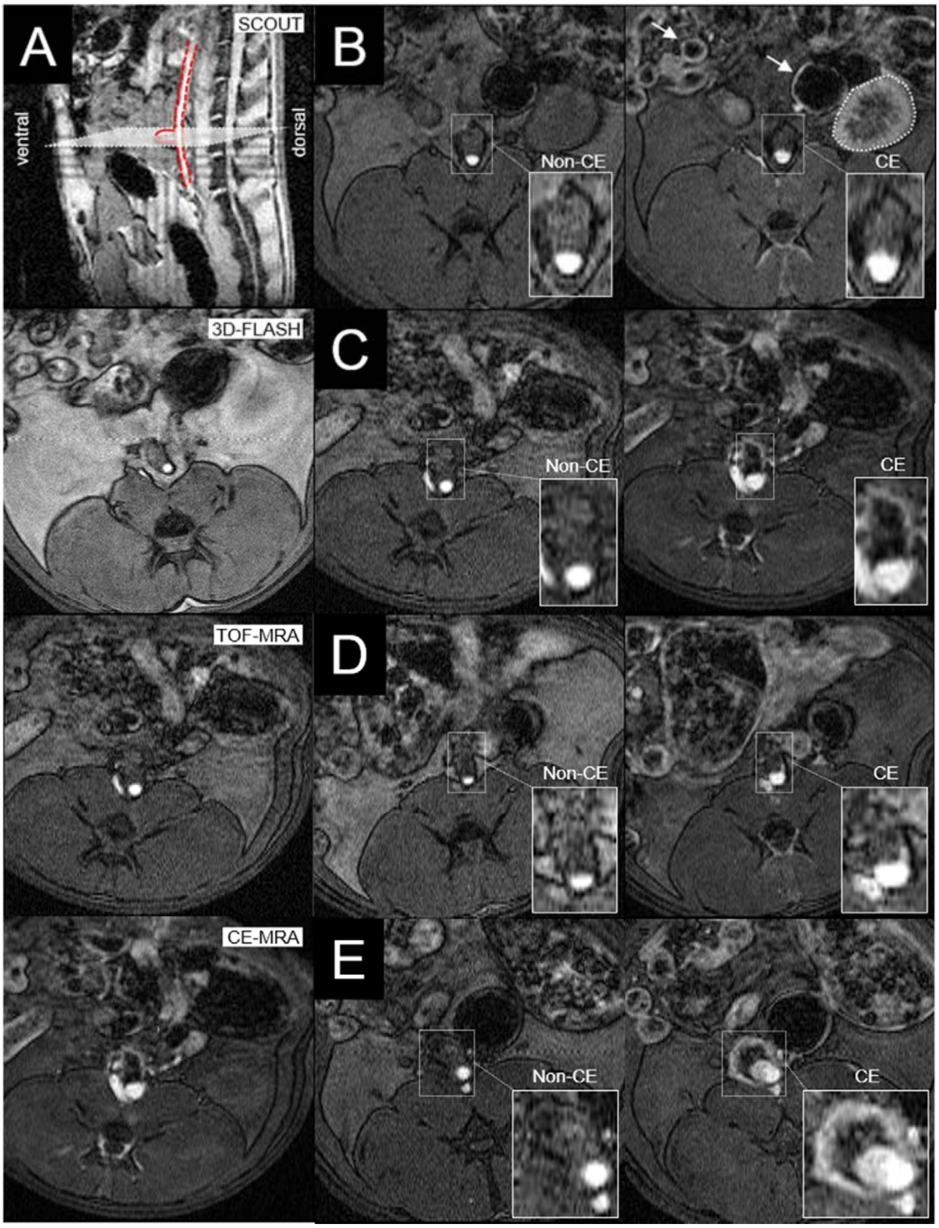

A, a sagittal scout was used to determine the field of view for subsequent 3D-FLASH images (anatomical overview), TOF-MRA, and CE-MRA. **B**, no enhancement of the aneurysm wall. Bowels (arrow) and the kidney (dashed line) demonstrate enhancement after contrast injection. **C**, aneurysm wall enhancement. **D**, minor aneurysm recurrence. **E**, major recurrence and aneurysm wall enhancement.

Figure 5. ITK-SNAP 3D active contour segmentation.

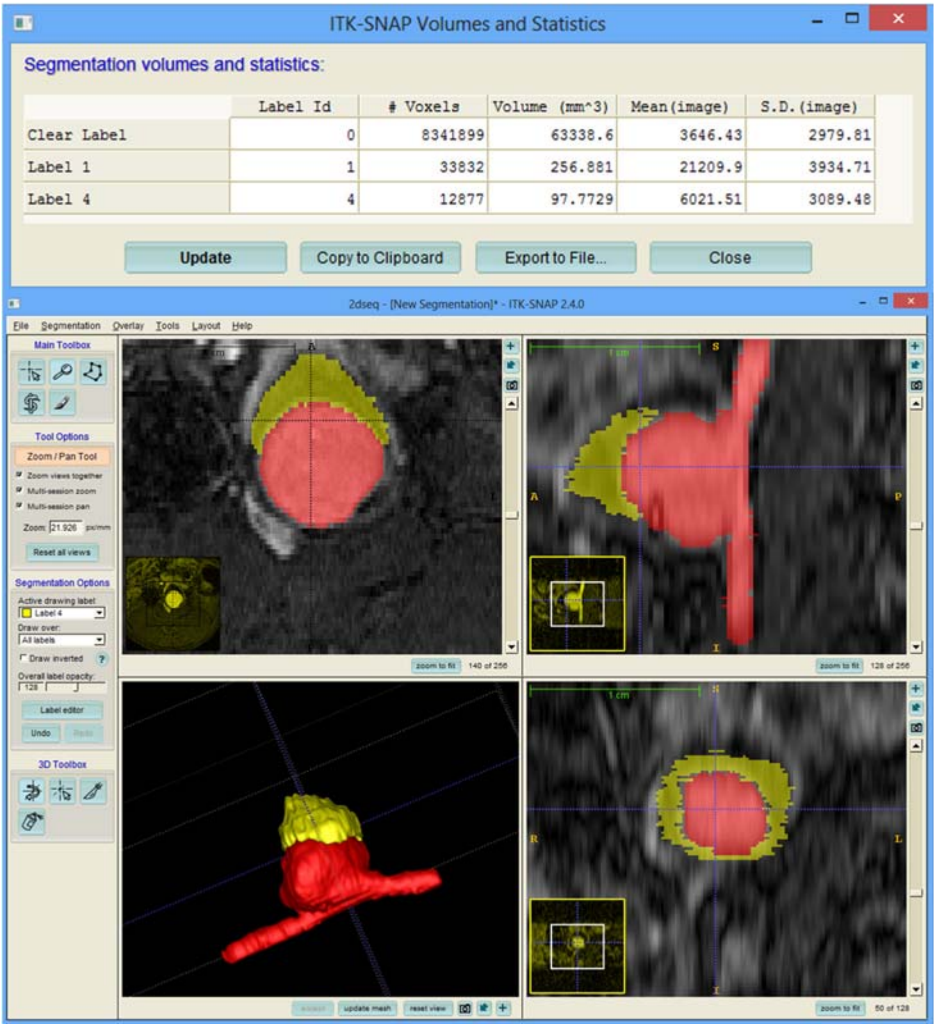

Screenshots of segmentation volume calculation, axial, sagittal and coronal clipping planes and 3D visualization. Anatomical structures of the aneurysm were delineated and extracted using the semi-automated segmentation tool (snake evolution) provided by ITK-SNAP. In each plane, closed curves are placed in regions of interest (ROI; contrast enhanced vessels). In relation to image intensities, the closed curve adjusts to take on the shape of the ROI. Single objects were created using the contour stack function and isosurface rendering. The volume of objects was calculated by adding up the contour areas.

4.3 Tissue processing and cell cultures

4.3.1 Graft decellularization

4.3.1.1 Physical decellularization method

Ex-vivo pilot series using various ischemia periods at four degrees Celsius (4 °C) and room temperature (RT) were performed in combination with multiple freeze-thaw cycles and centrifugation to assess physical decellularization. Detailed description of blinded counting of numbers of cell nuclei in random vessel walls of different decellularization methods at various time points is given in **Figure 6**.

4.3.1.2 Chemical decellularization method

To minimize SDS incubation time and consequent ECM disruption, the original description of rat abdominal aorta decellularization by Allaire et al. was adopted with slight modifications.[422] Donor grafts were harvested and frozen in PBS at -4 °C. The grafts were thawed the next day, rinsed with Milli-Q® water at room temperature and incubated for ten hours at 37 °C in 0.1% SDS in Milli-Q® water. The SDS-treated grafts were subsequently washed three times with gentle agitation, refrozen in PBS and kept at -4 °C until use. To assess the adapted decellularization process, thoracic aorta segments of four rats were harvested and assigned to various SDS incubation times (3h, 6h, 10h and 15h).

4.3.2 Cell culture, labeling, and immunofluorescence

4.3.2.1 Primary cell culture

Primary cell culture cells were obtained by the explant and enzymatic digestion method. A one-to-two centimeter abdominal aortic segment was excised and cleaned of fat tissue with sterile forceps and micro scissors, washed with PBS, transferred to warm Dulbeco's Modified Eagle's Medium, rinsed and cut into approximately 1 mm^2 squares. The tissue pieces underwent trypsin digestion for 20 minutes at 37 °C followed by incubation in fetal bovine serum for 15 min. After centrifugation, the supernatant was discarded and the tissue evenly distributed in a 6-well cell culture cluster containing Dulbeco's modified Eagle's medium (DMEM), supplemented with 10% fetal bovine serum (FBS) and a Penicillin (500 U/mL)-Streptomycin (5mg/ml)-L-Glutamine (5mM) solution. The primary cell cultures were passaged initially at a ratio of 1:2 when the cells became confluent. Cells were maintained in 25 and 75 cm^2 tissue culture flasks and underwent 6-10 passages before transplantation. Cells were labeled using a carbocyanine lipid cell membrane tracer and homogenously suspended in thrombin solution in a concentration of 1 x 10^6 cells/ml which was then mixed with the fibrinogen component to form a clot. The switch from the contractile to the synthetic smooth muscle cell phenotype was confirmed by immunostaining to cytoplasmic smooth muscle actin and vimentin (**Figure 7A**).

4.3.2.2 CM-Dil cell-labeling

The numbers of live cells obtained after trypsination were counted before labeling. In a typical experiment the percentage of dead cells did not exceed 1 - 2%. The cells were labeled by incubation in 1ml of 10µM 1,1-dioctadecyl-3,3,3,3-tetramethylindocarbocyanine perchlorate solution for five minutes at 37 °C and for another 15 minutes at 4 °C. After labeling, the cells were washed in PBS, centrifuged and homogenously re-suspended in the thrombin solution at a concentration of 1 x 10^6 cells/ml, followed by mixing with the fibrinogen component to form a clot. To determine the intensity of the fluorescence labeling ~50,000 cells of each sample were Cellspin mounted onto slides and analyzed using an Axiovision fluorescence microscope (Carl Zeiss). The nuclei were counterstained with 4',6-diamindino-2-phenylindole (DAPI) (**Figure 7B**).

4.3.2.3 Immunofluorescence in cell culture

Quantification of differentiation of smooth muscle cells into smooth muscle cells of synthetic phenotype was assessed by cell culture staining for smooth muscle actin and vimentin and viewed with fluorescence microscopy (Axiovision, Carl Zeiss) at 20x magnification. For immunocytochemical staining, the cells were cultured on coverslips until confluency, fixed with 4% PFA and permeabilized with 0.1% Triton X-100. Fixed cells were stained with antibodies against human smooth muscle actin and vimentin. Secondary antibodies were Cy3-conjugated donkey anti-mouse IgG and FITC-conjugated donkey anti-rabbit IgG. The nuclei were counterstained with DAPI. Cells were imaged using fluorescence confocal microscopy in multichannel scanning at 10x and 40x magnification. Negative control for staining was performed with species-matching unspecific antibody (**Figure 7C**).

4.3.3 Histology and histological analysis

4.3.3.1 Sample preparation and visualization

Aneurysms embedded in paraffin blocks were cut in the middle along the longitudinal axis and into consecutive 4 µm sections for hematoxylin-eosin, elastica van Gieson's, Masson-Goldner's trichrome and Prussian blue staining (**Figure 8**). All histological slides underwent qualitative analysis by two observers. Histological scoring was performed blinded to the treatment allocation. Slides were visualized under light and fluorescence microscope and post processed using Adobe Photoshop CS 6 -and Image J 1.47e (National Institutes of Health, Bethesda, MD, USA) software.[423]

Fluorescent images were examined to determine the fate of transplanted CM-Dil labeled smooth muscle cells: ingrowth in luminal thrombosis and organization of thrombosis and fibrin glue, neointima formation, infiltration of the adventitia, ingrowth in periadventitial environment, migration to the parent artery and CM-Dil uptake by macrophage cells. Detailed evaluation of periadventitial environment, aneurysm wall structure and endoluminal thrombus was performed on hematoxylin-eosin and elastica van Gieson's stain.

4.3.3.2 Quantitation of histology

The following characteristics were assessed and scored as follows (**Figure 9**): Periadventitial inflammation (0 = none, 1 = mild, 2 = moderate, 3 = severe), periadventitial fibrosis (0 = none, 1 = mild, 2 = moderate, 3 = severe), aneurysm wall inflammation (0 = none, 1 = few (1-3) spots, 2 = many (>4) spots, 3 = ubiquitous), aneurysm wall hematoma (0 = none, 1 = few (1-3) spots, 2 = many (>4) spots, 3 = ubiquitous), aneurysm wall cellularity (0 = none, 1 = few (1-3) spots, 2 = many (>4) spots, 3 = ubiquitous), aneurysm wall dissection (0 = none, 1 = few (1-3) spots, 2 = many (>4) spots, 3 = ubiquitous), endothelial cellularity (0 = none, 1 = few (1-3) spots, 2 = many (>4) spots, 3 = ubiquitous), luminal thrombus (0 = absent, 1 = present), neutrophils in the thrombus (0 = none, 1 = mild, 2 = moderate, 3 = severe) and neointima formation (0 = none, 1 = organizing thrombus, 2 = organizing thrombus and neointima formation, 3 = mature neointima). Scores were dichotomized as (1) none/mild and moderate/severe, (2) no/few cells and focal hypocellularity/normal cell count, and (3) no neointima/organizing thrombus and organizing neointima/mature neointima.

Figure 6. Cell count in decellularized walls.

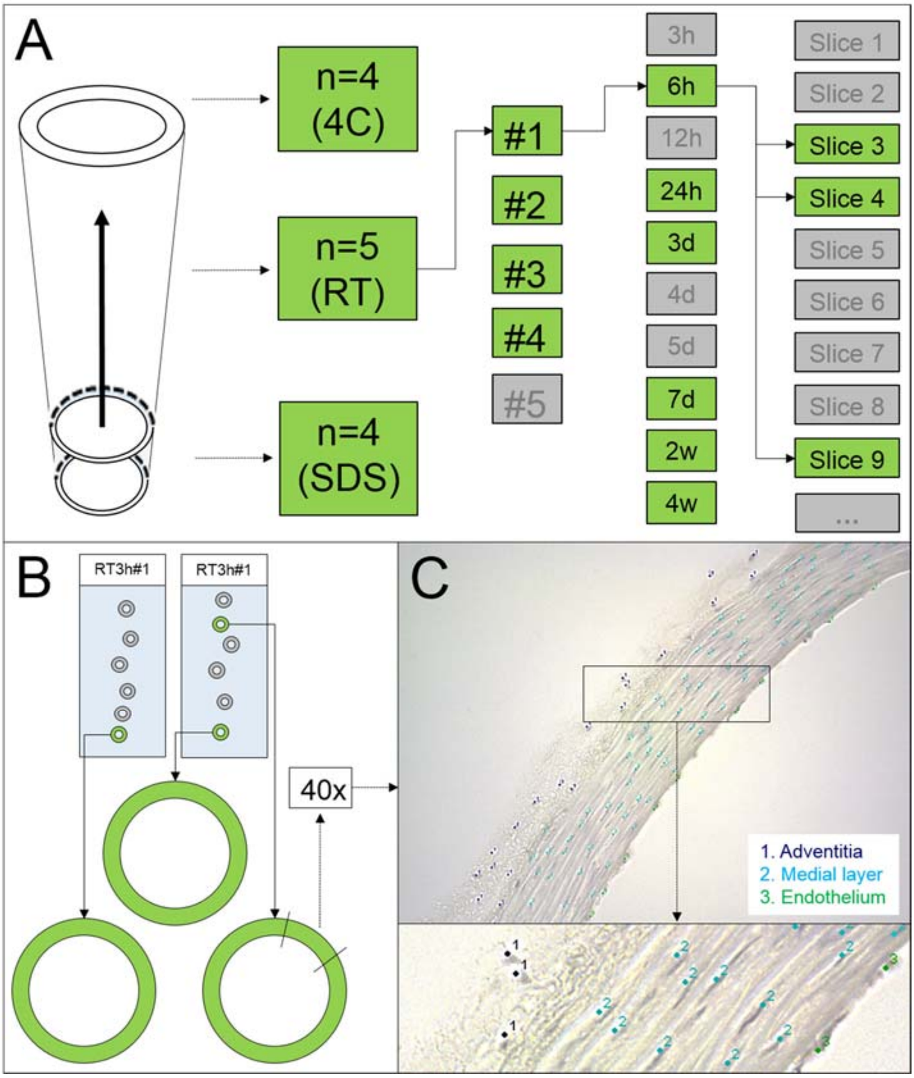

A, thoracic aorta segments were harvested and cell counts assessed over time (serial specimens in the same specimen at 3h, 6h, 12h, 24h, 3d, 4d, 5d, 7d, 1w, 2w, 4w). **B**, at each time point, three histological slides with four to six vessel cross sections were stained and hematoxylin positive cells counted in a random field of view at 6h, 24h, 3d, 7d, 2w and 4w. **C**, digitalized microphotographs of three vessel cross sections were taken at 40x magnification, blinded and analyzed separately for each vessel wall layer (adventitia, medial layer, and endothelium) using ImageJ software. RT = room temperature. SDS = sodium dodecyl sulfate.

Figure 7. Cell culture staining and labeling.

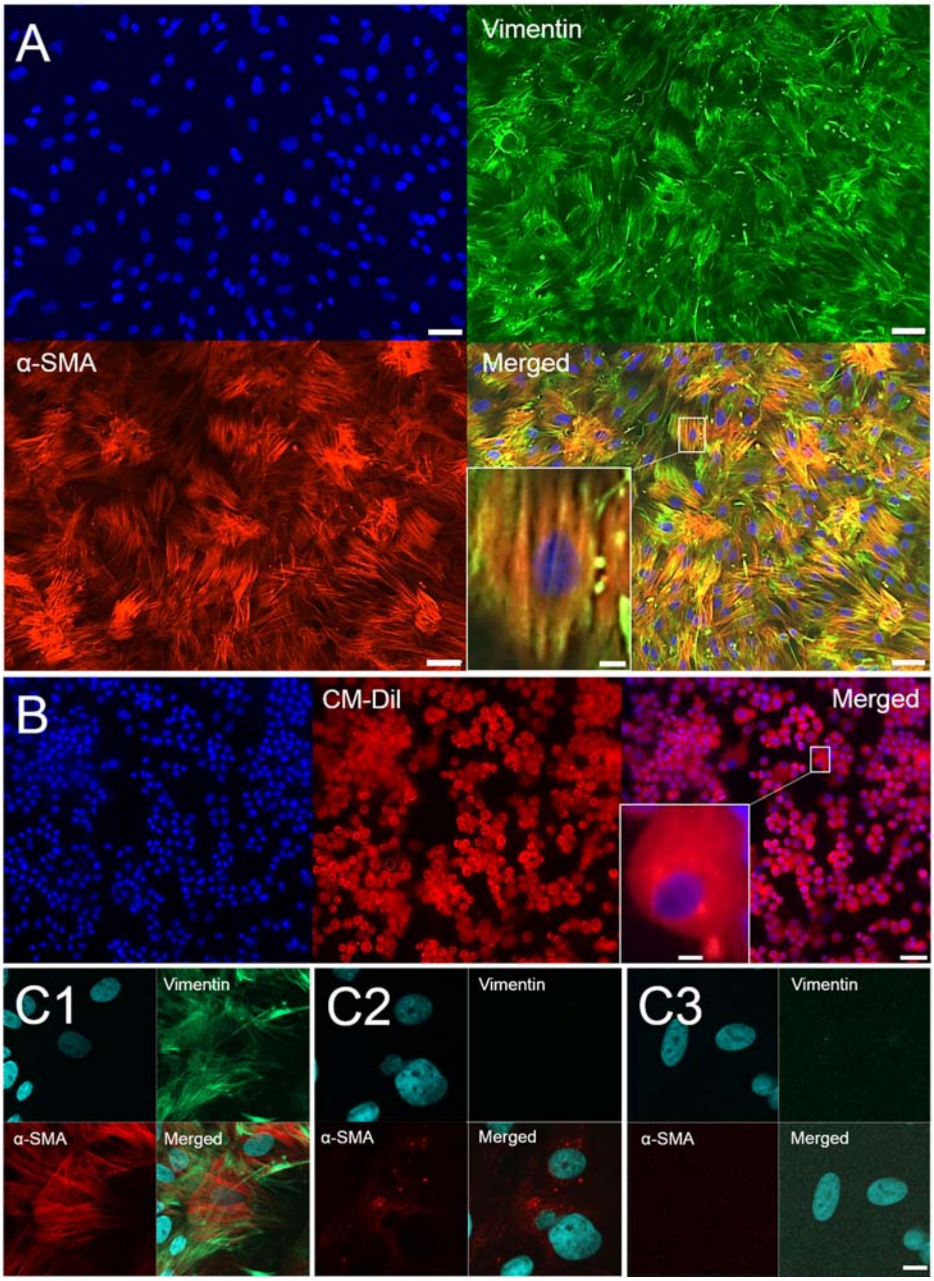

A, Double-labeled cells taken from cell culture indicating differentiation into SMCs of synthetic phenotype. **B**, Cellspin mounted samples of CM-Dil stained cells. **C1**, Concfocal microscopy of immunostaining for α-SMA and vimentin filaments confirmed phenotype change. **C2**, negative controls in unlabelled and CM-Dil-labeled (**C3**) cell cultures. 20x (A, B) and 40x (C) magnification. Scale bar = 50 µm (A, B); 10 µm (Inlet, C). α-SMA = α-smooth muscle actin.

Figure 8. Light microscope staining.

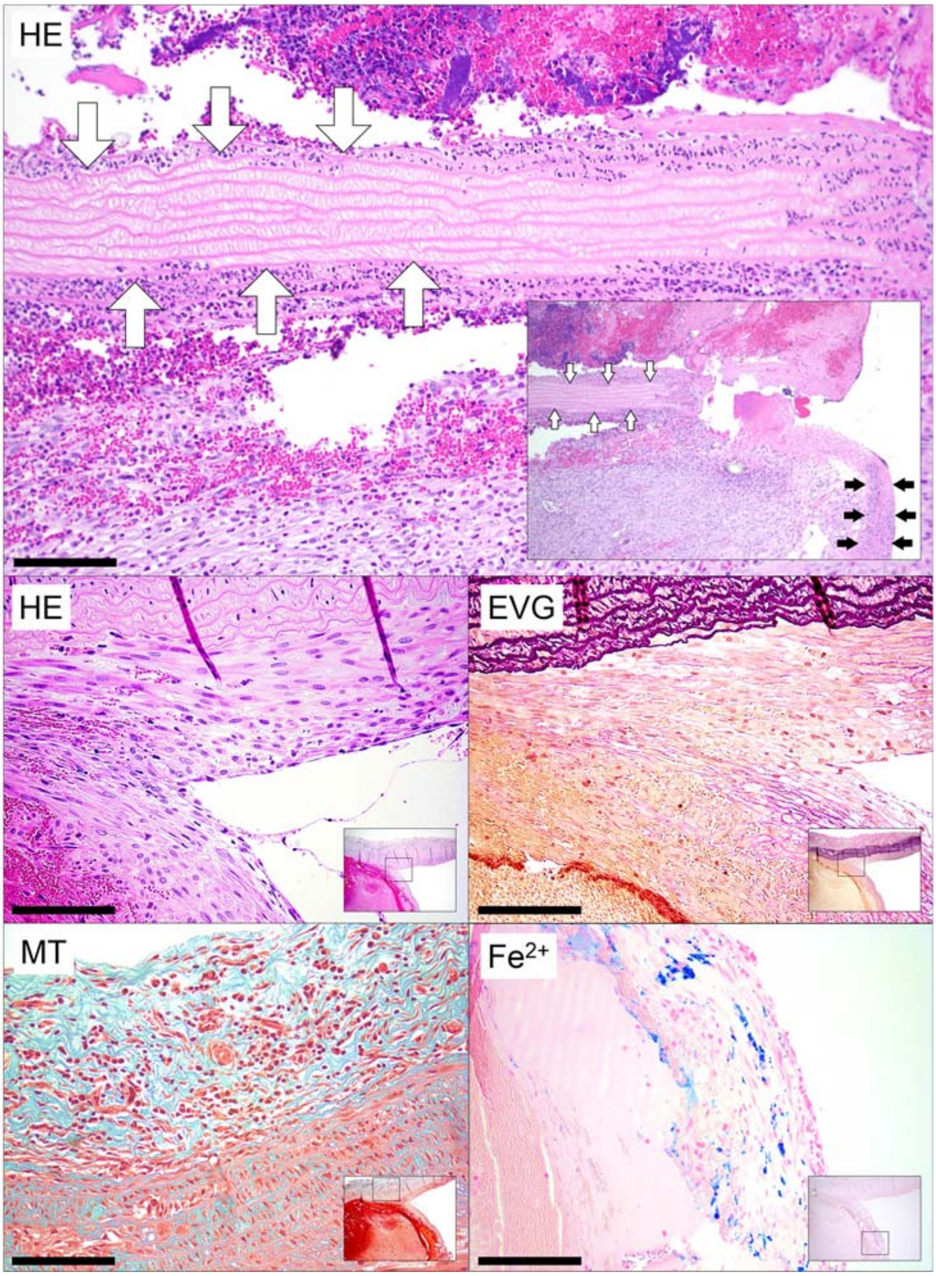

Overview: Decellularized aneurysm wall (white arrows) and healthy parent artery (black arrows). **HE**: Cell morphology; **EVG**: Connective tissue (violet). **MT**: Collagen (greenish blue). **FE2+**: Iron and hemosiderin (azure). Large panel 10x magnification, scale bar = 50 µm; Small panels 20x magnification, scale bar = 100 µm; Inlets 5x magnification.

Figure 9. Histological characteristics.

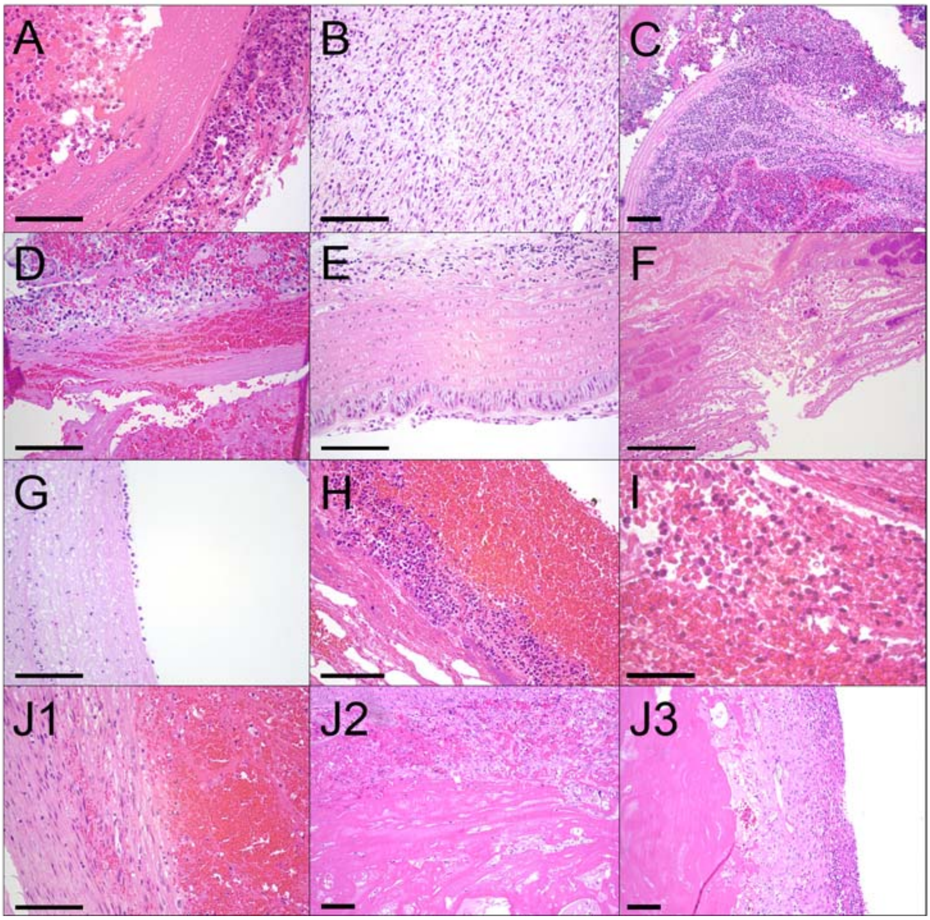

A, Periadventitial inflammation (strong adventitial inflammation); 20x magnification; scale bar = 100 µm. **B**, periadventitial fibrosis (severe fibrosis); 20x magnification; scale bar = 100 µm. **C**, aneurysm wall inflammation (ubiquitous inflammation); 10x magnification; Scale bar = 50 µm. **D**, aneurysm wall hematoma (ubiquitous); 20x magnification; scale bar = 100 µm. **E**, aneurysm wall cellularity (many spots); 20x magnification; scale bar = 100 µm. **F**, aneurysm wall dissection (ubiquitous); 20x magnification; scale bar = 100 µm. **G**, endothelial cellularity (none; neutrophils attached to the surface); 20x magnification; scale bar = 100 µm. **H**, luminal thrombus (present); 20x magnification; scale bar = 100 µm. **I**, neutrophils in the thrombus (severe inflammation); 40x magnification, oil; Scale bar = 50 µm. **J1**, unorganized thrombus; 20x magnification; scale bar = 100 µm. **J2**, thrombus and neointima formation; 10x magnification; Scale bar = 50 µm. **J3**, mature neointima; 10x magnification; Scale bar = 50 µm. All specimens are stained with HE.

4.4 Statistics

Two-tailed Fisher`s exact test was used for comparison of dichotomized histological grades, aneurysm growth, and rate of thrombosis between decellularized and non decellularized groups and growing and stable aneurysms, respectively. Two-tailed Student t-test was performed to assess differences in surgical characteristics of the sidewall aneurysm model and to evaluate differences between one-month and twelve-month morphometric measurements of complex bifurcation aneurysms. Data were analyzed and visualized using Graph Pad Prism statistical software V6.01 for Windows. Values are expressed as mean ± standard deviation (SD) and 95% confidence interval (CI). A probability value of less than 0.05 was considered statistically significant.

5 Results and Discussion

5.1 Microsurgical complex bifurcation aneurysms in rabbits

5.1.1 Surgical and neuroradiological findings

5.1.1.1 Mortality, morbidity, and surgical characteristics

Perioperative and one-month postoperative mortality and morbidity was 0% and 9% respectively.[I] One year follow-up mortality and morbidity increased to 18% and 24% for complications related to long-term housing.[I, II] Strict adherence to elaborated perioperative and postoperative management is needed to achieve such low rates of mortality and morbidity.[424, 425]

Despite relatively long operation times of approximate 2.5 hours[I, II], the mean clamping time of both CCA's did not exceed one hour, which is comparable to conventional surgical aneurysm creation.[426, 427] This indicates that it is not the anastomosis procedure itself but rather the harvest and creation of the venous graft/pouch that requires additional operation time. This may also explain why the complication rate did not rise despite an increase in overall operation time.

5.1.1.2 Aneurysm volume changes over time

There were no significant differences in aneurysm volume or parent artery configuration over the period of one year [II]. Volume of complexly shaped aneurysms is far larger than those in conventional berry-shaped venous pouch bifurcation aneurysms (< 100 mm^3)[428] or elastase-induced aneurysms (~ 30–100mm^3).[420]

It has been shown that elastase-induced[410], bifurcation aneurysms[369] and side-wall aneurysms[412] enlarge during the first weeks after creation. The most impressive growth has been documented in a rat venous pouch bifurcation model, with an increase of 145% in aneurysm size over a three-month period (SD=30%).[429] While some aneurysms from the presented series demonstrated an increase in volume, others decreased in volume by the one year follow-up. Aneurysm shrinking in absence of thrombosis can likely be explained by remodeling processes.[380] These remodeling processes provoked criticism of the microsurgical venous pouch model until recent studies demonstrated that a significant number of ruptured, and especially unruptured human aneurysms, do contain intimal thickening and inflammatory cell infiltration, therefore supporting the use of the model.[112, 140]

5.1.1.3 Patency rate and antithrombotic regimen

One month aneurysm and parent vessel patency was over 90% in both series.[I, II] Overall long-term follow-up of all three groups together revealed a patency rate of 86% with only one complete and one partial occlusion in bisaccular aneurysms.[II] Bilobular, bisaccular and broad-neck aneurysms represent different hemodynamic features. In future studies the three different shapes should be evaluated separately.

Previous studies report small numbers of early spontaneous thrombosis and stable long-term patency. More recent publication with large case numbers (224 canine and 40 rabbit sidewall vein pouch aneurysms) and excellent short term patency rates of 99.5%[430] and 95%[412] stand in contrast to the smaller series with more frequently reported early spontaneous thrombosis.[367, 368, 431] We assume that initial aggressive anticoagulation is important to protect the anastomotic complex from early thrombosis until endothelialization inhibits extrinsic activation of the coagulation system.[149]

However, especially when considering the reported excellent patency rates in very experienced hands[412, 430], it remains unknown whether other factors such as extensive microsurgical training[426, 427] and associated technical factors (suture line, badly placed sutures, or constricted neck of the aneurysm)[391, 431], shape of arteriotomy[13], aneurysm volume-to-neck ratio[28], number of sutures, tensionless anastomosis and perioperative and post-operative management (compensation for fluid loss, pain management, antibiotics, vitamin complexes) are as important as anticoagulation in preventing thrombosis.[426] Interestingly, in our series parent vessel and aneurysm thrombosis occurred only in the group with the greatest number of sutures (bisaccular aneurysms).[I, II]

Only a control study (one group with extended anti-coagulation, another only with anti-coagulation at the day of surgery) could answer the question of whether initial aggressive one month anticoagulation is necessary. The present study confirms that strict adherence to the mentioned measures prevents extensive early spontaneous thrombosis. The results further demonstrate that long-term patency can be achieved in absence of ongoing anticoagulation.

5.1.2 In vivo animal testing of human endovascular devices

Nowadays, the range of cerebral aneurysms found to be suitable for endovascular treatment is steadily increasing in the clinical setting. Nevertheless, the incidence of recanalization and recurrent aneurysms after endovascular treatment must be considered as a limitation of these techniques. The complexity and difficulty of cases demand further development of endovascular technology. The various angioarchitecture of the experimental aneurysm formations presented here offer a promising tool for in vivo animal testing of human devices in true bifurcation hemodynamics, and provide a valuable training opportunity for neurointerventional radiologists and endovascular neurosurgeons.

5.2 Microsurgical arterial sidewall aneurysms in rats

5.2.1 Mortality, morbidity and surgical characteristics

Anesthesia-related death occurred in five rats. Further non anesthesia related mortality was: two animals died during pilot transvascular embolization attempts, five animals deceased due to either proximal or distal dissection of the aorta with or without pseudoaneurysm formation, four rats died due to massive intra-abdominal bleeding from a ruptured enlarged aneurysm, one animal died due to thrombosis of the parent artery, one animal died due to abdominal cavity infection and in three animals the cause of death remained unclear due to delayed autopsy (>12h post-mortem). One animal was euthanized after occurrence of bilateral femoral artery thrombosis on day one after surgery. Key steps of the model and related surgical characteristics are given in **Figure 10**.[III]

5.2.1.1 Fast, simple and affordable

The basic principles of the rat aneurysm model can be mastered in a short period of time. An introductory course in rodent microsurgery is recommended for those researchers inexperienced in performing dissections and suture techniques under an operating microscope. An average total operation time of less than 60 minutes for microsurgical creation of a sidewall aneurysm in rats is much shorter than that needed for creation of more complex microsurgical venous pouch arterial bifurcation aneurysm in rabbits and dogs.[130, 432] Small animals such as the rat are inherently associated with lower experiment and housing costs and the reduced need for specialized equipment.

The advantages of low costs and faster methods of aneurysm creation may facilitate conduction of studies with larger number of experiments and subsequent increased statistical power. In addition, the rodent arterial sidewall aneurysm model has been successfully implemented to answer research questions requiring more sophisticated laboratory methodology, including transgenic animals.[140, 433]

5.2.1.2 The study of endovascular devices and aneurysm biology

Experimental models for saccular aneurysms are needed to study the biology of arterial aneurysms and for the testing of novel therapeutic devices and strategies. For these purposes, several different models in different species have been developed and published.[382] Larger aneurysm models in pigs, dogs and rabbits are preferred to test endovascular innovations in complex aneurysm architecture.[382, 432] Murine aneurysm models, on the other hand, allow research in genetically modified species.[140, 433] and facilitate clarification of aneurysm biology at cellular and molecular levels far better than larger species.[382] The model presented has been successfully implemented to answer research questions needing more sophisticated laboratory methodology, including transgenic animals.[140, 433]

Although endovascular trans-carotid and trans-iliac device deployment is limited to bigger rats (>400-500g) and to stents smaller than 2.0 mm and 1.5 mm in diameter[434], stents can also be placed through direct insertion into the abdominal aortic segment harboring the experimental aneurysms.[267, 419] Previous work using the rat microsurgical abdominal aortic sidewall aneurysm model demonstrated its feasibility in testing platinum- and polyglycolic-polylactic acid- coated coils.[267]

5.2.1.3 Robust, standardized model for multicenter preclinical trials

Preclinical trials should ideally be performed with the same standardized model in various institutions and labs, in order to allow better comparison of data, devices and treatments. To date, there are no guidelines for standardized testing of endovascular devices prior to clinical application and animal models remain underused.[382] Most of the proposed novel treatment modalities are single-center cases that lack validation and replication. Standardized models will gain importance once multicenter randomized preclinical trials also emerge in this field of research. The model presented is the most standardized and inexpensive one currently available and is of great interest to those working on the development of treatments for intracranial aneurysms, or in the field of vascular neurosurgery and neuroradiological interventions in general.

Microsurgical sidewall aneurysm creation in rodents allows standardization of graft origin, volume-to-orifice ratio and parent vessel to aneurysm long axis angle. The presented technique resulted in standardized aneurysms with minimal variation in aneurysm dimension, location and relation to the parent artery. Previous experiments revealed high overall patency rates of 92.5% at a median follow-up of six weeks after creation.[140, 267, 419] With the exception of a single case, significant growth or dilatation of native experimental aneurysms was not observed and none of the aneurysms ruptured during median follow-up of 6 weeks (range 3 days – 2 years).[140]

Figure 10. Saccular arterial sidewall aneurysm.

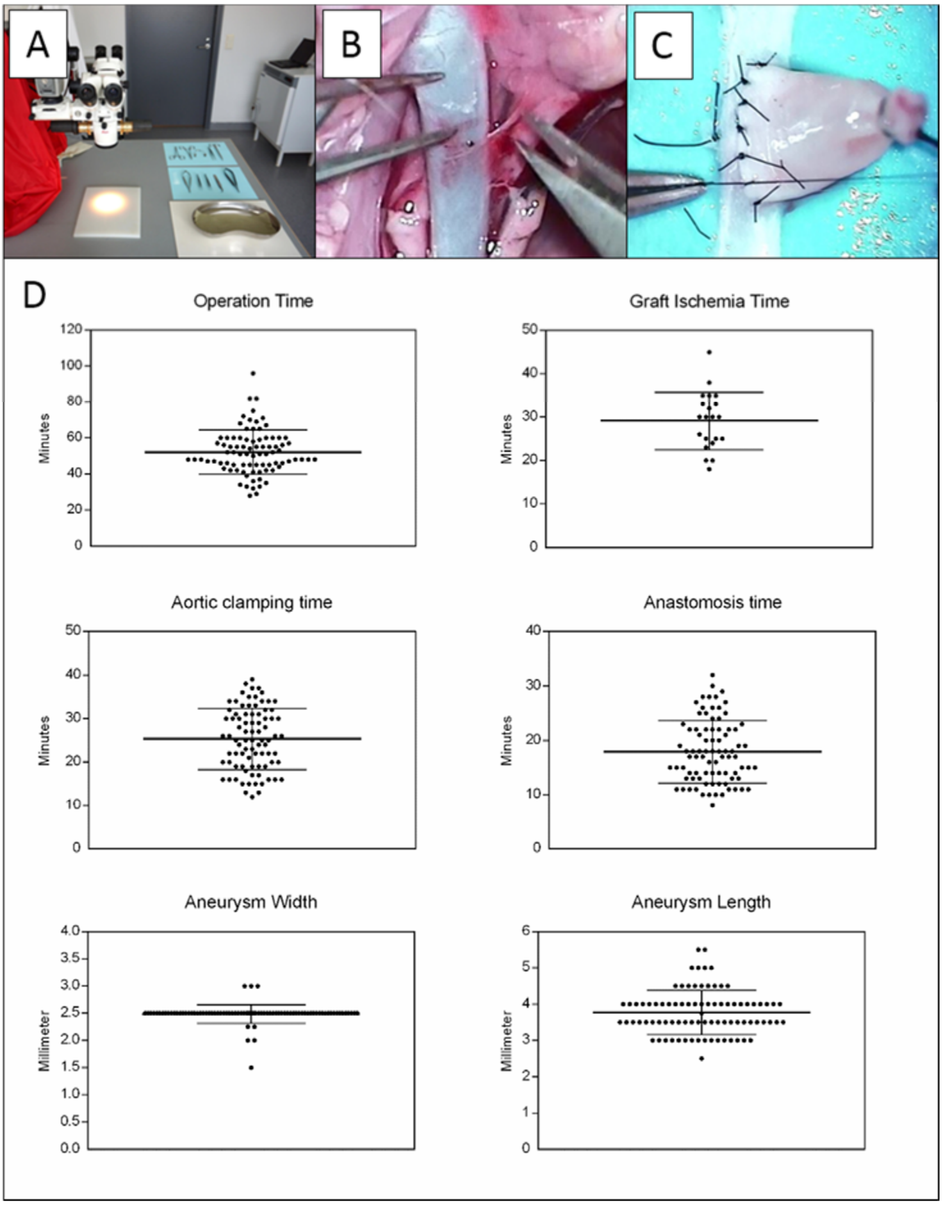

A, preparations. **B**, graft harvesting. **C**, end-to-side anastomosis. **D**, surgical characteristics: The graphs visualize the distribution of single data values (small black dots), data mean (bold long bar) and standard deviation (error bars).

5.3 Biological effect of mural cell loss

5.3.1 Physical and chemical decellularization

Any decellularization methods alter ECM and cause some ultrastructural disruption. Minimized damage to the ECM, coupled with complete decellularization is the aim of each decellularization method (chemical, biological, and physical) and depends on many factors, such as the tissue's cellularity, density, organization and thickness.[435] Agents and techniques need to be verified for the rat abdominal aorta.

Ex vivo pilot series using various physical decellularization including freezing/thawing cycles, pressure and ischemia periods at four degrees Celsius (4 °C) and RT proved to be insufficient to remove nuclear components unless further chemical or biological processing was added. Chemical decellularization using the ionic detergent SDS successfully removed nuclear remnants of the rat abdominal aorta in an incubation time-dependent manner (**Figure 11**).

After ten hour of SDS treatment, near-complete graft decellularization was documented in all three layers of the rat abdominal aorta. Following SDS treatment, matrix components of the extracellular matrix including medial elastin, collagen networks and adventitial extracellular matrix are known to be preserved.[422] Although there are no clear microscopic changes in the matrix it is still possible that the SDS treatment alters the mechanical strength of the vessel wall. It has been shown that SDS treatment decreases compliance of vessels.[436] Since no differences in the amount of collagen between native and decellularized vessels was found, collagen denaturation was ruled out and the authors hypothesized that the absence of vascular smooth muscle cells is causative for the altered vessel compliance.

5.3.2 Luminal thrombus formation

5.3.2.1 Failure of stable thrombus organization causes recanalization

There were no significant differences between the aneurysm patency rates in the two groups at any time during follow-up.[IV] Aneurysms in the non decellularized group showed a linear course of thrombosis over time. Decellularized aneurysms exhibited a heterogeneous pattern of thrombosis and recanalization.

Repeated follow-up MRA revealed that aneurysms with a "healthy" wall developed thrombosis stepwise, while decellularized aneurysms showed continually repeating cycles of clot formation, dissolution and aneurysm recanalization. Histologically-confirmed unorganized thrombus and failure of neointima formation was only noticed in decellularized aneurysms, which further supports the concept of impaired thrombus organization in aneurysms missing mural cells.

Together, the radiological and histological findings indicate that aneurysms with loss of mural cells are less likely to form a stable thrombus. Previous studies have already demonstrated the paramount importance of aneurysm wall smooth muscle cells in thrombus organization and neointima formation.[140, 437] Therefore, it can be hypothesized that loss of mural cells is causative for the failure of luminal thrombus transformation into stable fibrotic tissue.

Intraluminal thrombus (38% in non-giant IA radiographic series[438]; as an intraoperative finding, luminal thrombosis is even more common in giant aneurysms) and wall hematomas are common features of human giant intracranial aneurysms and in line with our histological findings. Fresh luminal thrombosis is seen in up to 25% of unruptured and 70% of ruptured non-giant aneurysms.[102] The histological changes of luminal thrombus formation and luminal thrombus organization found in the experimental aneurysm resemble those seen in human histopathological series.[100, 102, 105]

5.3.2.2 Increased neutrophil accumulation in the luminal thrombus

Decellularized aneurysm demonstrated a trend towards increased neutrophil accumulation in the thrombus ($p = 0.08$) when compared to non decellularized aneurysms. Analyses comparing stable and growing aneurysms revealed a significant increase in neutrophil accumulation ($p = 0.001$) in unorganized intraluminal thrombus formation. Failure of thrombus organization and neointima formation was seen only in decellularized aneurysms.[IV]

This interesting finding indicates that decellularized aneurysms are not only incapable of thrombus organization, or continually repeating cycles of clot formation, dissolution and aneurysm recanalization; but also induce increased neutrophil accumulation in the luminal thrombus. Fibrin deposition and platelet-derived neutrophil-attracting chemokine released from the thrombus attracts neutrophils per se.[439] The additional increased neutrophil content in the luminal thrombus of decellularized aneurysm could be explained by the fact that ongoing degeneration of red blood cells and degranulation of thrombocytes, platelets and neutrophils trapped in the fibrin scaffold of an unorganized thrombus initiates additional chemotropic responses and attracts even more neutrophils.[440] In abdominal artery aneurysms, intraluminal thrombus is associated with wall instability which appears to contribute to growth and rupture.[441]

Crompton has divided the IA into three parts and identified the most frequent rupture point in the distal third (IA fundus)[34]. In our series we did not perform multiple contiguous sections throughout the entire paraffin-embedded specimen. Therefore we cannot comment on the rupture site.

5.3.2.3 Benefits and limitations of the model

The behavior of aneurysm growth seen in our model does not mirror the growth pattern of human cerebral aneurysms exactly. Small aneurysms grew in to giant aneurysms within two weeks which is considerably faster than what was believed necessary for cerebral aneurysm formation and maturation. The loss of mural cells in human intracranial aneurysms is most likely a long term process requiring more time than in the experimental model presented. It therefore follows that the natural history of these experimental aneurysms is not the same as that of human aneurysms.

Animals are prone to sudden death due to aneurysm growth and rupture, which raises ethical concerns about acceptability of the severity of an experiment. The results revealed that aneurysm growth began within the first two weeks and first ruptures occurred no earlier than ten days after aneurysm creation. The foreseeable changes in aneurysm geometry can by tracked noninvasively by MRA, micro computed tomography and high-frequency ultrasound and guarantees an early discontinuation of the experiment.

The presented model aortic artery sidewall rat aneurysm model using decellularized aneurysms is based on a relatively small number of animals and needs further validation and replication. Despite all attempts to minimize surgical trauma, aortic clamping time and standardize aneurysm angioarchitecture, multiple complex factors can influence biological behavior and it is impossible to disentangle confounding factors from true causal factors and events. Aneurysms arising in the abdominal cavity are allowed to grow unrestricted without causing mass effect for a long time (up to more than tenfold increase in size), but inflammatory cells are more easily attracted than in other parts of the body.

The microsurgical sidewall aneurysm model using decellularized grafts can be used to study basic biological concepts of aneurysm formation although one must be aware of differences in hemodynamic characteristics and vascular biology between the aorta and cerebral arteries. With the exception of the Hashimoto model[365], in which induction of intracranial aneurysms is triggered by hypertension, this limitation should be considered in all currently used aneurysm models. Using the side-wall arterial out-pouch model, future experiments may allow testing the efficacy and interaction of endovascular devices on different wall conditions, including growing aneurysms.

5.3.3 Aneurysm wall degeneration, growth and rupture

5.3.3.1 Wall inflammation is associated with wall disruption

Decellularized aneurysms demonstrate higher grades of periadventitial fibrosis and significantly enhanced aneurysm wall inflammation ($p = 0.03$) when compared to non decellularized aneurysms. Wall dissection and mural hematomas were seen exclusively in decellularized aneurysms. Aneurysm with increased neutrophil accumulation in the thrombus and increased wall inflammation showed a trend for mural hematomas ($p = 0.05$ and $p = 0.08$).[IV]

A main source of matrix-degrading proteases are neutrophils trapped in unorganized thrombus.[141] In addition, intraluminal thrombosis is not only a site of protease release and activation itself, but also releases cytotoxic compounds and induces inflammation throughout the wall promoting further matrix degradation.[122]

The increased accumulation of neutrophils in aneurysm walls missing mural cells may also be linked to the lack of "cell barrier" meaning that macromolecular plasma components such as lipids, complement compounds and immunoglobulins diffuse freely to the decellularized wall matrix and induce inflammation. These results demonstrate that neutrophil accumulation in the thrombus and wall inflammation is associated with aneurysm wall dissections and mural hematomas. Aneurysm wall fragility is, in turn, associated with aneurysm growth and eventual rupture.

5.3.3.2 Aneurysm wall fragility is associated with growth

Aneurysm growth occurred in five out of twelve decellularized aneurysms (42%). Four of the growing aneurysms increased in size during the first week and continued to grow thereafter. One aneurysm started to grow during the second week. All non decellularized aneurysms remained stable (**Figure 12**).

Macroscopic measurement of width and length of non decellularized aneurysms at creation confirmed that these aneurysms remained stable over time. In the decellularized aneurysm group, four aneurysms (4/12; 33%) remained stable and four grew to giant aneurysms (4/12; 33%) that were as large as 43 mm x 38 mm x 24 mm (**Figure 13**). Three of the growing aneurysms in the decellularized group ruptured during the observation period (3/4; 75%). Endoscopy showed massive intraluminal thrombosis in two of these ruptured aneurysm (2/3; 66%). One suspected case of growth and rupture had to be excluded from final histological analysis due to delayed autopsy. Histology revealed that growing aneurysms had marked adventitial fibrosis and inflammation ($p = 0.002$ and 0.03), wall disruption ($p = 0.008$) with inflammation ($p = 0.003$) and intramural hematomas ($p = 0.05$) when compared to stable aneurysms.[IV]

In summary, the results show first, that neutrophil accumulation in the thrombus and wall inflammation is associated with aneurysm wall dissections and mural hematomas. Second, that aneurysm wall fragility is associated with aneurysm growth and eventual rupture. Lack of viable mural smooth muscle cells, matrix degeneration, intramural hematomas, aneurysm wall inflammation and intraluminal thrombus formation are known characteristics of ruptured human IA.[100, 102, 146]

Loss of mural cells also means loss of aneurysm wall repair (defense) mechanisms such as re-synthesis of degraded collagen[442], induction of antioxidant enzymes[443] or proteases inhibitors.[444] Together, these detrimental effects may shift the balance from aneurysm wall cicatrisation to wall destruction which promotes growth and eventual rupture.

Figure 11. Graft decellularization.

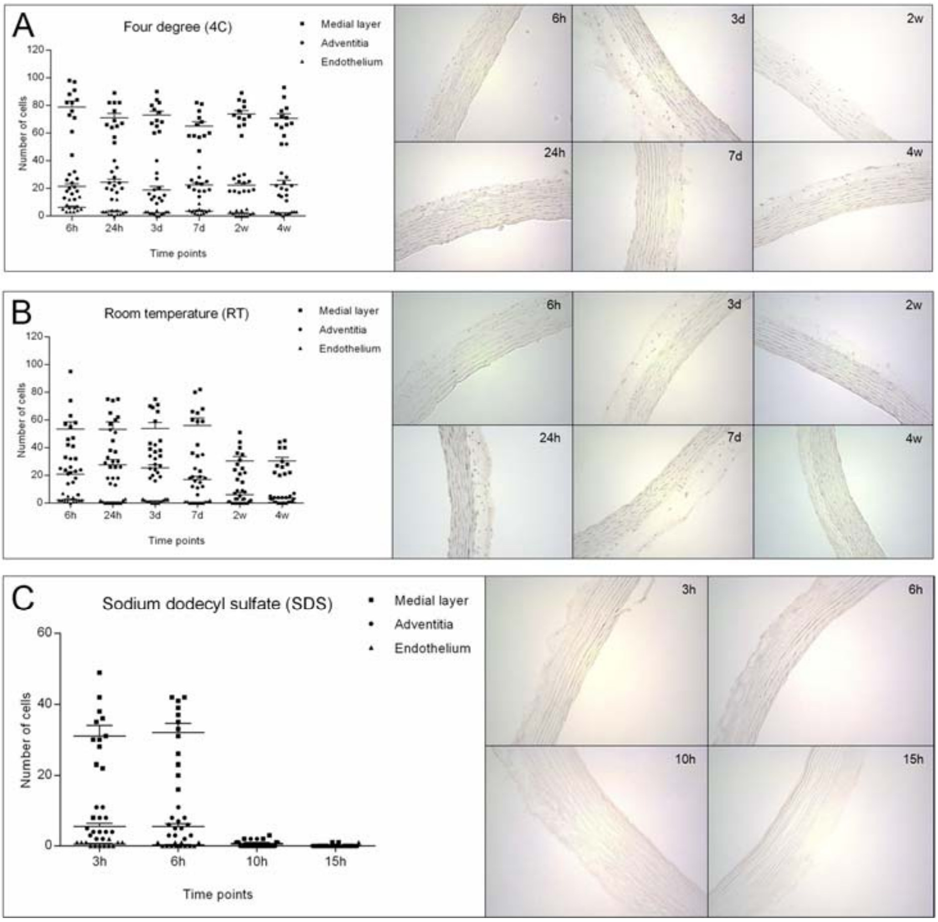

Physical decellularization using prolonged ischemia time at four degree (**A**) and room temperature (**B**) demonstrated insufficient cell removal. Chemical decellularization by incubation for 10 hours at 37 °C in 0.1% SDS (**C**) in Milli-Q® water reveals almost total loss of nuclear components. 40x magnification. All specimens are stained with hematoxylin.

Figure 12. Stable and growing aneurysm.

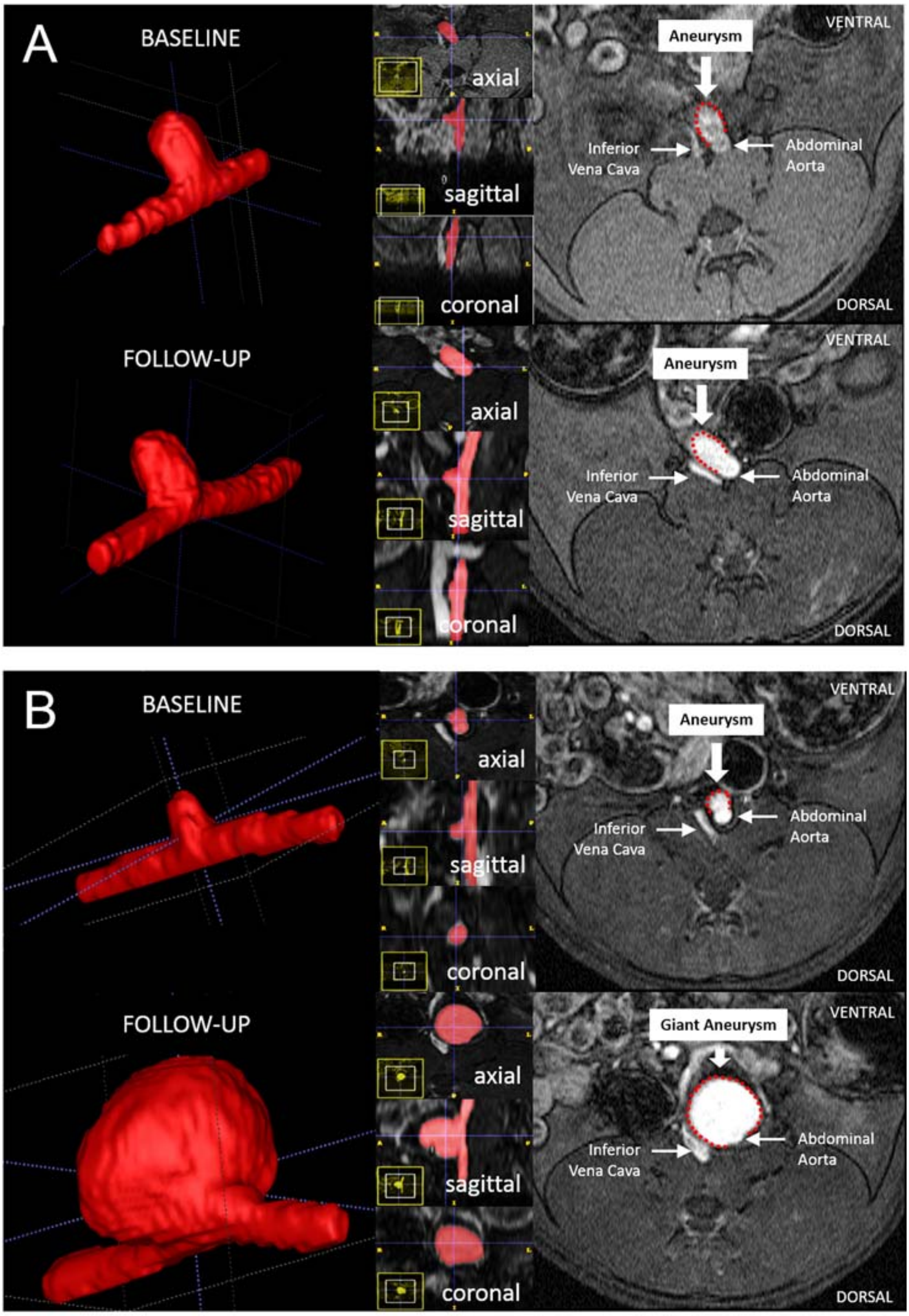

3D reconstructions, three main axis cutting planes and source CE-MRA at baseline and four weeks follow up. **A**, non-decellularized stable aneurysm. **B**, decellularized growing aneurysm.

Figure 13. Growth of decellularized aneurysms.

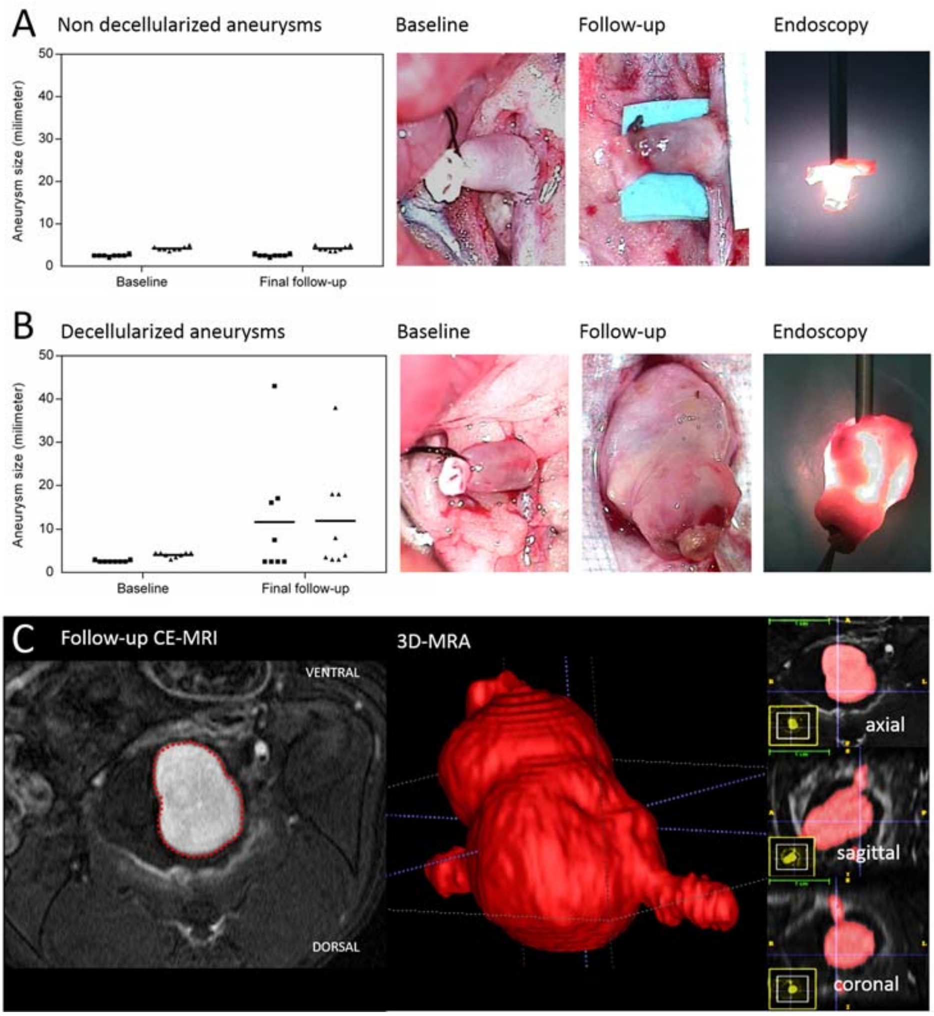

A, non-decellularized (control group). **B**, decellularized (sodium dodecyl sulphate treated group). The graphs depict aneurysm dimensions (width and length) in mm at baseline and final follow up four weeks after creation. All non decellularized aneurysms remained stable. Marked growth was documented in four decellularized aneurysms. **C**, some of the decellularized aneurysms grew to giant aneurysm proportions (largest length 4 cm) with irregular shape and secondary pouches.

5.4 Local cell therapy for decellularized aneurysms

5.4.1 Effect of luminal thrombosis on aneurysm walls

5.4.1.1 The role of luminal thrombosis in healthy aneurysms

Healthy untreated non decellularized aneurysms demonstrate a linear course of stepwise thrombosis over time and remained stable. Histology of these aneurysms revealed preserved aneurysm wall cellularity, virtually no wall disruption, minimal wall inflammation and rare neutrophil accumulation in the luminal thrombus. Organizing or mature neointima was observed in all healthy aneurysms that underwent spontaneous thrombosis.[V]

On the other hand, all except one healthy non decellularized rapid thrombus in the induced aneurysms were incapable of forming neointima. Almost half of the healthy non decellularized aneurysms showed complete loss of (or only a few remaining viable) mural cells. Aneurysms with an initially healthy wall that suffered mural cell loss showed significantly more wall inflammation ($P = 0.01$) and a trend to increased neutrophil accumulation in the thrombus ($P = 0.072$) as compared to aneurysms without loss of mural cells.[V]

All but one healthy aneurysm showed partial or complete recurrence after three weeks and three aneurysms increased in size. Two of these growing aneurysms in the healthy aneurysm group with acute thrombus induction demonstrated complete loss of mural cells, enhanced intrathrombus and intramural neutrophil accumulation, complete wall disruption and prominent periadventitial fibrosis.

The observed cell loss in “healthy” aneurysms could be attributed to ischemic or inflammatory reactions induced by the fibrin glue thrombus. It also seems possible that luminal fibrin glue impaired diffusion of nutrients to the healthy media and promoted inflammation as a secondary reaction. Inflammation or mural cell loss is rare in stepwise spontaneous thrombosis of healthy untreated aneurysms. A potential explanation might be that acute thrombosis induces inflammation to such a large scale that it overruns the aneurysm wall defense mechanisms. This results in wall destabilization, loss of mural cells, destructive remodeling, growth and eventual rupture prior to thrombus stabilization/organization caused by cell ingrowth promoting scar formation.

Our results are consistent with those of Raymond et al.[144] who found (in a swine sidewall aneurysm model), that wide-neck aneurysms (n = 6) with stepwise thrombosis demonstrated gradual healing with substantially thickened hypertrophied walls infiltrated with myofibroblasts and collagen, mature neointima and organized thrombus filling the aneurysm lumen. On the other hand, 50% of small-neck aneurysms (n =4) with fast thrombosis demonstrated aneurysm wall destabilization and rupture.

Acute thrombus induction has been linked to mural destabilization not only in experimental aneurysms[143, 144] but also in clinical settings following application of flow diverters to treat intracranial aneurysms.[145, 146] The studies consistently found histopathological characteristics comparable to those found in our study, with large numbers of inflammatory cells and loss of mural cells in destabilized aneurysm wall segments after rapid thrombosis.[143, 144, 146]

5.4.1.2 Luminal thrombosis in sick decellularized aneurysms

First recurrence in decellularized embolized aneurysms was seen seven days after thrombus induction. After three weeks, all decellularized embolized aneurysms were partially or completely recanalized. Three aneurysms had grown, including one aneurysm that developed into a giant partially thrombosed multilobulated aneurysm. One of the growing aneurysms ruptured ten days after creation. With the exception of two cases, neointima formation was incomplete in all aneurysms with a decellularized wall. In the replication series, half of the aneurysm demonstrated incapability of thrombus organization, recurrence and growth. All aneurysms that underwent growth demonstrated enhanced endoluminal and intrathrombus neutrophil accumulation, inflammatory and hemorrhagic transformation of the wall and enhanced periadventitial fibrosis.[V]

MRA, macro- and microscopic evaluation and histology confirmed that aneurysms with loss of mural cells are incapable of organizing induced thrombosis. If the intraluminal thrombus is not infiltrated by cells that turn it into fibrous tissue (neointima), the thrombus is absorbed and recanalized. Thrombus recurrence was noted as early as one week after induction and was present in all aneurysms at three weeks follow-up. At that time point, aneurysm recurrence was associated with fresh unorganized intraluminal thrombosis and marked inflammatory reactions.[V]

5.4.1.3 Cell loss triggers wall degeneration, growth and rupture

Loss of mural cells per se did not induce aneurysm wall inflammation. Decellularized embolized aneurysms without recurrence revealed less intrathrombus and intramural inflammation. A possible explanation for this might be that macromolecular plasma components capable of inducing inflammation were blocked by fibrin glue and only recurrence allowed free diffusion towards the aneurysm wall.

It is important to note that initially "healthy" aneurysms that acquired mural cell loss due to thrombus induction showed evolution similar to genuine decellularized embolized aneurysms; with recurrence, growth and significant increase in aneurysm wall inflammation, intrathrombus neutrophil accumulation, wall disruption and periadventitial fibrosis. Taken together, the findings corroborate that aneurysms missing mural cells are subjected to increased inflammatory reactions, severe wall degeneration, aneurysm growth and eventual rupture.

5.4.2 Luminal cell replacement heals decellularized aneurysm

To further test the hypothesis that mural cell loss impairs thrombus organization and neointima formation, we treated decellularized aneurysms with syngeneic smooth muscle cell transplantation. If mural cell loss causes impaired thrombus formation, recanalization, growth and rupture, cell replacement might reduce these events.

5.4.2.1 Cell transplantation promotes early thrombus organization

All but one aneurysm with transplanted cells and a decellularized wall remained occluded with complete or near complete neointima formation. This single case of incomplete neointima formation demonstrated an increase in aneurysm size at three weeks follow-up. There was no recurrence or growth in the replicate experiments. After transplantation, cells were equally distributed within the intraluminal thrombus, became confluent and demonstrated no migration trend towards the aneurysm wall or the aneurysm ostium. Thrombus-induced and cell transplanted aneurysms demonstrated progressive healing over time (**Figure 14**). Spindle-shaped CM-Dil labeled cells embedded in collagen bundles were found to organize the fibrin clot and noeintima along the neck. OPT revealed that transplanted cell infiltration of adventitia, ingrowth in periadventitional environment and migration to parent artery was absent. (**Figure 15**).[V]

5.4.2.2 Reduced inflammation and enhanced neointima formation

There was significantly more neutrophil accumulation in the thrombus in decellularized aneurysms ($P = 0.03$), and a trend ($P = 0.15$) towards increased neutrophils in the thrombus of non-decellularized aneurysms as compared to decellularized aneurysms with local cell transplantation. Healed aneurysms had significantly fewer neutrophils in the thrombus when compared to aneurysms with missing neointima formation ($P = 0.017$). Decellularized aneurysms treated with local cell replacement at the time of thrombosis demonstrated considerably better histological neointima formation than thrombosed non decellularized aneurysms ($P < 0.001$) and thrombosed decellularized aneurysms ($P = 0.002$) (**Figure 16**). Overall recurrence rate of thrombosed decellularized aneurysms was notably higher as compared to embolized decellularized aneurysms with concomitant cell replacement ($P = 0.037$).[V]

In summary, replacement of lost smooth muscle cells not only promoted fast thrombus organization within days after thrombus induction but also reduced neutrophil accumulation in the thrombus. It can be hypothesized that the presence of viable cells improves early thrombus reorganization and neointima formation, preventing recurrence and additional thrombus formation. Consequently, intraluminal amount of new red blood cells, platelets and macromolecular plasma components such as lipids, complement compounds and immunoglobulins are reduced which in turn attenuates fishing of neutrophils. This could explain the finding that healed aneurysms had significantly less neutrophils in the thrombus as compared to aneurysms with missing neointima formation.

Figure 14. Time course of aneurysm healing.

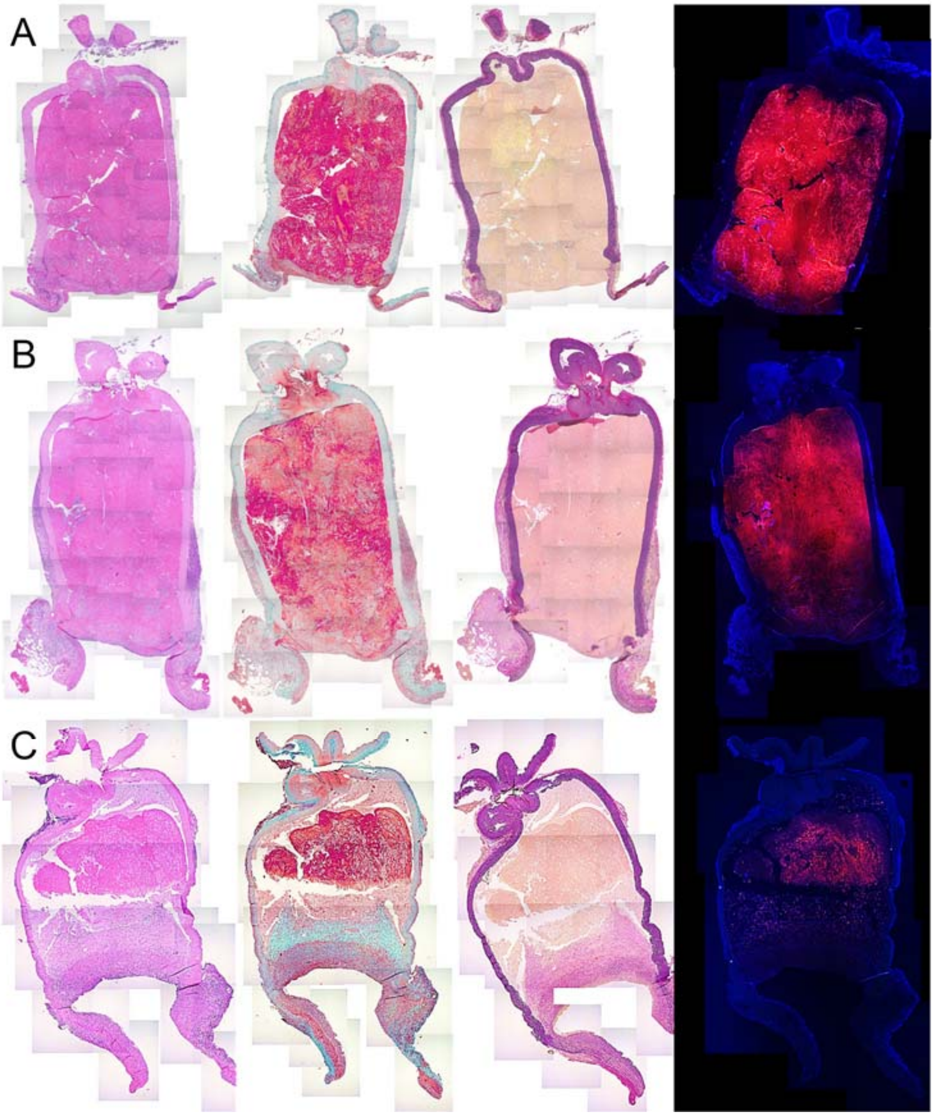

Panels from left to right demonstrate merged light microscope hematoxylin-eosin, Masson-Goldner's trichrome, elastica van Gieson's staining and fluorescent stained photomicrographs (10x magnification). **A**, organization of the fibrin clot and neointima formation starts three days after cell graft placement. **B**, organization progresses already after one week and thick neointima is formed at the aneurysm orifice. **C**, in week three the ostium is completely occluded by thick neointima and large amounts of collagen deposits.

Figure 15. Fibrin clot organization and spatial cell distribution.

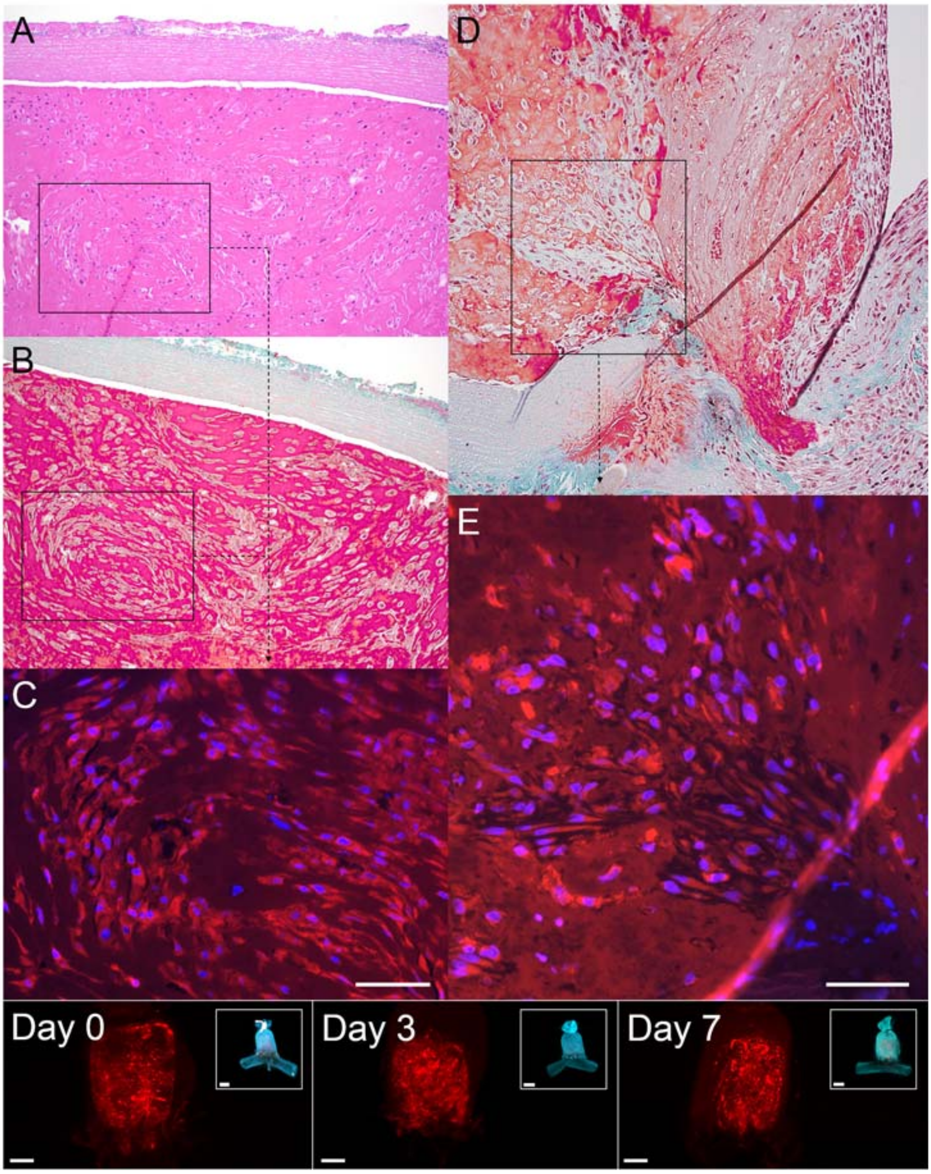

Day 3: **A**, cells trapped in the fibrin clot; HE, 10x; **B**, organization of cells; MT, 10x; **C**, CM-DiI-labeled cells in fibrin clot; 10x; Scale bar = 50 µm. Day 7: **D**, connective tissue formation; **E**, labeled cells in areas of collagen formation. 20x magnification; Scale bar = 50 µm. Panels below: OPT time profile (Day 0, 3, and 7) of spatial cell distribution within the aneurysm. Labeled cells appear in bright red; Scale bars = 500 µm. The whole aneurysm and part of its parent artery is displayed in translucent greenish-blue (scale bars = 1000 µm).

Figure 16. Healed aneurysm neck.

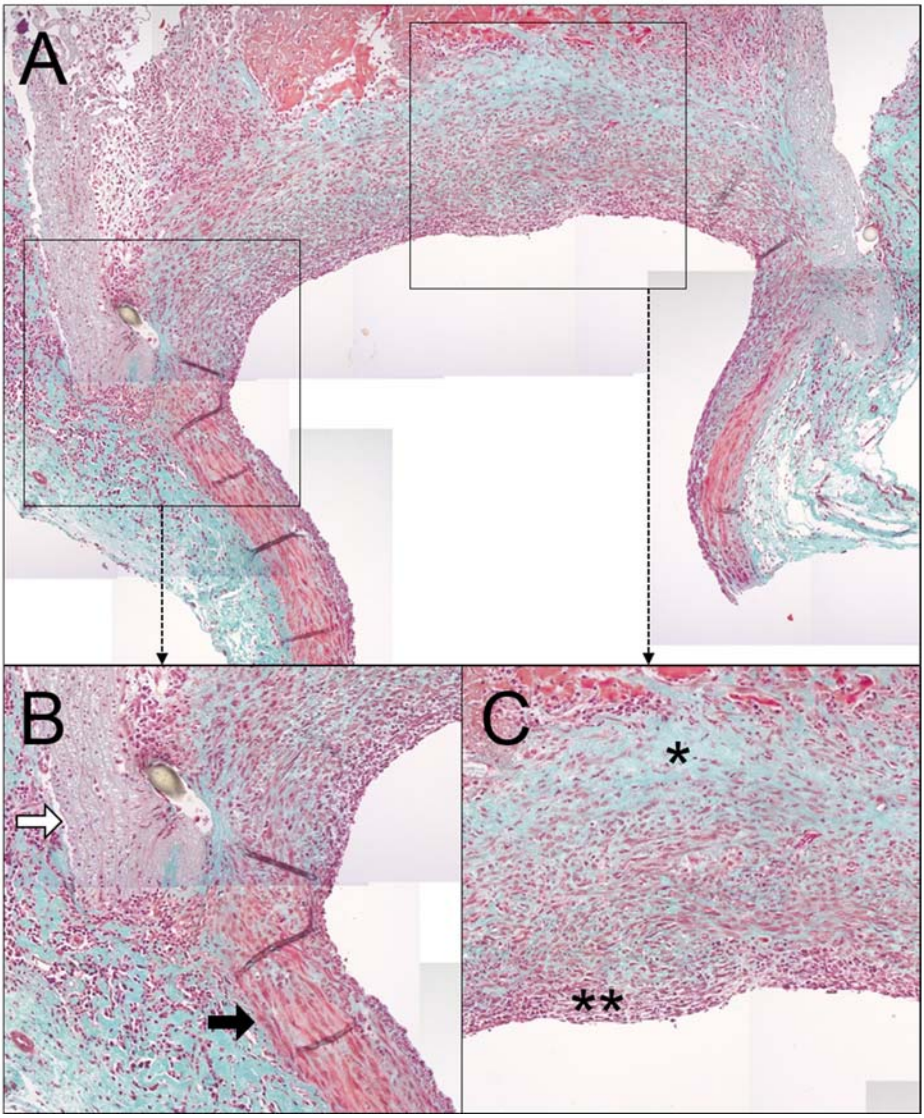

A, merged light microscope photomicrographs (MT; 10x magnification) depict aneurysm orifice covered with a thick neointima. **B**, transmission zone between healthy parent artery (black arrow) and decellularized aneurysm wall (white arrow). **C**, MT staining reveals connective tissue formation with abundant collagen deposits (*) and formation of a thick layer of hypercellular tissue (**) across the aneurysm's neck.

Conclusions

Rabbit and rats have become the most frequently used animal models in the field of IA research. The rabbit is customarily used to test EVT devices, while rats are mainly used for research concerning IA biology. Although coagulation and healing profiles similar to humans and true bifurcational hemodynamics are essential in determining the technical proficiency of novel EVT devices, biological principles are ideally tested in standardized models that facilitate analysis of efficacy and interaction of endovascular devices within different wall conditions, including growing aneurysms.

I Creation of complex venous pouch bifurcation aneurysms in the rabbit is feasible with low morbidity, mortality, and high short-term aneurysm patency. The necks, domes and volumes of the bilobular, bisaccular and broad-neck aneurysms created are larger than those previously described and provide a promising tool for in vivo animal testing of human endovascular devices.

II Long term patency without spontaneous thrombosis is one of the most important preconditions for analysis of embolization devices. Complex bilobular, bisaccular and broad-neck microsurgical aneurysm formation in the rabbit venous pouch bifurcation model demonstrates a high long term patency rate without need for prolonged (more than four weeks) anticoagulation.

III The microsurgical sidewall rat aneurysm model is a fast, affordable and consistent method to create experimental aneurysms with standardized categories for size, shape and geometric configuration in relation to the parent artery. The model allows the study of aneurysm growth and rupture and could potentially be used to assess biological responses induced by embolization devices in growing and rupture-prone aneurysms.

True understanding of IA reopening after EVT requires comprehensive knowledge of the biological mechanisms involved in aneurysm wall remodeling, intraluminal thrombosis formation and resorption, tissue response to EVT materials, and their interaction. Most of the EVT modalities currently available and large research efforts are directed towards the treatment of the visible lumen. However, it is becoming increasingly difficult to ignore the importance of IA wall pathobiology in aneurysm healing. Therefore, novel interventions should not only target the visible lumen, but also focus on the wall as such, and the molecular pathways relevant to IA wall pathobiology.

IV Aneurysms missing mural cells are incapable of organizing a luminal thrombus, leading to aneurysm recanalization and increased inflammatory reaction, which in turn causes severe wall degeneration, aneurysm growth and eventual rupture. The results suggest that mural cells are of paramount importance for thrombus organization and aneurysm wall homeostasis.

V Loss of smooth muscle cells from the aneurysm wall impairs thrombus organization and neointima formation in thrombosed aneurysms and drives the healing process towards destructive wall remodeling. This promotes recurrence, growth and eventual rupture of embolized aneurysms. The biologically active luminal thrombus can provoke mural cell loss and increased intramural and intrathrombus inflammation even in healthy aneurysms. Local smooth muscle cell transplantation compensates for the loss of mural cells, attenuates inflammatory reactions, promotes aneurysm healing and reduces recurrence, growth and rupture rate in a rat saccular sidewall aneurysm model.

Future perspectives

Despite numerous known clinical factors associated with IA rupture, estimation of rupture risk remains an educated guess. Over the last few years it has become apparent that shape and aspect ratio may be more effective than size in determining IA rupture risk.[47, 48, 53] These findings, and the discrepancies between the reported low risk of rupture in small anterior circulation aneurysms from ISUA[39, 42] and UCAS[37] as compared to other studies[34, 41, 445-447] with a significant numbers of IA rupture at 3-6 mm in size, highlight the need for improved parameters for the prediction of IA rupture risk. Perhaps in the future, imaging modalities allow better characterization of the IA wall, intraluminal space and periadventitial surroundings, either by use of molecular/cellular biomarkers and/or increased spatial image resolution. Adding such pathobiological characterization could improve IA rupture risk assessment.[448]

Improved pathobiological assessment of the IA wall could not only aid in better determination of the IA's natural history, but may also be advantageous in choosing the best possible treatment. Histopathology of human IA samples have long indicated that ruptured and unruptured IA represent different biological entities with increased inflammatory reactions, and the loss of mural cells in ruptured IAs.[100, 102, 107, 138] When considering the assumption that IA healing is primarily organized by cells originating in the IA wall[140], and the finding that unruptured IA present more stably following GCD embolization than ruptured IA[12, 13, 274, 275], it is intriguing that the best treatment modality for any given aneurysm might be influenced by the IA wall condition. In case of an IA with a severely degenerated acellular thin wall, it is likely that only surgical exclusion or endovascular bridging of the diseased vessel wall will result in successful IA occlusion. On the other hand, aneurysms with a healthier, less degenerated wall may have a greater chance to heal completely after standard endovascular coiling.

In the future, IA classification and treatment might be wall-oriented rather than lumen-oriented and vessel wall imaging may allow direct visualization of pathological processes and the degree of wall degeneration.[305, 449-451] Reports of successful visualization of IA wall pulsation and protuberances[452], site of rupture[172], measurement of IA wall thickness[453, 454], intravascular cerebral ultrasonography[455, 456], in vivo molecular enzyme-specific MRI of inflammation[457] and macrophage imaging[458-460] already demonstrate the current imaging possibilities. Further advances in diagnosis and better understanding of the underlying pathways in IA pathobiology will allow identification of IA wall types with different biological behaviors. Their influence on growth, susceptibility to rupture and reaction to endovascular treatment will provide clues to developing and selecting the best possible treatment options for the patient.

As with the dilemma of not knowing which IA will eventually rupture, we cannot anticipate which aneurysm will eventually reopen after EVT. However, there is growing evidence that healing after EVT is determined primarily by the IA wall condition. The rapidly growing body of knowledge on molecular biological pathways involved in IA formation, growth and rupture (obtained from intracranial animal models and human histopathological IA tissue samples) will support the development of EVT modalities, successfully addressing both the luminal part of the IA and the pathology within the vessel wall. Development of pharmacological treatments to repair the diseased vessel segment will not only provide stabilization of untreated IA, but most likely improve long term stability after EVT and result in a true clinical cure.

Figures

Tables

Supplementary videos

Video 1. Pulsating patent complex rabbit bilobular aneurysm at time of creation. Runtime: 13 sec.

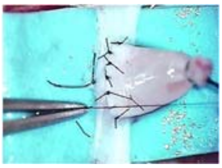

Video 2. Step-by-step procedural instructions of the rat sidewall aneurysm model. Runtime: 13 min. 53 sec.

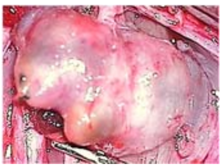

Video 3. Harvesting and measurement of a rat giant aneurysm. Runtime: 1 min. 32 sec.

Video 4. Endoscopy of a patent open and partially thrombosed growing rat aneurysm. Runtime: 1 min. 1 sec.

Video 5. 3D-CE-MRA complex angioarchitecture rabbit bifurcation aneurysms. Runtime: 1 min. 33 sec.

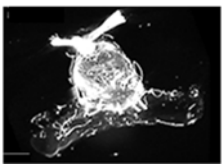

Video 6. Transparent 3D anatomical morphology of a rat sidewall aneurysm. Runtime: 21 sec.

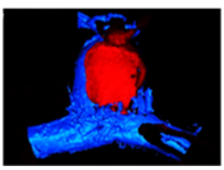

Video 7. Rotating 3D internal morphology of a cell transplanted rat sidewall aneurysm. Runtime: 21 sec.

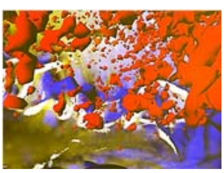

Video 8. High resolution 3D fly-through animation inside a cell transplanted aneurysm. Runtime: 50 sec.

Acknowledgements

Part I and II of this study was carried out in the Cerebrovascular Research Group at the Departments of Intensive Care Medicine and Neurosurgery, Bern University Hospital and University of Bern, Bern, Switzerland and at the Department of Neurosurgery and Division of Neuroradiology, Kantonsspital Aarau, Aarau, Switzerland in 2008-2011. Part III to V of this study was carried out in 2012-2014 in the Neurosurgery Research Group of the Neuroscience program of Biomedicum Helsinki, Helsinki, Finland and the Department of Neurosurgery, Helsinki University Central Hospital, Helsinki, Finland. I express my sincere gratitude to the following co-workers and friends who supported, guided, and encouraged me directly and indirectly during the past years.

Juhana Frösén, for his excellent support as a co-worker and supervisor. Without his guidance on planning, conducting and the evaluation of experiments, the studies would not have been possible. His profound knowledge in IA wall biology is truly remarkable and I feel fortunate to have learned the basic principles in this complex and fascinating area of research from him.

Mika Niemelä and **Javier Fandino** for their work as thesis supervisors. Javier Fandino, as my mentor during neurosurgical training, set the course for the research period in Helsinki. Mika Niemelä paved the way for the doctoral thesis in the very first month of my stay. Both gave unequivocal support for the proposed projects and have advanced the thesis and my career.

Juha Hernesniemi supported the idea of the doctoral thesis from the beginning and gave his full approval. I am lucky to have had the chance to be his fellow.

Pauli Helén and **Hannu Manninen**, reviewers of this thesis, for the excellent comments, suggestions, and constructive criticism which improved and complemented the thesis.

Stephan Jakob and **Jukka Takala** for providing their great support and collaboration in our Joint Cerebrovascular Research Laboratory. Without their support we would not have been able to establish the current laboratory and to form a growing research team.

Luca Remonda and his radiologic technologists for their support and diligent 3D-MRA reconstructions.

Daniel Coluccia, **Salome Erhardt**, **Camillo Sherif**, **Janine-Ai Schläppi**, **Ilhan Tastan**, **Volker Neuschmelting,** and **Lukas Andereggen**, as co-workers for their laboratory and experimental work, help in data analysis and sharing many good moments in the lab.

Daniel Mettler, **Max Müller**, **Daniel Zalokar**, and **Olgica Beslac** for their skillful management of animal care, anesthesia and operative assistance.

Hans Rudolf Widmer and **Andreas Raabe** for their ongoing support of our research activities in the Cerebrovascular Research Group.

Erica Holt for her editorial support in proofreading the manuscripts and language editing of this thesis.

Michael von Gunten and **Menja Berthold** for providing expertise in histopathology, tissue processing and staining.

Johan Marjamaa for his great support, humorous manner and generous hospitality.

Antti Huotarinen for daily support in the lab, concise scientific discussions and providing constant quantities of freshly brewed filter coffee and the best Karelian pies in town. **Petri Honkanen** for his help in MR data processing and analysis. He was a great man and I highly appreciated his calm manner. **Kateřina Bradáčová** for operative assistance and help in data analysis.

Emilia Gaal-Paavola for her motivating support. It was her that initially came up with the idea of starting the PhD program during my research stay.

Nancy Lim, **Olli Mattila**, and **Anne Reijula** for their excellent technical assistance.

Essam Abdelhameed for his excellent video editing job for the JOVE manuscript.

Jussi Kenkkilä for his comprehensive support in OPT imaging acquisition, image processing, and help in 3D-CE-MRA volumetry. The BIU team is acknowledged for microscopy services.

Andrey Anisimov for assistance with cell cultures and cell culture staining, **Gabriela D'Amico Lago** for sharing her expertise in OPT tissue processing, and **Tanja Holopainen** for assistance in-vivo FITC lectin staining. I am grateful for the support of aforementioned members of the Kari Alitalo laboratory and the laboratory itself for providing a contact point to solve everyday problems of laboratory science.

Usama Abo-Ramadan for inspiring scientific and religious discussions and his continuous commitment to make MRI sequences better and better.

Arthur, my uncle, and **Ines und Franco**, my parents, for the trust and confidence they have placed in me.

Janine, my wife, **Céline** and **Nic**, my children, for their enthusiasm and love.

This work was supported by the research funds of the Helsinki University Central Hospital, Helsinki, Finland and by grants from The Sigrid Juselius Foundation (Helsinki, Finland), the Department of Intensive Care Medicine, Inselspital, Bern University Hospital and University of Bern, Switzerland, the Research Fund from the Kantonsspital Aarau, Aarau, Switzerland and by a grant from the Swiss National Science Foundation (S.M.: PBSKP3-123454).

References

1. Sivenius J, Tuomilehto J, Immonen-Raiha P, Kaarisalo M, Sarti C, Torppa J, et al. Continuous 15-year decrease in incidence and mortality of stroke in finland: The finstroke study. *Stroke*. 2004;35:420-425

2. Hoffmann E, Marbacher S, Jakob S, Takala J, Remonda L, Fandino J. Incidence of vasospasm, outcome, and quality of life after endovascular and surgical treatment of ruptured intracranial aneurysms: Results of a single-center prospective study in switzerland. *ISRN Vascular Medicine*. 2011;Article ID 782568, 10 pages, 2011. doi:10.5402/2011/782568

3. Johnston SC, Selvin S, Gress DR. The burden, trends, and demographics of mortality from subarachnoid hemorrhage. *Neurology*. 1998;50:1413-1418

4. Stegmayr B, Eriksson M, Asplund K. Declining mortality from subarachnoid hemorrhage: Changes in incidence and case fatality from 1985 through 2000. *Stroke*. 2004;35:2059-2063

5. Nieuwkamp DJ, Setz LE, Algra A, Linn FH, de Rooij NK, Rinkel GJ. Changes in case fatality of aneurysmal subarachnoid haemorrhage over time, according to age, sex, and region: A meta-analysis. *Lancet neurology*. 2009;8:635-642

6. Hop JW, Rinkel GJ, Algra A, van Gijn J. Case-fatality rates and functional outcome after subarachnoid hemorrhage: A systematic review. *Stroke*. 1997;28:660-664

7. Naggara ON, Lecler A, Oppenheim C, Meder JF, Raymond J. Endovascular treatment of intracranial unruptured aneurysms: A systematic review of the literature on safety with emphasis on subgroup analyses. *Radiology*. 2012;263:828-835

8. Kotowski M, Naggara O, Darsaut TE, Nolet S, Gevry G, Kouznetsov E, et al. Safety and occlusion rates of surgical treatment of unruptured intracranial aneurysms: A systematic review and meta-analysis of the literature from 1990 to 2011. *J Neurol Neurosurg Psychiatry*. 2013;84:42-48

9. Molyneux A, Kerr R, Stratton I, Sandercock P, Clarke M, Shrimpton J, et al. International subarachnoid aneurysm trial (isat) of neurosurgical clipping versus endovascular coiling in 2143 patients with ruptured intracranial aneurysms: A randomized trial. *J Stroke Cerebrovasc Dis*. 2002;11:304-314

10. Molyneux AJ, Kerr RS, Yu LM, Clarke M, Sneade M, Yarnold JA, et al. International subarachnoid aneurysm trial (isat) of neurosurgical clipping versus endovascular coiling in 2143 patients with ruptured intracranial aneurysms: A randomised comparison of effects on survival, dependency, seizures, rebleeding, subgroups, and aneurysm occlusion. *Lancet*. 2005;366:809-817

11. Mitchell P, Kerr R, Mendelow AD, Molyneux A. Could late rebleeding overturn the superiority of cranial aneurysm coil embolization over clip ligation seen in the international subarachnoid aneurysm trial? *J Neurosurg*. 2008;108:437-442

12. Raymond J, Guilbert F, Weill A, Georganos SA, Juravsky L, Lambert A, et al. Long-term angiographic recurrences after selective endovascular treatment of aneurysms with detachable coils. *Stroke*. 2003;34:1398-1403

13. Ferns SP, Sprengers MES, van Rooij WJ, Rinkel GJE, van Rijn JC, Bipat S, et al. Coiling of intracranial aneurysms: A systematic review on initial occlusion and reopening and retreatment rates. *Stroke*. 2009;40:e523-529

14. Murayama Y, Nien YL, Duckwiler G, Gobin YP, Jahan R, Frazee J, et al. Guglielmi detachable coil embolization of cerebral aneurysms: 11 years' experience. *J Neurosurg*. 2003;98:959-966

15. Dorfer C, Gruber A, Standhardt H, Bavinzski G, Knosp E. Management of residual and recurrent aneurysms after initial endovascular treatment. *Neurosurgery*. 2012;70:537-553; discussion 553-534

16. Campi A, Ramzi N, Molyneux AJ, Summers PE, Kerr RS, Sneade M, et al. Retreatment of ruptured cerebral aneurysms in patients randomized by coiling or clipping in the international subarachnoid aneurysm trial (isat). *Stroke*. 2007;38:1538-1544

17. Willinsky RA, Peltz J, da Costa L, Agid R, Farb RI, terBrugge KG. Clinical and angiographic follow-up of ruptured intracranial aneurysms treated with endovascular embolization. *AJNR Am J Neuroradiol*. 2009;30:1035-1040

18. Frosen J, Tulamo R, Paetau A, Laaksamo E, Korja M, Laakso A, et al. Saccular intracranial aneurysm: Pathology and mechanisms. *Acta neuropathologica*. 2012;123:773-786

19. Rinkel GJ, Djibuti M, Algra A, van Gijn J. Prevalence and risk of rupture of intracranial aneurysms: A systematic review. *Stroke*. 1998;29:251-256

20. Vlak MH, Algra A, Brandenburg R, Rinkel GJ. Prevalence of unruptured intracranial aneurysms, with emphasis on sex, age, comorbidity, country,

and time period: A systematic review and meta-analysis. *Lancet neurology*. 2011;10:626-636

21. Inagawa T, Hirano A. Autopsy study of unruptured incidental intracranial aneurysms. *Surg Neurol*. 1990;34:361-365

22. Iwamoto H, Kiyohara Y, Fujishima M, Kato I, Nakayama K, Sueishi K, et al. Prevalence of intracranial saccular aneurysms in a japanese community based on a consecutive autopsy series during a 30-year observation period. The hisayama study. *Stroke*. 1999;30:1390-1395

23. McCormick WF, Nofzinger JD. Saccular intracranial aneurysms: An autopsy study. *J Neurosurg*. 1965;22:155-159

24. Igase K, Matsubara I, Igase M, Miyazaki H, Sadamoto K. Initial experience in evaluating the prevalence of unruptured intracranial aneurysms detected on 3-tesla mri. *Cerebrovasc Dis*. 2012;33:348-353

25. Housepian EM, Pool JL. A systematic analysis of intracranial aneurysms from the autopsy file of the presbyterian hospital, 1914 to 1956. *Journal of neuropathology and experimental neurology*. 1958;17:409-423

26. Kassell NF, Torner JC, Haley EC, Jr., Jane JA, Adams HP, Kongable GL. The international cooperative study on the timing of aneurysm surgery. Part 1: Overall management results. *J Neurosurg*. 1990;73:18-36

27. Dashti R, Hernesniemi J, Niemela M, Rinne J, Porras M, Lehecka M, et al. Microneurosurgical management of middle cerebral artery bifurcation aneurysms. *Surg Neurol*. 2007;67:441-456

28. Brisman JL, Song JK, Newell DW. Cerebral aneurysms. *The New England journal of medicine*. 2006;355:928-939

29. Schievink WI. Intracranial aneurysms. *The New England journal of medicine*. 1997;336:28-40

30. Cedzich C, Schramm J, Rockelein G. Multiple middle cerebral artery aneurysms in an infant. Case report. *J Neurosurg*. 1990;72:806-809

31. Inagawa T. Incidence and risk factors for multiple intracranial saccular aneurysms in patients with subarachnoid hemorrhage in izumo city, japan. *Acta Neurochir (Wien)*. 2009;151:1623-1630

32. Juvela S. Risk factors for multiple intracranial aneurysms. *Stroke*. 2000;31:392-397

33. Qureshi AI, Suarez JI, Parekh PD, Sung G, Geocadin R, Bhardwaj A, et al. Risk factors for multiple intracranial aneurysms. *Neurosurgery*. 1998;43:22-26; discussion 26-27

34. Crompton MR. Mechanism of growth and rupture in cerebral berry aneurysms. *British medical journal*. 1966;1:1138-1142

35. Juvela S, Hillbom M, Numminen H, Koskinen P. Cigarette smoking and alcohol consumption as risk factors for aneurysmal subarachnoid hemorrhage. *Stroke*. 1993;24:639-646

36. Kissela BM, Sauerbeck L, Woo D, Khoury J, Carrozzella J, Pancioli A, et al. Subarachnoid hemorrhage: A preventable disease with a heritable component. *Stroke*. 2002;33:1321-1326

37. Investigators UJ, Morita A, Kirino T, Hashi K, Aoki N, Fukuhara S, et al. The natural course of unruptured cerebral aneurysms in a japanese cohort. *The New England journal of medicine*. 2012;366:2474-2482

38. Beck J, Rohde S, Berkefeld J, Seifert V, Raabe A. Size and location of ruptured and unruptured intracranial aneurysms measured by 3-dimensional rotational angiography. *Surg Neurol*. 2006;65:18-25; discussion 25-17

39. Kemp WJ, 3rd, Fulkerson DH, Payner TD, Leipzig TJ, Horner TG, Palmer EL, et al. Risk of hemorrhage from de novo cerebral aneurysms. *J Neurosurg*. 2013;118:58-62

40. Villablanca JP, Duckwiler GR, Jahan R, Tateshima S, Martin NA, Frazee J, et al. Natural history of asymptomatic unruptured cerebral aneurysms evaluated at ct angiography: Growth and rupture incidence and correlation with epidemiologic risk factors. *Radiology*. 2013;269:258-265

41. Guresir E, Vatter H, Schuss P, Platz J, Konczalla J, de Rochement Rdu M, et al. Natural history of small unruptured anterior circulation aneurysms: A prospective cohort study. *Stroke*. 2013;44:3027-3031

42. Wiebers DO, Whisnant JP, Huston J, 3rd, Meissner I, Brown RD, Jr., Piepgras DG, et al. Unruptured intracranial aneurysms: Natural history, clinical outcome, and risks of surgical and endovascular treatment. *Lancet*. 2003;362:103-110

43. Raymond J, Guillemin F, Proust F, Molyneux AJ, Fox AJ, Claiborne JS, et al. Unruptured intracranial aneurysms. A critical review of the international study of unruptured intracranial aneurysms (isuia) and of appropriate methods to address the clinical problem. *Interv Neuroradiol*. 2008;14:85-96

44. Ujiie H, Tachibana H, Hiramatsu O, Hazel AL, Matsumoto T, Ogasawara Y, et al. Effects of size and shape (aspect ratio) on the hemodynamics of saccular aneurysms: A possible index for surgical treatment of intracranial aneurysms. *Neurosurgery*. 1999;45:119-129; discussion 129-130

45. Beck J, Rohde S, el Beltagy M, Zimmermann M, Berkefeld J, Seifert V, et al. Difference in configuration of ruptured and unruptured intracranial aneurysms determined by biplanar digital subtraction angiography. *Acta Neurochir (Wien)*. 2003;145:861-865; discussion 865

46. San Millan Ruiz D, Yilmaz H, Dehdashti AR, Alimenti A, de Tribolet N, Rufenacht DA. The perianeurysmal environment: Influence on saccular aneurysm shape and rupture. *AJNR Am J Neuroradiol*. 2006;27:504-512

47. Lin N, Ho A, Gross BA, Pieper S, Frerichs KU, Day AL, et al. Differences in simple morphological variables in ruptured and unruptured middle cerebral artery aneurysms. *J Neurosurg*. 2012;117:913-919

48. Raghavan ML, Ma B, Harbaugh RE. Quantified aneurysm shape and rupture risk. *J Neurosurg*. 2005;102:355-362

49. Kadasi LM, Dent WC, Malek AM. Colocalization of thin-walled dome regions with low hemodynamic wall shear stress in unruptured cerebral aneurysms. *J Neurosurg*. 2013;119:172-179

50. Kawaguchi T, Nishimura S, Kanamori M, Takazawa H, Omodaka S, Sato K, et al. Distinctive flow pattern of wall shear stress and oscillatory shear index: Similarity and dissimilarity in ruptured and unruptured cerebral aneurysm blebs. *J Neurosurg*. 2012;117:774-780

51. Xiang J, Natarajan SK, Tremmel M, Ma D, Mocco J, Hopkins LN, et al. Hemodynamic-morphologic discriminants for intracranial aneurysm rupture. *Stroke*. 2011;42:144-152

52. de Rooij NK, Velthuis BK, Algra A, Rinkel GJ. Configuration of the circle of willis, direction of flow, and shape of the aneurysm as risk factors for rupture of intracranial aneurysms. *J Neurol*. 2009;256:45-50

53. Rahman M, Smietana J, Hauck E, Hoh B, Hopkins N, Siddiqui A, et al. Size ratio correlates with intracranial aneurysm rupture status: A prospective study. *Stroke*. 2010;41:916-920

54. Kallmes DF. Point: Cfd--computational fluid dynamics or confounding factor dissemination. *AJNR Am J Neuroradiol*. 2012;33:395-396

55. Juvela S, Poussa K, Porras M. Factors affecting formation and growth of intracranial aneurysms: A long-term follow-up study. *Stroke*. 2001;32:485-491

56. Ishibashi T, Murayama Y, Urashima M, Saguchi T, Ebara M, Arakawa H, et al. Unruptured intracranial aneurysms: Incidence of rupture and risk factors. *Stroke*. 2009;40:313-316

57. Sonobe M, Yamazaki T, Yonekura M, Kikuchi H. Small unruptured intracranial aneurysm verification study: Suave study, japan. *Stroke*. 2010;41:1969-1977

58. Chien A, Liang F, Sayre J, Salamon N, Villablanca P, Vinuela F. Enlargement of small, asymptomatic, unruptured intracranial aneurysms in patients with no history of subarachnoid hemorrhage: The different factors related to the growth of single and multiple aneurysms. *J Neurosurg*. 2013;119:190-197

59. Juvela S. Prevalence of and risk factors for intracranial aneurysms. *Lancet neurology*. 2011;10:595-597

60. Feigin VL, Rinkel GJ, Lawes CM, Algra A, Bennett DA, van Gijn J, et al. Risk factors for subarachnoid hemorrhage: An updated systematic review of epidemiological studies. *Stroke*. 2005;36:2773-2780

61. Mhurchu CN, Anderson C, Jamrozik K, Hankey G, Dunbabin D, Australasian Cooperative Research on Subarachnoid Hemorrhage Study G. Hormonal factors and risk of aneurysmal subarachnoid hemorrhage: An international population-based, case-control study. *Stroke*. 2001;32:606-612

62. Ding C, Toll V, Ouyang B, Chen M. Younger age of menopause in women with cerebral aneurysms. *Journal of neurointerventional surgery*. 2013;5:327-331

63. Jamous MA, Nagahiro S, Kitazato KT, Satomi J, Satoh K. Role of estrogen deficiency in the formation and progression of cerebral aneurysms. Part i: Experimental study of the effect of oophorectomy in rats. *J Neurosurg*. 2005;103:1046-1051

64. Jamous MA, Nagahiro S, Kitazato KT, Tamura T, Kuwayama K, Satoh K. Role of estrogen deficiency in the formation and progression of cerebral aneurysms. Part ii: Experimental study of the effects of hormone replacement therapy in rats. *J Neurosurg*. 2005;103:1052-1057

65. Kim YW, Neal D, Hoh BL. Cerebral aneurysms in pregnancy and delivery: Pregnancy and delivery do not increase the risk of aneurysm rupture. *Neurosurgery*. 2013;72:143-149; discussion 150

66. Vlak MH, Rinkel GJ, Greebe P, Algra A. Risk of rupture of an intracranial aneurysm based on patient characteristics: A case-control study. *Stroke*. 2013;44:1256-1259

67. Inagawa T. Risk factors for the formation and rupture of intracranial saccular aneurysms in shimane, japan. *World neurosurgery*. 2010;73:155-164; discussion e123

68. Ariesen MJ, Claus SP, Rinkel GJ, Algra A. Risk factors for intracerebral hemorrhage in the general population: A systematic review. *Stroke*. 2003;34:2060-2065

69. Inagawa T. Risk factors for aneurysmal subarachnoid hemorrhage in patients in izumo city, japan. *J Neurosurg*. 2005;102:60-67

70. Marbacher S, Schlappi JA, Fung C, Husler J, Beck J, Raabe A. Do statins reduce the risk of aneurysm development? A case-control study. *J Neurosurg*. 2012;116:638-642

71. Vlak MH, Rinkel GJ, Greebe P, Algra A. Independent risk factors for intracranial aneurysms and their joint effect: A case-control study. *Stroke*. 2013;44:984-987

72. Ruigrok YM, Buskens E, Rinkel GJ. Attributable risk of common and rare determinants of subarachnoid hemorrhage. *Stroke*. 2001;32:1173-1175

73. Raaymakers D, Buijs P. Magnetic resonance angiography detection of four asymptomatic intracranial aneurysms. *Cerebrovasc Dis*. 1998;8:78

74. Ronkainen A, Hernesniemi J, Puranen M, Niemitukia L, Vanninen R, Ryynanen M, et al. Familial intracranial aneurysms. *Lancet*. 1997;349:380-384

75. Mackey J, Brown RD, Jr., Moomaw CJ, Sauerbeck L, Hornung R, Gandhi D, et al. Unruptured intracranial aneurysms in the familial intracranial aneurysm and international study of unruptured intracranial aneurysms cohorts: Differences in multiplicity and location. *J Neurosurg*. 2012;117:60-64

76. Ruigrok YM, Rinkel GJ, Algra A, Raaymakers TW, Van Gijn J. Characteristics of intracranial aneurysms in patients with familial subarachnoid hemorrhage. *Neurology*. 2004;62:891-894

77. van den Berg JS, Limburg M, Hennekam RC. Is marfan syndrome associated with symptomatic intracranial aneurysms? *Stroke*. 1996;27:10-12

78. Schievink WI. Marfan syndrome and intracranial aneurysms. *Stroke*. 1999;30:2767-2768

79. Korja M, Silventoinen K, McCarron P, Zdravkovic S, Skytthe A, Haapanen A, et al. Genetic epidemiology of spontaneous subarachnoid hemorrhage: Nordic twin study. *Stroke*. 2010;41:2458-2462

80. Ruigrok YM, Rinkel GJ. Genetics of intracranial aneurysms. *Stroke*. 2008;39:1049-1055

81. Krischek B, Inoue I. The genetics of intracranial aneurysms. *J Hum Genet*. 2006;51:587-594

82. Alg VS, Sofat R, Houlden H, Werring DJ. Genetic risk factors for intracranial aneurysms: A meta-analysis in more than 116,000 individuals. *Neurology*. 2013;80:2154-2165

83. Ruigrok YM, Wijmenga C, Rinkel GJ, van't Slot R, Baas F, Wolfs M, et al. Genomewide linkage in a large dutch family with intracranial aneurysms: Replication of 2 loci for intracranial aneurysms to chromosome 1p36.11-p36.13 and xp22.2-p22.32. *Stroke*. 2008;39:1096-1102

84. Bilguvar K, Yasuno K, Niemela M, Ruigrok YM, von Und Zu Fraunberg M, van Duijn CM, et al. Susceptibility loci for intracranial aneurysm in european and japanese populations. *Nature genetics*. 2008;40:1472-1477

85. Helgadottir A, Thorleifsson G, Magnusson KP, Gretarsdottir S, Steinthorsdottir V, Manolescu A, et al. The same sequence variant on 9p21 associates with myocardial infarction, abdominal aortic aneurysm and intracranial aneurysm. *Nature genetics*. 2008;40:217-224

86. Leeper NJ, Raiesdana A, Kojima Y, Kundu RK, Cheng H, Maegdefessel L, et al. Loss of cdkn2b promotes p53-dependent smooth muscle cell apoptosis and aneurysm formation. *Arteriosclerosis, thrombosis, and vascular biology*. 2013;33:e1-e10

87. Matsui T, Kanai-Azuma M, Hara K, Matoba S, Hiramatsu R, Kawakami H, et al. Redundant roles of sox17 and sox18 in postnatal angiogenesis in mice. *Journal of cell science*. 2006;119:3513-3526

88. Kim I, Saunders TL, Morrison SJ. Sox17 dependence distinguishes the transcriptional regulation of fetal from adult hematopoietic stem cells. *Cell*. 2007;130:470-483

89. Yasuno K, Bilguvar K, Bijlenga P, Low SK, Krischek B, Auburger G, et al. Genome-wide association study of intracranial aneurysm identifies three new risk loci. *Nature genetics*. 2010;42:420-425

90. Yasuno K, Bakircioglu M, Low SK, Bilguvar K, Gaal E, Ruigrok YM, et al. Common variant near the endothelin receptor type a (ednra) gene is associated with intracranial aneurysm risk. *Proceedings of the National Academy of Sciences of the United States of America*. 2011;108:19707-19712

91. Low SK, Takahashi A, Cha PC, Zembutsu H, Kamatani N, Kubo M, et al. Genome-wide association study for intracranial aneurysm in the japanese population identifies three candidate susceptible loci and a functional genetic variant at ednra. *Human molecular genetics*. 2012;21:2102-2110

92. Gaetani P, Tartara F, Grazioli V, Tancioni F, Infuso L, Rodriguez y Baena R. Collagen cross-linkage, elastolytic and collagenolytic activities in cerebral aneurysms: A preliminary investigation. *Life Sci*. 1998;63:285-292

93. Stehbens WE. Etiology of intracranial berry aneurysms. *J Neurosurg*. 1989;70:823-831

94. Nystroem SH. Development of intracranial aneurysms as revealed by electron microscopy. *J Neurosurg*. 1963;20:329-337

95. Alpers BJ, Berry RG, Paddison RM. Anatomical studies of the circle of willis in normal brain. *A.M.A. archives of neurology and psychiatry*. 1959;81:409-418

96. Connolly ES, Jr., Huang J, Goldman JE, Holtzman RN. Immunohistochemical detection of intracranial vasa vasorum: A human autopsy study. *Neurosurgery*. 1996;38:789-793

97. Forbus W. On the origin of miliary aneurysms of superficial cerebral arteries. *Bull Johns Hopkins Hosp*. 1930;47:239-284

98. Stehbens WE. Aneurysms and anatomical variation of cerebral arteries. *Archives of pathology*. 1963;75:45-64

99. Finlay HM, Whittaker P, Canham PB. Collagen organization in the branching region of human brain arteries. *Stroke*. 1998;29:1595-1601

100. Kataoka K, Taneda M, Asai T, Kinoshita A, Ito M, Kuroda R. Structural fragility and inflammatory response of ruptured cerebral aneurysms. A comparative study between ruptured and unruptured cerebral aneurysms. *Stroke*. 1999;30:1396-1401

101. Scanarini M, Mingrino S, Giordano R, Baroni A. Histological and ultrastructural study of intracranial saccular aneurysmal wall. *Acta Neurochir (Wien)*. 1978;43:171-182

102. Frosen J, Piippo A, Paetau A, Kangasniemi M, Niemela M, Hernesniemi J, et al. Remodeling of saccular cerebral artery aneurysm wall is associated with rupture: Histological analysis of 24 unruptured and 42 ruptured cases. *Stroke*. 2004;35:2287-2293

103. Schlote W, Gaus C. Histologic aspects from ruptured and nonruptured aneurysms. *Neurol Res*. 1994;16:59-62

104. Thyberg J. Phenotypic modulation of smooth muscle cells during formation of neointimal thickenings following vascular injury. *Histology and histopathology*. 1998;13:871-891

105. Kosierkiewicz TA, Factor SM, Dickson DW. Immunocytochemical studies of atherosclerotic lesions of cerebral berry aneurysms. *Journal of neuropathology and experimental neurology*. 1994;53:399-406

106. Nakajima N, Nagahiro S, Sano T, Satomi J, Satoh K. Phenotypic modulation of smooth muscle cells in human cerebral aneurysmal walls. *Acta neuropathologica*. 2000;100:475-480

107. Kilic T, Sohrabifar M, Kurtkaya O, Yildirim O, Elmaci I, Gunel M, et al. Expression of structural proteins and angiogenic factors in normal arterial and unruptured and ruptured aneurysm walls. *Neurosurgery*. 2005;57:997-1007; discussion 1997-1007

108. Kurki MI, Hakkinen SK, Frosen J, Tulamo R, von und zu Fraunberg M, Wong G, et al. Upregulated signaling pathways in ruptured human saccular intracranial aneurysm wall: An emerging regulative role of toll-like receptor signaling and nuclear factor-kappab, hypoxia-inducible factor-1a, and ets transcription factors. *Neurosurgery*. 2011;68:1667-1675; discussion 1675-1666

109. Jayaraman T, Berenstein V, Li X, Mayer J, Silane M, Shin YS, et al. Tumor necrosis factor alpha is a key modulator of inflammation in cerebral aneurysms. *Neurosurgery*. 2005;57:558-564; discussion 558-564

110. Moriwaki T, Takagi Y, Sadamasa N, Aoki T, Nozaki K, Hashimoto N. Impaired progression of cerebral aneurysms in interleukin-1beta-deficient mice. *Stroke*. 2006;37:900-905

111. Chyatte D, Bruno G, Desai S, Todor DR. Inflammation and intracranial aneurysms. *Neurosurgery*. 1999;45:1137-1146; discussion 1146-1137

112. Tulamo R, Frosen J, Junnikkala S, Paetau A, Pitkaniemi J, Kangasniemi M, et al. Complement activation associates with saccular cerebral artery aneurysm wall degeneration and rupture. *Neurosurgery*. 2006;59:1069-1076; discussion 1076-1067

113. Tulamo R, Frosen J, Paetau A, Seitsonen S, Hernesniemi J, Niemela M, et al. Lack of complement inhibitors in the outer intracranial artery aneurysm wall associates with complement terminal pathway activation. *The American journal of pathology*. 2010;177:3224-3232

114. Tulamo R, Frosen J, Junnikkala S, Paetau A, Kangasniemi M, Pelaez J, et al. Complement system becomes activated by the classical pathway in intracranial aneurysm walls. *Laboratory investigation; a journal of technical methods and pathology*. 2010;90:168-179

115. Laaksamo E, Tulamo R, Liiman A, Baumann M, Friedlander RM, Hernesniemi J, et al. Oxidative stress is associated with cell death, wall degradation, and increased risk of rupture of the intracranial aneurysm wall. *Neurosurgery*. 2013;72:109-117

116. Aoki T, Nishimura M, Kataoka H, Ishibashi R, Nozaki K, Hashimoto N. Reactive oxygen species modulate growth of cerebral aneurysms: A study using the free radical scavenger edaravone and p47phox(-/-) mice. *Laboratory investigation; a journal of technical methods and pathology*. 2009;89:730-741

117. Sadamasa N, Nozaki K, Hashimoto N. Disruption of gene for inducible nitric oxide synthase reduces progression of cerebral aneurysms. *Stroke*. 2003;34:2980-2984

118. Inci S, Spetzler RF. Intracranial aneurysms and arterial hypertension: A review and hypothesis. *Surg Neurol*. 2000;53:530-540; discussion 540-532

119. Sakaki T, Kohmura E, Kishiguchi T, Yuguchi T, Yamashita T, Hayakawa T. Loss and apoptosis of smooth muscle cells in intracranial aneurysms. Studies with in situ DNA end labeling and antibody against single-stranded DNA. *Acta Neurochir (Wien)*. 1997;139:469-474; discussion 474-465

120. Pentimalli L, Modesti A, Vignati A, Marchese E, Albanese A, Di Rocco F, et al. Role of apoptosis in intracranial aneurysm rupture. *J Neurosurg*. 2004;101:1018-1025

121. Guo F, Li Z, Song L, Han T, Feng Q, Guo Y, et al. Increased apoptosis and cysteinyl aspartate specific protease-3 gene expression in human intracranial aneurysm. *J Clin Neurosci*. 2007;14:550-555

122. Martin-Ventura JL, Madrigal-Matute J, Martinez-Pinna R, Ramos-Mozo P, Blanco-Colio LM, Moreno JA, et al. Erythrocytes, leukocytes and platelets as a source of oxidative stress in chronic vascular diseases: Detoxifying mechanisms and potential therapeutic options. *Thrombosis and haemostasis*. 2012;108:435-442

123. Zheng Y, Gardner SE, Clarke MC. Cell death, damage-associated molecular patterns, and sterile inflammation in cardiovascular disease. *Arteriosclerosis, thrombosis, and vascular biology*. 2011;31:2781-2786

124. Lee S, Birukov KG, Romanoski CE, Springstead JR, Lusis AJ, Berliner JA. Role of phospholipid oxidation products in atherosclerosis. *Circ Res*. 2012;111:778-799

125. Aoki T, Kataoka H, Ishibashi R, Nozaki K, Hashimoto N. Gene expression profile of the intima and media of experimentally induced cerebral aneurysms in rats by laser-microdissection and microarray techniques. *International journal of molecular medicine*. 2008;22:595-603

126. Kondo S, Hashimoto N, Kikuchi H, Hazama F, Nagata I, Kataoka H. Apoptosis of medial smooth muscle cells in the development of saccular cerebral aneurysms in rats. *Stroke*. 1998;29:181-188; discussion 189

127. Aoki T, Kataoka H, Ishibashi R, Nozaki K, Morishita R, Hashimoto N. Reduced collagen biosynthesis is the hallmark of cerebral aneurysm: Contribution of interleukin-1beta and nuclear factor-kappab. *Arteriosclerosis, thrombosis, and vascular biology*. 2009;29:1080-1086

128. Bygglin H, Laaksamo E, Myllarniemi M, Tulamo R, Hernesniemi J, Niemela M, et al. Isolation, culture, and characterization of smooth muscle cells from human intracranial aneurysms. *Acta Neurochir (Wien)*. 2011;153:311-318

129. Aoki T, Kataoka H, Ishibashi R, Nozaki K, Egashira K, Hashimoto N. Impact of monocyte chemoattractant protein-1 deficiency on cerebral aneurysm formation. *Stroke*. 2009;40:942-951

130. Kanematsu Y, Kanematsu M, Kurihara C, Tada Y, Tsou TL, van Rooijen N, et al. Critical roles of macrophages in the formation of intracranial aneurysm. *Stroke*. 2011;42:173-178

131. Aoki T, Kataoka H, Shimamura M, Nakagami H, Wakayama K, Moriwaki T, et al. Nf-kappab is a key mediator of cerebral aneurysm formation. *Circulation*. 2007;116:2830-2840

132. Aoki T, Kataoka H, Nishimura M, Ishibashi R, Morishita R, Miyamoto S. Regression of intracranial aneurysms by simultaneous inhibition of nuclear

factor-kappab and ets with chimeric decoy oligodeoxynucleotide treatment. *Neurosurgery*. 2012;70:1534-1543; discussion 1543

133. Ishibashi R, Aoki T, Nishimura M, Hashimoto N, Miyamoto S. Contribution of mast cells to cerebral aneurysm formation. *Current neurovascular research*. 2010;7:113-124

134. Morgan L, Cooper J, Montgomery H, Kitchen N, Humphries SE. The interleukin-6 gene -174g>c and -572g>c promoter polymorphisms are related to cerebral aneurysms. *J Neurol Neurosurg Psychiatry*. 2006;77:915-917

135. de Gast AN, Altes TA, Marx WF, Do HM, Helm GA, Kallmes DF. Transforming growth factor beta-coated platinum coils for endovascular treatment of aneurysms: An animal study. *Neurosurgery*. 2001;49:690-694; discussion 694-696

136. Grosskreutz CL, Anand-Apte B, Duplaa C, Quinn TP, Terman BI, Zetter B, et al. Vascular endothelial growth factor-induced migration of vascular smooth muscle cells in vitro. *Microvascular research*. 1999;58:128-136

137. Futami K, Yamashita J, Tachibana O, Kida S, Higashi S, Ikeda K, et al. Basic fibroblast growth factor may repair experimental cerebral aneurysms in rats. *Stroke*. 1995;26:1649-1654

138. Frosen J, Piippo A, Paetau A, Kangasniemi M, Niemela M, Hernesniemi J, et al. Growth factor receptor expression and remodeling of saccular cerebral artery aneurysm walls: Implications for biological therapy preventing rupture. *Neurosurgery*. 2006;58:534-541; discussion 534-541

139. Aoki T, Nishimura M, Kataoka H, Ishibashi R, Nozaki K, Miyamoto S. Complementary inhibition of cerebral aneurysm formation by enos and nnos. *Laboratory investigation; a journal of technical methods and pathology*. 2011;91:619-626

140. Frosen J, Marjamaa J, Myllarniemi M, Abo-Ramadan U, Tulamo R, Niemela M, et al. Contribution of mural and bone marrow-derived neointimal cells to thrombus organization and wall remodeling in a microsurgical murine saccular aneurysm model. *Neurosurgery*. 2006;58:936-944; discussion 936-944

141. Fontaine V, Jacob MP, Houard X, Rossignol P, Plissonnier D, Angles-Cano E, et al. Involvement of the mural thrombus as a site of protease release and activation in human aortic aneurysms. *The American journal of pathology*. 2002;161:1701-1710

142. Fontaine V, Touat Z, Mtairag el M, Vranckx R, Louedec L, Houard X, et al. Role of leukocyte elastase in preventing cellular re-colonization of the mural thrombus. *The American journal of pathology*. 2004;164:2077-2087

143. Becker TA, Preul MC, Bichard WD, Kipke DR, McDougall CG. Preliminary investigation of calcium alginate gel as a biocompatible material for endovascular aneurysm embolization in vivo. *Neurosurgery*. 2007;60:1119-1127; discussion 1127-1118

144. Raymond J, Darsaut TE, Kotowski M, Makoyeva A, Gevry G, Berthelet F, et al. Thrombosis heralding aneurysmal rupture: An exploration of potential mechanisms in a novel giant swine aneurysm model. *AJNR Am J Neuroradiol*. 2012

145. Hampton T, Walsh D, Tolias C, Fiorella D. Mural destabilization after aneurysm treatment with a flow-diverting device: A report of two cases. *Journal of neurointerventional surgery*. 2011;3:167-171

146. Kulcsar Z, Houdart E, Bonafe A, Parker G, Millar J, Goddard AJ, et al. Intra-aneurysmal thrombosis as a possible cause of delayed aneurysm rupture after flow-diversion treatment. *AJNR Am J Neuroradiol*. 2011;32:20-25

147. Tamatani S, Ito Y, Abe H, Koike T, Takeuchi S, Tanaka R. Evaluation of the stability of aneurysms after embolization using detachable coils: Correlation between stability of aneurysms and embolized volume of aneurysms. *AJNR Am J Neuroradiol*. 2002;23:762-767

148. Cloft HJ, Kallmes DF. Aneurysm packing with hydrocoil embolic system versus platinum coils: Initial clinical experience. *AJNR Am J Neuroradiol*. 2004;25:60-62

149. Sherif C, Plenk H, Jr., Grossschmidt K, Kanz F, Bavinzski G. Computer-assisted quantification of occlusion and coil densities on angiographic and histological images of experimental aneurysms. *Neurosurgery*. 2006;58:559-566; discussion 559-566

150. Crobeddu E, Lanzino G, Kallmes DF, Cloft HJ. Review of 2 decades of aneurysm-recurrence literature, part 2: Managing recurrence after endovascular coiling. *AJNR Am J Neuroradiol*. 2013;34:481-485

151. Satoh K, Matsubara S, Hondoh H, Nagahiro S. Intracranial aneurysm embolization using interlocking detachable coils. Correlation between volume embolization rate and coil compaction. *Interv Neuroradiol*. 1997;3 Suppl 2:125-128

152. Kawanabe Y, Sadato A, Taki W, Hashimoto N. Endovascular occlusion of intracranial aneurysms with guglielmi detachable coils: Correlation between coil packing density and coil compaction. *Acta Neurochir (Wien)*. 2001;143:451-455

153. Uchiyama N, Kida S, Nomura M, Hasegawa M, Yamashima T, Yamashita J, et al. Significance of volume embolization ratio as a predictor of recanalization on endovascular treatment of cerebral aneurysms with guglielmi detachable coils. *Interv Neuroradiol*. 2000;6 Suppl 1:59-63

154. Chalouhi N, Tjoumakaris S, Gonzalez LF, Dumont AS, Starke RM, Hasan D, et al. Coiling of large and giant aneurysms: Complications and long-term results of 334 cases. *AJNR Am J Neuroradiol*. 2013

155. Sluzewski M, Menovsky T, van Rooij WJ, Wijnalda D. Coiling of very large or giant cerebral aneurysms: Long-term clinical and serial angiographic results. *AJNR Am J Neuroradiol*. 2003;24:257-262

156. van Rooij WJ, Sluzewski M. Coiling of very large and giant basilar tip aneurysms: Midterm clinical and angiographic results. *AJNR Am J Neuroradiol*. 2007;28:1405-1408

157. Molyneux AJ, Ellison DW, Morris J, Byrne JV. Histological findings in giant aneurysms treated with guglielmi detachable coils. Report of two cases with autopsy correlation. *J Neurosurg*. 1995;83:129-132

158. Byrne JV, Adams CB, Kerr RS, Molyneux AJ. Endosaccular treatment of inoperable intracranial aneurysms with platinum coils. *Br J Neurosurg*. 1995;9:585-592

159. Tateshima S, Murayama Y, Gobin YP, Duckwiler GR, Guglielmi G, Vinuela F. Endovascular treatment of basilar tip aneurysms using guglielmi detachable coils: Anatomic and clinical outcomes in 73 patients from a single institution. *Neurosurgery*. 2000;47:1332-1339; discussion 1339-1342

160. Ferns SP, van Rooij WJ, Sluzewski M, van den Berg R, Majoie CB. Partially thrombosed intracranial aneurysms presenting with mass effect: Long-term clinical and imaging follow-up after endovascular treatment. *AJNR Am J Neuroradiol*. 2010;31:1197-1205

161. van Rooij WJ, Sprengers ME, Sluzewski M, Beute GN. Intracranial aneurysms that repeatedly reopen over time after coiling: Imaging characteristics and treatment outcome. *Neuroradiology*. 2007;49:343-349

162. de Rooij NK, Linn FH, van der Plas JA, Algra A, Rinkel GJ. Incidence of subarachnoid haemorrhage: A systematic review with emphasis on region,

age, gender and time trends. *J Neurol Neurosurg Psychiatry*. 2007;78:1365-1372

163. Ingall T, Asplund K, Mahonen M, Bonita R. A multinational comparison of subarachnoid hemorrhage epidemiology in the who monica stroke study. *Stroke*. 2000;31:1054-1061

164. Broderick JP, Brott T, Tomsick T, Huster G, Miller R. The risk of subarachnoid and intracerebral hemorrhages in blacks as compared with whites. *The New England journal of medicine*. 1992;326:733-736

165. Mayberg MR, Batjer HH, Dacey R, Diringer M, Haley EC, Heros RC, et al. Guidelines for the management of aneurysmal subarachnoid hemorrhage. A statement for healthcare professionals from a special writing group of the stroke council, american heart association. *Stroke*. 1994;25:2315-2328

166. Hajat C, Dundas R, Stewart JA, Lawrence E, Rudd AG, Howard R, et al. Cerebrovascular risk factors and stroke subtypes: Differences between ethnic groups. *Stroke*. 2001;32:37-42

167. Ohkuma H, Fujita S, Suzuki S. Incidence of aneurysmal subarachnoid hemorrhage in shimokita, japan, from 1989 to 1998. *Stroke*. 2002;33:195-199

168. Taylor TN, Davis PH, Torner JC, Holmes J, Meyer JW, Jacobson MF. Lifetime cost of stroke in the united states. *Stroke*. 1996;27:1459-1466

169. Feigin VL, Lawes CM, Bennett DA, Barker-Collo SL, Parag V. Worldwide stroke incidence and early case fatality reported in 56 population-based studies: A systematic review. *Lancet neurology*. 2009;8:355-369

170. Beck J, Raabe A, Szelenyi A, Berkefeld J, Gerlach R, Setzer M, et al. Sentinel headache and the risk of rebleeding after aneurysmal subarachnoid hemorrhage. *Stroke*. 2006;37:2733-2737

171. Sames TA, Storrow AB, Finkelstein JA, Magoon MR. Sensitivity of new-generation computed tomography in subarachnoid hemorrhage. *Academic emergency medicine : official journal of the Society for Academic Emergency Medicine*. 1996;3:16-20

172. Matouk CC, Mandell DM, Gunel M, Bulsara KR, Malhotra A, Hebert R, et al. Vessel wall magnetic resonance imaging identifies the site of rupture in patients with multiple intracranial aneurysms: Proof of principle. *Neurosurgery*. 2013;72:492-496; discussion 496

173. Edlow JA, Caplan LR. Avoiding pitfalls in the diagnosis of subarachnoid hemorrhage. *The New England journal of medicine*. 2000;342:29-36

174. Backes D, Rinkel GJ, Kemperman H, Linn FH, Vergouwen MD. Time-dependent test characteristics of head computed tomography in patients suspected of nontraumatic subarachnoid hemorrhage. *Stroke*. 2012;43:2115-2119

175. Perry JJ, Stiell IG, Sivilotti ML, Bullard MJ, Emond M, Symington C, et al. Sensitivity of computed tomography performed within six hours of onset of headache for diagnosis of subarachnoid haemorrhage: Prospective cohort study. *Bmj*. 2011;343:d4277

176. Horstman P, Linn FH, Voorbij HA, Rinkel GJ. Chance of aneurysm in patients suspected of sah who have a 'negative' ct scan but a 'positive' lumbar puncture. *J Neurol*. 2012;259:649-652

177. Dalyai R, Chalouhi N, Theofanis T, Jabbour PM, Dumont AS, Gonzalez LF, et al. Subarachnoid hemorrhage with negative initial catheter angiography: A review of 254 cases evaluating patient clinical outcome and efficacy of short- and long-term repeat angiography. *Neurosurgery*. 2013;72:646-652; discussion 651-642

178. Hunt WE, Hess RM. Surgical risk as related to time of intervention in the repair of intracranial aneurysms. *J Neurosurg*. 1968;28:14-20

179. Botterell EH, Lougheed WM, Scott JW, Vandewater SL. Hypothermia, and interruption of carotid, or carotid and vertebral circulation, in the surgical management of intracranial aneurysms. *J Neurosurg*. 1956;13:1-42

180. Teasdale GM, Drake CG, Hunt W, Kassell N, Sano K, Pertuiset B, et al. A universal subarachnoid hemorrhage scale: Report of a committee of the world federation of neurosurgical societies. *J Neurol Neurosurg Psychiatry*. 1988;51:1457

181. Teasdale G, Jennett B. Assessment of coma and impaired consciousness. A practical scale. *Lancet*. 1974;2:81-84

182. Aulmann C, Steudl WI, Feldmann U. [validation of the prognostic accuracy of neurosurgical admission scales after rupture of cerebral aneurysms]. *Zentralblatt fur Neurochirurgie*. 1998;59:171-180

183. Wilson DA, Nakaji P, Abla AA, Uschold TD, Fusco DJ, Oppenlander ME, et al. A simple and quantitative method to predict symptomatic vasospasm after subarachnoid hemorrhage based on computed tomography: Beyond the fisher scale. *Neurosurgery*. 2012;71:869-875

184. Molyneux A, Kerr R, Stratton I, Sandercock P, Clarke M, Shrimpton J, et al. International subarachnoid aneurysm trial (isat) of neurosurgical clipping versus endovascular coiling in 2143 patients with ruptured intracranial aneurysms: A randomised trial. *Lancet*. 2002;360:1267-1274

185. Fujii Y, Takeuchi S, Sasaki O, Minakawa T, Koike T, Tanaka R. Ultra-early rebleeding in spontaneous subarachnoid hemorrhage. *J Neurosurg*. 1996;84:35-42

186. Lord AS, Fernandez L, Schmidt JM, Mayer SA, Claassen J, Lee K, et al. Effect of rebleeding on the course and incidence of vasospasm after subarachnoid hemorrhage. *Neurology*. 2012;78:31-37

187. De Marchis GM, Lantigua H, Schmidt JM, Lord AS, Velander AJ, Fernandez A, et al. Impact of premorbid hypertension on haemorrhage severity and aneurysm rebleeding risk after subarachnoid haemorrhage. *J Neurol Neurosurg Psychiatry*. 2013

188. Starke RM, Connolly ES, Jr., Participants in the International Multi-Disciplinary Consensus Conference on the Critical Care Management of Subarachnoid H. Rebleeding after aneurysmal subarachnoid hemorrhage. *Neurocrit Care*. 2011;15:241-246

189. Kassell NF, Sasaki T, Colohan AR, Nazar G. Cerebral vasospasm following aneurysmal subarachnoid hemorrhage. *Stroke*. 1985;16:562-572

190. Macdonald RL, Higashida RT, Keller E, Mayer SA, Molyneux A, Raabe A, et al. Clazosentan, an endothelin receptor antagonist, in patients with aneurysmal subarachnoid haemorrhage undergoing surgical clipping: A randomised, double-blind, placebo-controlled phase 3 trial (conscious-2). *Lancet neurology*. 2011;10:618-625

191. Macdonald RL, Kassell NF, Mayer S, Ruefenacht D, Schmiedek P, Weidauer S, et al. Clazosentan to overcome neurological ischemia and infarction occurring after subarachnoid hemorrhage (conscious-1): Randomized, double-blind, placebo-controlled phase 2 dose-finding trial. *Stroke*. 2008;39:3015-3021

192. Vajkoczy P, Meyer B, Weidauer S, Raabe A, Thome C, Ringel F, et al. Clazosentan (axv-034343), a selective endothelin a receptor antagonist, in the prevention of cerebral vasospasm following severe aneurysmal subarachnoid hemorrhage: Results of a randomized, double-blind, placebo-controlled, multicenter phase iia study. *J Neurosurg*. 2005;103:9-17

193. Crowley RW, Medel R, Dumont AS, Ilodigwe D, Kassell NF, Mayer SA, et al. Angiographic vasospasm is strongly correlated with cerebral infarction after subarachnoid hemorrhage. *Stroke*. 2011;42:919-923

124

194. Wartenberg KE, Mayer SA. Medical complications after subarachnoid hemorrhage. *Neurosurg Clin N Am*. 2010;21:325-338

195. Broderick JP, Brott TG, Duldner JE, Tomsick T, Leach A. Initial and recurrent bleeding are the major causes of death following subarachnoid hemorrhage. *Stroke*. 1994;25:1342-1347

196. Al-Khindi T, Macdonald RL, Schweizer TA. Decision-making deficits persist after aneurysmal subarachnoid hemorrhage. *Neuropsychology*. 2013

197. Ronkainen A, Niskanen M, Rinne J, Koivisto T, Hernesniemi J, Vapalahti M. Evidence for excess long-term mortality after treated subarachnoid hemorrhage. *Stroke*. 2001;32:2850-2853

198. Bernal J, Baldwin M, Gleason T, Kuhlman S, Moore G, Talcott M. Guidelines for rodent survival surgery. *Journal of investigative surgery : the official journal of the Academy of Surgical Research*. 2009;22:445-451

199. Pyysalo L, Luostarinen T, Keski-Nisula L, Ohman J. Long-term excess mortality of patients with treated and untreated unruptured intracranial aneurysms. *J Neurol Neurosurg Psychiatry*. 2013;84:888-892

200. Connolly ES, Jr., Rabinstein AA, Carhuapoma JR, Derdeyn CP, Dion J, Higashida RT, et al. Guidelines for the management of aneurysmal subarachnoid hemorrhage: A guideline for healthcare professionals from the american heart association/american stroke association. *Stroke*. 2012;43:1711-1737

201. Bederson JB, Connolly ES, Jr., Batjer HH, Dacey RG, Dion JE, Diringer MN, et al. Guidelines for the management of aneurysmal subarachnoid hemorrhage: A statement for healthcare professionals from a special writing group of the stroke council, american heart association. *Stroke*. 2009;40:994-1025

202. Steiner T, Juvela S, Unterberg A, Jung C, Forsting M, Rinkel G, et al. European stroke organization guidelines for the management of intracranial aneurysms and subarachnoid haemorrhage. *Cerebrovasc Dis*. 2013;35:93-112

203. Boogaarts HD, van Amerongen MJ, de Vries J, Westert GP, Verbeek AL, Grotenhuis JA, et al. Caseload as a factor for outcome in aneurysmal subarachnoid hemorrhage: A systematic review and meta-analysis. *J Neurosurg*. 2013

204. Kassell NF, Torner JC, Jane JA, Haley EC, Jr., Adams HP. The international cooperative study on the timing of aneurysm surgery. Part 2: Surgical results. *J Neurosurg*. 1990;73:37-47

205. Ohman J, Heiskanen O. Timing of operation for ruptured supratentorial aneurysms: A prospective randomized study. *J Neurosurg*. 1989;70:55-60

206. Lawson MF, Chi YY, Velat GJ, Mocco JD, Hoh BL. Timing of aneurysm surgery: The international cooperative study revisited in the era of endovascular coiling. *Journal of neurointerventional surgery*. 2010;2:131-134

207. McDougall CG, Spetzler RF, Zabramski JM, Partovi S, Hills NK, Nakaji P, et al. The barrow ruptured aneurysm trial. *J Neurosurg*. 2012;116:135-144

208. Spetzler RF, McDougall CG, Albuquerque FC, Zabramski JM, Hills NK, Partovi S, et al. The barrow ruptured aneurysm trial: 3-year results. *J Neurosurg*. 2013;119:146-157

209. Proust F, Martinaud O, Gerardin E, Derrey S, Leveque S, Bioux S, et al. Quality of life and brain damage after microsurgical clip occlusion or endovascular coil embolization for ruptured anterior communicating artery aneurysms: Neuropsychological assessment. *J Neurosurg*. 2009;110:19-29

210. Li H, Pan R, Wang H, Rong X, Yin Z, Milgrom DP, et al. Clipping versus coiling for ruptured intracranial aneurysms: A systematic review and meta-analysis. *Stroke*. 2013;44:29-37

211. Hernesniemi J, Dashti R, Niemela M, Romani R, Rinne J, Jaaskelainen JE. Microsurgical and angiographic anatomy of middle cerebral artery aneurysm. *Neurosurgery*. 2010;66:E1030

212. Rinne J, Hernesniemi J, Niskanen M, Vapalahti M. Analysis of 561 patients with 690 middle cerebral artery aneurysms: Anatomic and clinical features as correlated to management outcome. *Neurosurgery*. 1996;38:2-11

213. Marbacher S, Fandino J, Lukes A. Acute subdural hematoma from ruptured cerebral aneurysm. *Acta Neurochir (Wien)*. 2010;152:501-507

214. Regli L, Dehdashti AR, Uske A, de Tribolet N. Endovascular coiling compared with surgical clipping for the treatment of unruptured middle cerebral artery aneurysms: An update. *Acta Neurochir Suppl*. 2002;82:41-46

215. Sturiale CL, Brinjikji W, Murad MH, Lanzino G. Endovascular treatment of intracranial aneurysms in elderly patients: A systematic review and meta-analysis. *Stroke*. 2013;44:1897-1902

216. Lubicz B, Leclerc X, Gauvrit JY, Lejeune JP, Pruvo JP. Endovascular treatment of ruptured intracranial aneurysms in elderly people. *AJNR Am J Neuroradiol*. 2004;25:592-595

217. Kremer C, Groden C, Hansen HC, Grzyska U, Zeumer H. Outcome after endovascular treatment of hunt and hess grade iv or v aneurysms: Comparison of anterior versus posterior circulation. *Stroke*. 1999;30:2617-2622

218. Lusseveld E, Brilstra EH, Nijssen PC, van Rooij WJ, Sluzewski M, Tulleken CA, et al. Endovascular coiling versus neurosurgical clipping in patients with a ruptured basilar tip aneurysm. *J Neurol Neurosurg Psychiatry*. 2002;73:591-593

219. Darsaut TE, Jack AS, Kerr RS, Raymond J. International subarachnoid aneurysm trial - isat part ii: Study protocol for a randomized controlled trial. *Trials*. 2013;14:156

220. Johnston SC, Dowd CF, Higashida RT, Lawton MT, Duckwiler GR, Gress DR, et al. Predictors of rehemorrhage after treatment of ruptured intracranial aneurysms: The cerebral aneurysm rerupture after treatment (carat) study. *Stroke*. 2008;39:120-125

221. Ormond DR, Dressler A, Kim S, Ronecker J, Murali R. Lumbar drains may reduce the need for permanent csf diversion in spontaneous subarachnoid haemorrhage. *Br J Neurosurg*. 2013;27:171-174

222. Klopfenstein JD, Kim LJ, Feiz-Erfan I, Hott JS, Goslar P, Zabramski JM, et al. Comparison of rapid and gradual weaning from external ventricular drainage in patients with aneurysmal subarachnoid hemorrhage: A prospective randomized trial. *J Neurosurg*. 2004;100:225-229

223. Dorhout Mees SM, Rinkel GJ, Feigin VL, Algra A, van den Bergh WM, Vermeulen M, et al. Calcium antagonists for aneurysmal subarachnoid haemorrhage. *Cochrane Database Syst Rev*. 2007:CD000277

224. Allen GS, Ahn HS, Preziosi TJ, Battye R, Boone SC, Boone SC, et al. Cerebral arterial spasm--a controlled trial of nimodipine in patients with subarachnoid hemorrhage. *The New England journal of medicine*. 1983;308:619-624

225. Senbokuya N, Kinouchi H, Kanemaru K, Ohashi Y, Fukamachi A, Yagi S, et al. Effects of cilostazol on cerebral vasospasm after aneurysmal

subarachnoid hemorrhage: A multicenter prospective, randomized, open-label blinded end point trial. *J Neurosurg*. 2013;118:121-130

226. Tseng MY, Hutchinson PJ, Turner CL, Czosnyka M, Richards H, Pickard JD, et al. Biological effects of acute pravastatin treatment in patients after aneurysmal subarachnoid hemorrhage: A double-blind, placebo-controlled trial. *J Neurosurg*. 2007;107:1092-1100

227. Chou SH, Smith EE, Badjatia N, Nogueira RG, Sims JR, 2nd, Ogilvy CS, et al. A randomized, double-blind, placebo-controlled pilot study of simvastatin in aneurysmal subarachnoid hemorrhage. *Stroke*. 2008;39:2891-2893

228. Vergouwen MD, Algra A, Rinkel GJ. Endothelin receptor antagonists for aneurysmal subarachnoid hemorrhage: A systematic review and meta-analysis update. *Stroke*. 2012;43:2671-2676

229. Macdonald RL, Higashida RT, Keller E, Mayer SA, Molyneux A, Raabe A, et al. Preventing vasospasm improves outcome after aneurysmal subarachnoid hemorrhage: Rationale and design of conscious-2 and conscious-3 trials. *Neurocrit Care*. 2010;13:416-424

230. Macdonald RL, Higashida RT, Keller E, Mayer SA, Molyneux A, Raabe A, et al. Randomized trial of clazosentan in patients with aneurysmal subarachnoid hemorrhage undergoing endovascular coiling. *Stroke*. 2012;43:1463-1469

231. Wong GK, Poon WS, Chan MT, Boet R, Gin T, Ng SC, et al. Intravenous magnesium sulphate for aneurysmal subarachnoid hemorrhage (imash): A randomized, double-blinded, placebo-controlled, multicenter phase iii trial. *Stroke*. 2010;41:921-926

232. Raabe A, Beck J, Berkefeld J, Deinsberger W, Meixensberger J, Schmiedek P, et al. [recommendations for the management of patients with aneurysmal subarachnoid hemorrhage]. *Zentralblatt fur Neurochirurgie*. 2005;66:79-91

233. Raabe A, Beck J, Keller M, Vatter H, Zimmermann M, Seifert V. Relative importance of hypertension compared with hypervolemia for increasing cerebral oxygenation in patients with cerebral vasospasm after subarachnoid hemorrhage. *J Neurosurg*. 2005;103:974-981

234. Aaslid R, Markwalder TM, Nornes H. Noninvasive transcranial doppler ultrasound recording of flow velocity in basal cerebral arteries. *J Neurosurg*. 1982;57:769-774

235. Dankbaar JW, Slooter AJ, Rinkel GJ, Schaaf IC. Effect of different components of triple-h therapy on cerebral perfusion in patients with aneurysmal subarachnoid haemorrhage: A systematic review. *Crit Care*. 2010;14:R23

236. Keen W. Intracranial lesions. *M News New York*. 1890;57:439-449

237. Dott N. Intracranial aneurysm: Cerebral arteriography: Surgical treatment. *Edinb Med J*. 1933;40:219-234

238. Dandy WE. Intracranial aneurysm of the internal carotid artery: Cured by operation. *Ann Surg*. 1938;107:654-659

239. Cushing H. I. The control of bleeding in operations for brain tumors: With the description of silver "clips" for the occlusion of vessels inaccessible to the ligature. *Ann Surg*. 1911;54:1-19

240. Moniz E. Lencephalographie arterielle, son importance dans la localization des tumours cerebrales. *Rev Neurol (Paris)*. 1927;2:72-90

241. Werner S, Blakemore A, King B. Aneurysm of the internal carotid artery within the skull. Wiring and electrothermic coagulation. *JAMA*. 1941;116:578-582

242. Mullan S, Beckman F, Vailati G, Karasick J, Dobben G. An experimental approach to the problem of cerebral aneurysm. *J Neurosurg*. 1964;21:838-845

243. Yasargil MG. A legacy of microneurosurgery: Memoirs, lessons, and axioms. *Neurosurgery*. 1999;45:1025-1092

244. Kanaan Y, Kaneshiro D, Fraser K, Wang D, Lanzino G. Evolution of endovascular therapy for aneurysm treatment. Historical overview. *Neurosurg Focus*. 2005;18:E2

245. Alksne JF. Stereotactic thrombosis of intracranial aneurysms. *The New England journal of medicine*. 1971;284:171-174

246. Smith RW, Alksne JF. Stereotaxic thrombosis of inaccessible intracranial aneurysms. *J Neurosurg*. 1977;47:833-839

247. Alksne JF, Smith RW. Stereotaxic occlusion of 22 consecutive anterior communicating artery aneurysms. *J Neurosurg*. 1980;52:790-793

248. Gallagher JP. Obliteration of intracranial aneurysms by pilojection. *JAMA*. 1963;183:231-236

249. Luessenhop AJ, Velasquez AC. Observations on the tolerance of the intracranial arteries to catheterization. *J Neurosurg*. 1964;21:85-91

250. Frei EH, Driller J, Neufeld HN, Barr I, Bleiden L, Askenazy HN. The pod and its applications. *Medical research engineering*. 1966;5:11-18

251. Fogarty TJ, Cranley JJ, Krause RJ, Strasser ES, Hafner CD. A method for extraction of arterial emboli and thrombi. *Surgery, gynecology & obstetrics*. 1963;116:241-244

252. Wolpert SM. In re: Serbinenko fa. Balloon catheterization and occlusion of major cerebral vessels. J neurosurg 1974;41:1974. *AJNR Am J Neuroradiol*. 2000;21:1359-1360

253. Serbinenko FA. Balloon catheterization and occlusion of major cerebral vessels. *J Neurosurg*. 1974;41:125-145

254. Higashida RT, Halbach VV, Barnwell SL, Dowd C, Dormandy B, Bell J, et al. Treatment of intracranial aneurysms with preservation of the parent vessel: Results of percutaneous balloon embolization in 84 patients. *AJNR Am J Neuroradiol*. 1990;11:633-640

255. Hilal S, Khandji A, Chi T. Synthetic fibre-coated platinum coils successfully used for endovascular treatment of arteriovenous malformations, aneurysms and direct arteriovenous fistulas of cns. *AJNR Am J Neuroradiol*. 1988;9:1030

256. Guglielmi G, Guerrisi R, Guidetti B. L`elettrotrombosi intravasale nelle malformazioni vascolari sperimentalmente provocate, in carella (ed). *Proceedings of III Congress of the Italian Society of Neuroradiology.* 1983:pp 139-146

257. Gallas S, Pasco A, Cottier JP, Gabrillargues J, Drouineau J, Cognard C, et al. A multicenter study of 705 ruptured intracranial aneurysms treated with guglielmi detachable coils. *AJNR Am J Neuroradiol*. 2005;26:1723-1731

258. Gallas S, Drouineau J, Gabrillargues J, Pasco A, Cognard C, Pierot L, et al. Feasibility, procedural morbidity and mortality, and long-term follow-up of endovascular treatment of 321 unruptured aneurysms. *AJNR Am J Neuroradiol*. 2008;29:63-68

259. Cognard C, Pierot L, Anxionnat R, Ricolfi F, Clarity Study G. Results of embolization used as the first treatment choice in a consecutive nonselected population of ruptured aneurysms: Clinical results of the clarity gdc study. *Neurosurgery*. 2011;69:837-841; discussion 842

260. Szikora I, Seifert P, Hanzely Z, Kulcsar Z, Berentei Z, Marosfoi M, et al. Histopathologic evaluation of aneurysms treated with guglielmi detachable coils or matrix detachable microcoils. *AJNR Am J Neuroradiol*. 2006;27:283-288

261. White PM, Lewis SC, Nahser H, Sellar RJ, Goddard T, Gholkar A, et al. Hydrocoil endovascular aneurysm occlusion and packing study (helps trial): Procedural safety and operator-assessed efficacy results. *AJNR Am J Neuroradiol*. 2008;29:217-223

262. O'Hare AM, Fanning NF, Ti JP, Dunne R, Brennan PR, Thornton JM. Hydrocoils, occlusion rates, and outcomes: A large single-center study. *AJNR Am J Neuroradiol*. 2010;31:1917-1922

263. Vallée J-N, Pierot L, Bonafé A, Turjman F, Flandroy P, Berge J, et al. Endovascular treatment of intracranial wide-necked aneurysms using three-dimensional coils: Predictors of immediate anatomic and clinical results. *AJNR Am J Neuroradiol*. 2004;25:298-306

264. Taschner CA, Thines L, El-Mahdy M, Rachdi H, Gauvrit J-Y, Lejeune J-P, et al. Gdc 360 degrees for the endovascular treatment of intracranial aneurysms: A matched-pair study analysing angiographic outcomes with gdc 3d coils in 38 patients. *Neuroradiology*. 2009;51:45-52

265. Liebig T, Henkes H, Fischer S, Weber W, Miloslavski E, Mariushi W, et al. Fibered electrolytically detachable platinum coils used for the endovascular treatment of intracranial aneurysms. Initial experiences and mid-term results in 474 aneurysms. *Interv Neuroradiol*. 2004;10:5-26

266. Murayama Y, Tateshima S, Gonzalez NR, Vinuela F. Matrix and bioabsorbable polymeric coils accelerate healing of intracranial aneurysms: Long-term experimental study. *Stroke*. 2003;34:2031-2037

267. Marjamaa J, Tulamo R, Frosen J, Abo-Ramadan U, Hernesniemi JA, Niemela MR, et al. Occlusion of neck remnant in experimental rat aneurysms after treatment with platinum- or polyglycolic-polylactic acid-coated coils. *Surg Neurol*. 2009;71:458-465; discussion 465

268. Smith MJ, Mascitelli J, Santillan A, Brennan JS, Tsiouris AJ, Riina HA, et al. Bare platinum vs matrix detachable coils for the endovascular treatment of intracranial aneurysms: A multivariate logistic regression analysis and review of the literature. *Neurosurgery*. 2011;69:557-564; discussion 565

269. Youn SW, Cha S-H, Kang H-S, Cho YD, Han MH. Matrix^2 coils in embolization of intracranial aneurysms: 1-year outcome and comparison with bare platinum coil group in a single institution. *AJNR Am J Neuroradiol*. 2011;32:1745-1750

270. Bendszus M, Solymosi L. Cerecyte coils in the treatment of intracranial aneurysms: A preliminary clinical study. *AJNR Am J Neuroradiol*. 2006;27:2053-2057

271. Molyneux AJ, Clarke A, Sneade M, Mehta Z, Coley S, Roy D, et al. Cerecyte coil trial: Angiographic outcomes of a prospective randomized trial comparing endovascular coiling of cerebral aneurysms with either cerecyte or bare platinum coils. *Stroke*. 2012;43:2544-2550

272. White PM, Raymond J. Endovascular coiling of cerebral aneurysms using "bioactive" or coated-coil technologies: A systematic review of the literature. *AJNR Am J Neuroradiol*. 2009;30:219-226

273. Rezek I, Mousan G, Wang Z, Murad MH, Kallmes DF. Coil type does not affect angiographic follow-up outcomes of cerebral aneurysm coiling: A systematic review and meta-analysis. *AJNR Am J Neuroradiol*. 2013;34:1769-1773

274. Ferns SP, Sprengers MES, van Rooij WJ, van Zwam WH, de Kort GAP, Velthuis BK, et al. Late reopening of adequately coiled intracranial aneurysms: Frequency and risk factors in 400 patients with 440 aneurysms. *Stroke*. 2011;42:1331-1337

275. Cognard C, Weill A, Spelle L, Piotin M, Castaings L, Rey A, et al. Long-term angiographic follow-up of 169 intracranial berry aneurysms occluded with detachable coils. *Radiology*. 1999;212:348-356

276. Nguyen TN, Hoh BL, Amin-Hanjani S, Pryor JC, Ogilvy CS. Comparison of ruptured vs unruptured aneurysms in recanalization after coil embolization. *Surg Neurol*. 2007;68:19-23

277. Henkes H, Fischer S, Mariushi W, Weber W, Liebig T, Miloslavski E, et al. Angiographic and clinical results in 316 coil-treated basilar artery bifurcation aneurysms. *J Neurosurg*. 2005;103:990-999

278. Moret J, Cognard C, Weill A, Castaings L, Rey A. The "remodelling technique" in the treatment of wide neck intracranial aneurysms. Angiographic results and clinical follow-up in 56 cases. *Interv Neuroradiol*. 1997;3:21-35

279. Sluzewski M, van Rooij WJ, Beute GN, Nijssen PC. Balloon-assisted coil embolization of intracranial aneurysms: Incidence, complications, and angiography results. *J Neurosurg*. 2006;105:396-399

280. Pierot L, Spelle L, Leclerc X, Cognard C, Bonafe A, Moret J. Endovascular treatment of unruptured intracranial aneurysms: Comparison of safety of

remodeling technique and standard treatment with coils. *Radiology*. 2009;251:846-855

281. Pierot L, Cognard C, Anxionnat R, Ricolfi F, Investigators C. Remodeling technique for endovascular treatment of ruptured intracranial aneurysms had a higher rate of adequate postoperative occlusion than did conventional coil embolization with comparable safety. *Radiology*. 2011;258:546-553

282. Chalouhi N, Jabbour P, Tjoumakaris S, Dumont AS, Chitale R, Rosenwasser RH, et al. Single-center experience with balloon-assisted coil embolization of intracranial aneurysms: Safety, efficacy and indications. *Clin Neurol Neurosurg*. 2013;115:607-613

283. Santillan A, Gobin YP, Mazura JC, Meausoone V, Leng LZ, Greenberg E, et al. Balloon-assisted coil embolization of intracranial aneurysms is not associated with increased periprocedural complications. *Journal of neurointerventional surgery*. 2013;5 Suppl 3:iii56-iii61

284. Higashida RT, Halbach VV, Dowd CF, Juravsky L, Meagher S. Initial clinical experience with a new self-expanding nitinol stent for the treatment of intracranial cerebral aneurysms: The cordis enterprise stent. *AJNR Am J Neuroradiol*. 2005;26:1751-1756

285. Piotin M, Blanc R, Spelle L, Mounayer C, Piantino R, Schmidt PJ, et al. Stent-assisted coiling of intracranial aneurysms: Clinical and angiographic results in 216 consecutive aneurysms. *Stroke*. 2010;41:110-115

286. Shapiro M, Becske T, Sahlein D, Babb J, Nelson PK. Stent-supported aneurysm coiling: A literature survey of treatment and follow-up. *AJNR Am J Neuroradiol*. 2012;33:159-163

287. Gao X, Liang G, Li Z, Wei X, Hong Q. Complications and adverse events associated with neuroform stent-assisted coiling of wide-neck intracranial aneurysms. *Neurol Res*. 2011;33:841-852

288. Lee SJ, Cho YD, Kang HS, Kim JE, Han MH. Coil embolization using the self-expandable closed-cell stent for intracranial saccular aneurysm: A single-center experience of 289 consecutive aneurysms. *Clinical radiology*. 2013;68:256-263

289. Chalouhi N, Jabbour P, Singhal S, Drueding R, Starke RM, Dalyai RT, et al. Stent-assisted coiling of intracranial aneurysms: Predictors of complications, recanalization, and outcome in 508 cases. *Stroke*. 2013;44:1348-1353

290. Kulcsar Z, Goricke SL, Gizewski ER, Schlamann M, Sure U, Sandalcioglu IE, et al. Neuroform stent-assisted treatment of intracranial aneurysms:

Long-term follow-up study of aneurysm recurrence and in-stent stenosis rates. *Neuroradiology*. 2013;55:459-465

291. Santillan A, Greenberg E, Patsalides A, Salvaggio K, Riina HA, Gobin YP. Long-term clinical and angiographic results of neuroform stent-assisted coil embolization in wide-necked intracranial aneurysms. *Neurosurgery*. 2012;70:1232-1237; discussion 1237

292. Fargen KM, Hoh BL, Welch BG, Pride GL, Lanzino G, Boulos AS, et al. Long-term results of enterprise stent-assisted coiling of cerebral aneurysms. *Neurosurgery*. 2012;71:239-244; discussion 244

293. Izar B, Rai A, Raghuram K, Rotruck J, Carpenter J. Comparison of devices used for stent-assisted coiling of intracranial aneurysms. *PloS one*. 2011;6:e24875

294. Pierot L, Cognard C, Spelle L, Moret J. Safety and efficacy of balloon remodeling technique during endovascular treatment of intracranial aneurysms: Critical review of the literature. *AJNR Am J Neuroradiol*. 2012;33:12-15

295. Chalouhi N, Starke RM, Koltz MT, Jabbour PM, Tjoumakaris SI, Dumont AS, et al. Stent-assisted coiling versus balloon remodeling of wide-neck aneurysms: Comparison of angiographic outcomes. *AJNR Am J Neuroradiol*. 2013;34:1987-1992

296. Pierot L, Wakhloo AK. Endovascular treatment of intracranial aneurysms: Current status. *Stroke*. 2013;44:2046-2054

297. Brinjikji W, Murad MH, Lanzino G, Cloft HJ, Kallmes DF. Endovascular treatment of intracranial aneurysms with flow diverters: A meta-analysis. *Stroke*. 2013;44:442-447

298. Turowski B, Macht S, Kulcsar Z, Hanggi D, Stummer W. Early fatal hemorrhage after endovascular cerebral aneurysm treatment with a flow diverter (silk-stent): Do we need to rethink our concepts? *Neuroradiology*. 2011;53:37-41

299. Mustafa W, Kadziolka K, Anxionnat R, Pierot L. Direct carotid-cavernous fistula following intracavernous carotid aneurysm treatment with a flow-diverter stent. A case report. *Interv Neuroradiol*. 2010;16:447-450

300. Fanning NF, Willinsky RA, ter Brugge KG. Wall enhancement, edema, and hydrocephalus after endovascular coil occlusion of intradural cerebral aneurysms. *J Neurosurg*. 2008;108:1074-1086

301. Berge J, Tourdias T, Moreau JF, Barreau X, Dousset V. Perianeurysmal brain inflammation after flow-diversion treatment. *AJNR Am J Neuroradiol*. 2011;32:1930-1934

302. Darsaut TE, Rayner-Hartley E, Makoyeva A, Salazkin I, Berthelet F, Raymond J. Aneurysm rupture after endovascular flow diversion: The possible role of persistent flows through the transition zone associated with device deformation. *Interv Neuroradiol*. 2013;19:180-185

303. Horie N, Kitagawa N, Morikawa M, Tsutsumi K, Kaminogo M, Nagata I. Progressive perianeurysmal edema induced after endovascular coil embolization. Report of three cases and review of the literature. *J Neurosurg*. 2007;106:916-920

304. Stracke CP, Krings T, Moller-Hartmann W, Mahdavi A, Klug N. Severe inflammatory reaction of the optic system after endovascular treatment of a supraophthalmic aneurysm with bioactive coils. *AJNR Am J Neuroradiol*. 2007;28:1401-1402

305. Krings T, Alvarez H, Reinacher P, Ozanne A, Baccin CE, Gandolfo C, et al. Growth and rupture mechanism of partially thrombosed aneurysms. *Interv Neuroradiol*. 2007;13:117-126

306. Fiorella D, Sadasivan C, Woo HH, Lieber B. Regarding "aneurysm rupture following treatment with flow-diverting stents: Computational hemodynamics analysis of treatment". *AJNR Am J Neuroradiol*. 2011;32:E95-97; author reply E98-100

307. Cruz JP, Chow M, O'Kelly C, Marotta B, Spears J, Montanera W, et al. Delayed ipsilateral parenchymal hemorrhage following flow diversion for the treatment of anterior circulation aneurysms. *AJNR Am J Neuroradiol*. 2012;33:603-608

308. Kulcsar Z, Ernemann U, Wetzel SG, Bock A, Goericke S, Panagiotopoulos V, et al. High-profile flow diverter (silk) implantation in the basilar artery: Efficacy in the treatment of aneurysms and the role of the perforators. *Stroke*. 2010;41:1690-1696

309. Pistocchi S, Blanc R, Bartolini B, Piotin M. Flow diverters at and beyond the level of the circle of willis for the treatment of intracranial aneurysms. *Stroke*. 2012;43:1032-1038

310. Fiorella D, Hsu D, Woo HH, Tarr RW, Nelson PK. Very late thrombosis of a pipeline embolization device construct: Case report. *Neurosurgery*. 2010;67:onsE313-314; discussion onsE314

311. Briganti F, Napoli M, Tortora F, Solari D, Bergui M, Boccardi E, et al. Italian multicenter experience with flow-diverter devices for intracranial unruptured aneurysm treatment with periprocedural complications--a retrospective data analysis. *Neuroradiology*. 2012;54:1145-1152

312. Saatci I, Yavuz K, Ozer C, Geyik S, Cekirge HS. Treatment of intracranial aneurysms using the pipeline flow-diverter embolization device: A single-center experience with long-term follow-up results. *AJNR Am J Neuroradiol*. 2012;33:1436-1446

313. Pierot L, Klisch J, Cognard C, Szikora I, Mine B, Kadziolka K, et al. Endovascular web flow disruption in middle cerebral artery aneurysms: Preliminary feasibility, clinical, and anatomical results in a multicenter study. *Neurosurgery*. 2013;73:27-34; discussion 34-25

314. Klisch J, Sychra V, Strasilla C, Liebig T, Fiorella D. The woven endobridge cerebral aneurysm embolization device (web ii): Initial clinical experience. *Neuroradiology*. 2011;53:599-607

315. Molyneux AJ, Cekirge S, Saatci I, Gal G. Cerebral aneurysm multicenter european onyx (cameo) trial: Results of a prospective observational study in 20 european centers. *AJNR Am J Neuroradiol*. 2004;25:39-51

316. Carlson AP, Alaraj A, Amin-Hanjani S, Charbel FT, Aletich VA. Continued concern about parent vessel steno-occlusive progression with onyx hd-500 and the utility of quantitative magnetic resonance imaging in serial assessment. *Neurosurgery*. 2013;72:341-352; discussion 352

317. Li MH, Zhu YQ, Fang C, Wang W, Zhang PL, Cheng YS, et al. The feasibility and efficacy of treatment with a willis covered stent in recurrent intracranial aneurysms after coiling. *AJNR Am J Neuroradiol*. 2008;29:1395-1400

318. Li MH, Li YD, Tan HQ, Luo QY, Cheng YS. Treatment of distal internal carotid artery aneurysm with the willis covered stent: A prospective pilot study. *Radiology*. 2009;253:470-477

319. Zhu YQ, Li MH, Lin F, Song DL, Tan HQ, Gu BX, et al. Frequency and predictors of endoleaks and long-term patency after covered stent placement for the treatment of intracranial aneurysms: A prospective, non-randomised multicentre experience. *European radiology*. 2013;23:287-297

320. Byrne JV, Sohn MJ, Molyneux AJ, Chir B. Five-year experience in using coil embolization for ruptured intracranial aneurysms: Outcomes and incidence of late rebleeding. *J Neurosurg*. 1999;90:656-663

321. Krings T, Busch C, Sellhaus B, Drexler AY, Bovi M, Hermanns-Sachweh B, et al. Long-term histological and scanning electron microscopy results of endovascular and operative treatments of experimentally induced aneurysms in the rabbit. *Neurosurgery*. 2006;59:911-923; discussion 923-914

322. Bavinzski G, Talazoglu V, Killer M, Richling B, Gruber A, Gross CE, et al. Gross and microscopic histopathological findings in aneurysms of the human brain treated with guglielmi detachable coils. *J Neurosurg*. 1999;91:284-293

323. Dai D, Ding YH, Danielson MA, Kadirvel R, Lewis DA, Cloft HJ, et al. Histopathologic and immunohistochemical comparison of human, rabbit, and swine aneurysms embolized with platinum coils. *AJNR Am J Neuroradiol*. 2005;26:2560-2568

324. Raymond J, Venne D, Allas S, Roy D, Oliva VL, Denbow N, et al. Healing mechanisms in experimental aneurysms. I. Vascular smooth muscle cells and neointima formation. *Journal of neuroradiology. Journal de neuroradiologie*. 1999;26:7-20

325. Raymond J, Darsaut T, Salazkin I, Gevry G, Bouzeghrane F. Mechanisms of occlusion and recanalization in canine carotid bifurcation aneurysms embolized with platinum coils: An alternative concept. *AJNR Am J Neuroradiol*. 2008;29:745-752

326. Raymond J, Sauvageau E, Salazkin I, Ribourtout E, Gevry G, Desfaits AC. Role of the endothelial lining in persistence of residual lesions and growth of recurrences after endovascular treatment of experimental aneurysms. *Stroke*. 2002;33:850-855

327. Raymond J, Guilbert F, Metcalfe A, Gevry G, Salazkin I, Robledo O. Role of the endothelial lining in recurrences after coil embolization: Prevention of recanalization by endothelial denudation. *Stroke*. 2004;35:1471-1475

328. Hasan DM, Nadareyshvili AI, Hoppe AL, Mahaney KB, Kung DK, Raghavan ML. Cerebral aneurysm sac growth as the etiology of recurrence after successful coil embolization. *Stroke*. 2012;43:866-868

329. Abdihalim M, Watanabe M, Chaudhry SA, Jagadeesan B, Suri MF, Qureshi AI. Are coil compaction and aneurysmal growth two distinct etiologies leading to recurrence following endovascular treatment of intracranial aneurysm? *Journal of neuroimaging : official journal of the American Society of Neuroimaging*. 2014;24:171-175

330. Holmin S, Krings T, Ozanne A, Alt JP, Claes A, Zhao W, et al. Intradural saccular aneurysms treated by guglielmi detachable bare coils at a single

institution between 1993 and 2005: Clinical long-term follow-up for a total of 1810 patient-years in relation to morphological treatment results. *Stroke*. 2008;39:2288-2297

331. Ortiz R, Stefanski M, Rosenwasser R, Veznedaroglu E. Cigarette smoking as a risk factor for recurrence of aneurysms treated by endosaccular occlusion. *J Neurosurg*. 2008;108:672-675

332. Platz J, Guresir E, Seifert V, Vatter H, Berkefeld J. Long-term effects of antiplatelet drugs on aneurysm occlusion after endovascular treatment. *Journal of neurointerventional surgery*. 2012;4:345-350

333. Vanzin JR, Mounayer C, Abud DG, D'Agostini Annes R, Moret J. Angiographic results in intracranial aneurysms treated with inert platinum coils. *Interv Neuroradiol*. 2012;18:391-400

334. Pyysalo LM, Keski-Nisula LH, Niskakangas TT, Kahara VJ, Ohman JE. Long-term follow-up study of endovascularly treated intracranial aneurysms. *Interv Neuroradiol*. 2010;16:231-239

335. Finitsis S, Anxionnat R, Lebedinsky A, Albuquerque PC, Clayton MF, Picard L, et al. Endovascular treatment of acom intracranial aneurysms. Report on series of 280 patients. *Interv Neuroradiol*. 2010;16:7-16

336. Kang HS, Kwon BJ, Kwon OK, Jung C, Kim JE, Oh CW, et al. Endovascular coil embolization of anterior choroidal artery aneurysms. Clinical article. *J Neurosurg*. 2009;111:963-969

337. Tan IY, Agid RF, Willinsky RA. Recanalization rates after endovascular coil embolization in a cohort of matched ruptured and unruptured cerebral aneurysms. *Interv Neuroradiol*. 2011;17:27-35

338. Gruber A, Killer M, Bavinzski G, Richling B. Clinical and angiographic results of endosaccular coiling treatment of giant and very large intracranial aneurysms: A 7-year, single-center experience. *Neurosurgery*. 1999;45:793-803; discussion 803-794

339. Gao X, Liang G, Li Z, Wei X, Cao P. A single-centre experience and follow-up of patients with endovascular coiling of large and giant intracranial aneurysms with parent artery preservation. *J Clin Neurosci*. 2012;19:364-369

340. Sluzewski M, van Rooij WJ, Slob MJ, Bescos JO, Slump CH, Wijnalda D. Relation between aneurysm volume, packing, and compaction in 145 cerebral aneurysms treated with coils. *Radiology*. 2004;231:653-658

341. Ng P, Khangure MS, Phatouros CC, Bynevelt M, ApSimon H, McAuliffe W. Endovascular treatment of intracranial aneurysms with guglielmi detachable coils: Analysis of midterm angiographic and clinical outcomes. *Stroke*. 2002;33:210-217

342. David CA, Vishteh AG, Spetzler RF, Lemole M, Lawton MT, Partovi S. Late angiographic follow-up review of surgically treated aneurysms. *J Neurosurg*. 1999;91:396-401

343. Celik O, Niemela M, Romani R, Hernesniemi J. Inappropriate application of yasargil aneurysm clips: A new observation and technical remark. *Neurosurgery*. 2010;66:84-87; discussion 87

344. Reul J, Weis J, Spetzger U, Konert T, Fricke C, Thron A. Long-term angiographic and histopathologic findings in experimental aneurysms of the carotid bifurcation embolized with platinum and tungsten coils. *AJNR Am J Neuroradiol*. 1997;18:35-42

345. Ringer AJ, Lanzino G, Veznedaroglu E, Rodriguez R, Mericle RA, Levy EI, et al. Does angiographic surveillance pose a risk in the management of coiled intracranial aneurysms? A multicenter study of 2243 patients. *Neurosurgery*. 2008;63:845-849; discussion 849

346. Standhardt H, Boecher-Schwarz H, Gruber A, Benesch T, Knosp E, Bavinzski G. Endovascular treatment of unruptured intracranial aneurysms with guglielmi detachable coils: Short- and long-term results of a single-centre series. *Stroke*. 2008;39:899-904

347. Plowman RS, Clarke A, Clarke M, Byrne JV. Sixteen-year single-surgeon experience with coil embolization for ruptured intracranial aneurysms: Recurrence rates and incidence of late rebleeding. Clinical article. *J Neurosurg*. 2011;114:863-874

348. Chalouhi N, Tjoumakaris S, Gonzalez LF, Dumont AS, Starke RM, Hasan D, et al. Coiling of large and giant aneurysms: Complications and long-term results of 334 cases. *AJNR Am J Neuroradiol*. 2014;35:546-552

349. Bavinzski G, Killer M, Gruber A, Reinprecht A, Gross CE, Richling B. Treatment of basilar artery bifurcation aneurysms by using guglielmi detachable coils: A 6-year experience. *J Neurosurg*. 1999;90:843-852

350. Peluso JP, van Rooij WJ, Sluzewski M, Beute GN. Coiling of basilar tip aneurysms: Results in 154 consecutive patients with emphasis on recurrent haemorrhage and re-treatment during mid- and long-term follow-up. *J Neurol Neurosurg Psychiatry*. 2008;79:706-711

351. Lempert TE, Malek AM, Halbach VV, Phatouros CC, Meyers PM, Dowd CF, et al. Endovascular treatment of ruptured posterior circulation cerebral aneurysms. Clinical and angiographic outcomes. *Stroke*. 2000;31:100-110

352. Pandey AS, Koebbe C, Rosenwasser RH, Veznedaroglu E. Endovascular coil embolization of ruptured and unruptured posterior circulation aneurysms: Review of a 10-year experience. *Neurosurgery*. 2007;60:626-636; discussion 636-627

353. Yadla S, Campbell PG, Grobelny B, Jallo J, Gonzalez LF, Rosenwasser RH, et al. Open and endovascular treatment of unruptured carotid-ophthalmic aneurysms: Clinical and radiographic outcomes. *Neurosurgery*. 2011;68:1434-1443; discussion 1443

354. Guglielmi G, Vinuela F, Duckwiler G, Jahan R, Cotroneo E, Gigli R. Endovascular treatment of 306 anterior communicating artery aneurysms: Overall, perioperative results. *J Neurosurg*. 2009;110:874-879

355. Corns R, Zebian B, Tait MJ, Walsh D, Hampton T, Deasy N, et al. Prevalence of recurrence and retreatment of ruptured intracranial aneurysms treated with endovascular coil occlusion. *Br J Neurosurg*. 2013;27:30-33

356. van Rooij WJ, Sluzewski M, Beute GN. Internal carotid bifurcation aneurysms: Frequency, angiographic anatomy and results of coiling in 50 aneurysms. *Neuroradiology*. 2008;50:583-587

357. Oishi H, Yamamoto M, Nonaka S, Arai H. Endovascular therapy of internal carotid artery bifurcation aneurysms. *Journal of neurointerventional surgery*. 2013;5:400-404

358. Oishi H, Nonaka S, Yamamoto M, Arai H. Feasibility and efficacy of endovascular therapy for ruptured distal anterior cerebral artery aneurysms. *Neurol Med Chir (Tokyo)*. 2013;53:304-309

359. Park HS, Kwon SC, Kim MH, Park ES, Sim HB, Lyo IU. Endovascular coil embolization of distal anterior cerebral artery aneurysms: Angiographic and clinical follow-up results. *Neurointervention*. 2013;8:87-91

360. Iijima A, Piotin M, Mounayer C, Spelle L, Weill A, Moret J. Endovascular treatment with coils of 149 middle cerebral artery berry aneurysms. *Radiology*. 2005;237:611-619

361. Quadros RS, Gallas S, Noudel R, Rousseaux P, Pierot L. Endovascular treatment of middle cerebral artery aneurysms as first option: A single

center experience of 92 aneurysms. *AJNR Am J Neuroradiol*. 2007;28:1567-1572

362. Vendrell JF, Menjot N, Costalat V, Hoa D, Moritz J, Brunel H, et al. Endovascular treatment of 174 middle cerebral artery aneurysms: Clinical outcome and radiologic results at long-term follow-up. *Radiology*. 2009;253:191-198

363. Brinjikji W, Lanzino G, Cloft HJ, Rabinstein A, Kallmes DF. Endovascular treatment of middle cerebral artery aneurysms: A systematic review and single-center series. *Neurosurgery*. 2011;68:397-402; discussion 402

364. Mortimer AM, Bradley MD, Mews P, Molyneux AJ, Renowden SA. Endovascular treatment of 300 consecutive middle cerebral artery aneurysms: Clinical and radiologic outcomes. *AJNR Am J Neuroradiol*. 2014;35:706-714

365. Hashimoto N, Handa H, Hazama F. Experimentally induced cerebral aneurysms in rats. *Surg Neurol*. 1978;10:3-8

366. Cawley CM, Dawson RC, Shengelaia G, Bonner G, Barrow DL, Colohan AR. Arterial saccular aneurysm model in the rabbit. *AJNR Am J Neuroradiol*. 1996;17:1761-1766

367. Byrne JV, Hope JK, Hubbard N, Morris JH. The nature of thrombosis induced by platinum and tungsten coils in saccular aneurysms. *AJNR Am J Neuroradiol*. 1997;18:29-33

368. Guglielmi G, Ji C, Massoud TF, Kurata A, Lownie SP, Vinuela F, et al. Experimental saccular aneurysms. Ii. A new model in swine. *Neuroradiology*. 1994;36:547-550

369. Tsumoto T, Song JK, Niimi Y, Berenstein A. Interval change in size of venous pouch canine bifurcation aneurysms over a 10-month period. *AJNR Am J Neuroradiol*. 2008;29:1067-1070

370. Mawad ME, Mawad JK, Cartwright J, Jr., Gokaslan Z. Long-term histopathologic changes in canine aneurysms embolized with guglielmi detachable coils. *AJNR Am J Neuroradiol*. 1995;16:7-13

371. Kallmes DF, Helm GA, Hudson SB, Altes TA, Do HM, Mandell JW, et al. Histologic evaluation of platinum coil embolization in an aneurysm model in rabbits. *Radiology*. 1999;213:217-222

372. Zeng Z, Kallmes DF, Durka MJ, Ding Y, Lewis D, Kadirvel R, et al. Hemodynamics and anatomy of elastase-induced rabbit aneurysm models:

Similarity to human cerebral aneurysms? *AJNR Am J Neuroradiol*. 2011;32:595-601

373. Vilahur G, Padro T, Badimon L. Atherosclerosis and thrombosis: Insights from large animal models. *Journal of biomedicine & biotechnology*. 2011;2011:907575

374. Zeng Z, Durka MJ, Kallmes DF, Ding Y, Robertson AM. Can aspect ratio be used to categorize intra-aneurysmal hemodynamics?--a study of elastase induced aneurysms in rabbit. *Journal of biomechanics*. 2011;44:2809-2816

375. Ding Y, Dai D, Kadirvel R, Lewis DA, Kallmes DF. Five-year follow-up in elastase-induced aneurysms in rabbits. *AJNR Am J Neuroradiol*.

376. Hoh BL, Rabinov JD, Pryor JC, Ogilvy CS. A modified technique for using elastase to create saccular aneurysms in animals that histologically and hemodynamically resemble aneurysms in human. *Acta Neurochir (Wien)*. 2004;146:705-711

377. Villano JS, Boehm CA, Carney EL, Cooper TK. Complications of elastase-induced arterial saccular aneurysm in rabbits: Case reports and literature review. *Comp Med*. 2012;62:480-486

378. Cruise G, Shum JC, Plenk H. Hydrogel-coated and platinum coils for intracranial aneurysm embolization compared in three experimental models using computerized angiographic and histologic morphometry. *J Mater Chem*. 2007;17:3965-3973

379. Sherif C, Marbacher S, Erhardt S, Fandino J. Improved microsurgical creation of venous pouch arterial bifurcation aneurysms in rabbits. *AJNR Am J Neuroradiol*. 2011;32:165-169

380. Abruzzo T, Shengelaia GG, Dawson RC, 3rd, Owens DS, Cawley CM, Gravanis MB. Histologic and morphologic comparison of experimental aneurysms with human intracranial aneurysms. *AJNR Am J Neuroradiol*. 1998;19:1309-1314

381. Stehbens WE. In re: Histological and morphologic comparison of experimental aneurysms with human intracranial aneurysms. *AJNR Am J Neuroradiol*. 2000;21:1769-1773

382. Bouzeghrane F, Naggara O, Kallmes DF, Berenstein A, Raymond J, International Consortium of Neuroendovascular C. In vivo experimental intracranial aneurysm models: A systematic review. *AJNR Am J Neuroradiol*. 2010;31:418-423

383. Marbacher S, Erhardt S, Schlappi JA, Coluccia D, Remonda L, Fandino J, et al. Complex bilobular, bisaccular, and broad-neck microsurgical aneurysm formation in the rabbit bifurcation model for the study of upcoming endovascular techniques. *AJNR Am J Neuroradiol*. 2011;32:772-777

384. Ding YH, Danielson MA, Kadirvel R, Dai D, Lewis DA, Cloft HJ, et al. Modified technique to create morphologically reproducible elastase-induced aneurysms in rabbits. *Neuroradiology*. 2006;48:528-532

385. Aoki T, Nishimura M. The development and the use of experimental animal models to study the underlying mechanisms of ca formation. *Journal of biomedicine & biotechnology*. 2011;2011:535921

386. McCune WS, Samadi A, Blades B. Experimental aneurysms. *Ann Surg*. 1953;138:216-218

387. German WJ, Black SP. Experimental production of carotid aneurysms. *The New England journal of medicine*. 1954;250:104-106

388. White JC, Sayre GP, Whisnant JP. Experimental destruction of the media for the production of intracranial arterial aneurysms. *J Neurosurg*. 1961;18:741-745

389. Troupp H, Rinne T. Methyl-2-cyanoacrylate (eastman 910) in experimental vascular surgery with a note on experimental arterial aneurysms. *J Neurosurg*. 1964;21:1067-1069

390. Nishikawa M, Yonekawa Y, Matsuda I. Experimental aneurysms. *Surg Neurol*. 1976;5:15-18

391. Kerber CW, Buschman RW. Experimental carotid aneurysms: I. Simple surgical production and radiographic evaluation. *Investigative radiology*. 1977;12:154-157

392. Nagata I, Handa H, Hashimoto N, Hazama F. Experimentally induced cerebral aneurysms in rats: Part vi. Hypertension. *Surg Neurol*. 1980;14:477-479

393. Handa H, Hashimoto N, Nagata I, Hazama F. Saccular cerebral aneurysms in rats: A newly developed animal model of the disease. *Stroke*. 1983;14:857-866

394. Coutard M, Osborne-Pellegrin M. Genetic susceptibility to experimental cerebral aneurysm formation in the rat. *Stroke*. 1997;28:1035-1041; discussion 1042

395. Hashimoto N, Kim C, Kikuchi H, Kojima M, Kang Y, Hazama F. Experimental induction of cerebral aneurysms in monkeys. *J Neurosurg*. 1987;67:903-905

396. Meng H, Swartz DD, Wang Z, Hoi Y, Kolega J, Metaxa EM, et al. A model system for mapping vascular responses to complex hemodynamics at arterial bifurcations in vivo. *Neurosurgery*. 2006;59:1094-1100; discussion 1100-1091

397. Gao L, Hoi Y, Swartz DD, Kolega J, Siddiqui A, Meng H. Nascent aneurysm formation at the basilar terminus induced by hemodynamics. *Stroke*. 2008;39:2085-2090

398. Morimoto M, Miyamoto S, Mizoguchi A, Kume N, Kita T, Hashimoto N. Mouse model of cerebral aneurysm: Experimental induction by renal hypertension and local hemodynamic changes. *Stroke*. 2002;33:1911-1915

399. Kim C, Kikuchi H, Hashimoto N, Hazama F. Histopathological study of induced cerebral aneurysms in primates. *Surg Neurol*. 1989;32:45-50

400. Wang Z, Kolega J, Hoi Y, Gao L, Swartz DD, Levy EI, et al. Molecular alterations associated with aneurysmal remodeling are localized in the high hemodynamic stress region of a created carotid bifurcation. *Neurosurgery*. 2009;65:169-177; discussion 177-168

401. Hassler O. Experimental carotid ligation followed by aneurysmal formation and other morphological changes in the circle of willis. *J Neurosurg*. 1963;20:1-7

402. Dai D, Ding YH, Kadirvel R, Lewis DA, Kallmes DF. Experience with microaneurysm formation at the basilar terminus in the rabbit elastase aneurysm model. *AJNR Am J Neuroradiol*. 2010;31:300-303

403. Meng H, Metaxa E, Gao L, Liaw N, Natarajan SK, Swartz DD, et al. Progressive aneurysm development following hemodynamic insult. *J Neurosurg*. 2011;114:1095-1103

404. Mandelbaum M, Kolega J, Dolan JM, Siddiqui AH, Meng H. A critical role for proinflammatory behavior of smooth muscle cells in hemodynamic initiation of intracranial aneurysm. *PloS one*. 2013;8:e74357

405. Tada Y, Kanematsu Y, Kanematsu M, Nuki Y, Liang EI, Wada K, et al. A mouse model of intracranial aneurysm: Technical considerations. *Acta Neurochir Suppl*. 2011;111:31-35

406. Nuki Y, Tsou TL, Kurihara C, Kanematsu M, Kanematsu Y, Hashimoto T. Elastase-induced intracranial aneurysms in hypertensive mice. *Hypertension*. 2009;54:1337-1344

407. Yan T, Chopp M, Ning R, Zacharek A, Roberts C, Chen J. Intracranial aneurysm formation in type-one diabetes rats. *PloS one*. 2013;8:e67949

408. Hosaka K, Downes DP, Nowicki KW, Hoh BL. Modified murine intracranial aneurysm model: Aneurysm formation and rupture by elastase and hypertension. *Journal of neurointerventional surgery*. 2013

409. Aassar OS, Fujiwara NH, Marx WF, Matsumoto AH, Kallmes DF. Aneurysm growth, elastinolysis, and attempted doxycycline inhibition of elastase-induced aneurysms in rabbits. *Journal of Vascular and Interventional Radiology*. 2003;14:1427-1432

410. Fujiwara NH, Cloft HJ, Marx WF, Short JG, Jensen ME, Kallmes DF. Serial angiography in an elastase-induced aneurysm model in rabbits: Evidence for progressive aneurysm enlargement after creation. *AJNR Am J Neuroradiol*. 2001;22:698-703

411. Yang X-j, Li L, Wu Z-x. A novel arterial pouch model of saccular aneurysm by concomitant elastase and collagenase digestion. *Journal of Zhejiang University. Science. B*. 2007;8:697-703

412. Ding YH, Tieu T, Kallmes DF. Creation of sidewall aneurysm in rabbits: Aneurysm patency and growth follow-up. *Journal of neurointerventional surgery*. 2012

413. Byrne JV, Hubbard N, Morris JH. Endovascular coil occlusion of experimental aneurysms: Partial treatment does not prevent subsequent rupture. *Neurol Res*. 1994;16:425-427

414. Yang X, Wu Z, Li Y, Tang J, Sun Y, Liu Z, et al. Re-evaluation of cellulose acetate polymer: Angiographic findings and histological studies. *Surg Neurol*. 2001;55:116-122

415. Yoshino Y, Niimi Y, Song JK, Khoyama S, Shin YS, Berenstein A. Preventing spontaneous thrombosis of experimental sidewall aneurysms: The oblique cut. *AJNR Am J Neuroradiol*. 2005;26:1363-1365

416. Black SP, German WJ. Observations on the relationship between the volume and the size of the orifice of experimental aneurysms. *J Neurosurg*. 1960;17:984-990

417. O'Reilly GV, Utsunomiya R, Rumbaugh CL, Colucci VM. Experimental arterial aneurysms:Modification of the production technique. *Journal of microsurgery*. 1981;2:219-223

418. Raymond J, Salazkin I, Georganos S, Guilbert F, Desfaits AC, Gevry G, et al. Endovascular treatment of experimental wide neck aneurysms: Comparison of results using coils or cyanoacrylate with the assistance of an aneurysm neck bridge device. *AJNR Am J Neuroradiol*. 2002;23:1710-1716

419. Marjamaa J, Antell H, Abo-Ramadan U, Hernesniemi JA, Niemela MR, Kangasniemi M. High-resolution tof mr angiography at 4.7 tesla for volumetric and morphologic evaluation of coiled aneurysm neck remnants in a rat model. *Acta Radiol*. 2011;52:340-348

420. Ding YH, Dai D, Danielson MA, Kadirvel R, Lewis DA, Cloft HJ, et al. Control of aneurysm volume by adjusting the position of ligation during creation of elastase-induced aneurysms: A prospective study. *AJNR Am J Neuroradiol*. 2007;28:857-859

421. Yushkevich PA, Piven J, Hazlett HC, Smith RG, Ho S, Gee JC, et al. User-guided 3d active contour segmentation of anatomical structures: Significantly improved efficiency and reliability. *NeuroImage*. 2006;31:1116-1128

422. Allaire E, Guettier C, Bruneval P, Plissonnier D, Michel JB. Cell-free arterial grafts: Morphologic characteristics of aortic isografts, allografts, and xenografts in rats. *J Vasc Surg*. 1994;19:446-456

423. Schneider CA, Rasband WS, Eliceiri KW. Nih image to imagej: 25 years of image analysis. *Nature methods*. 2012;9:671-675

424. Sherif C, Fandino J, Erhardt S, di Ieva A, Killer M, Kleinpeter G, et al. Microsurgical venous pouch arterial-bifurcation aneurysms in the rabbit model: Technical aspects. *Journal of visualized experiments : JoVE*. 2011

425. Sherif C, Marbacher S, Erhardt S, Plenk HJ, Fandino J. Improved microsurgical creation of venous-pouch arterial-bifurcation aneurysms in rabbits. *AJNR Am J Neuroradiol*. 2010; In Press

426. Bavinzski G, al-Schameri A, Killer M, Schwendenwein I, Gruber A, Saringer W, et al. Experimental bifurcation aneurysm: A model for in vivo evaluation of endovascular techniques. *Minim Invasive Neurosurg*. 1998;41:129-132

427. Spetzger U, Reul J, Weis J, Bertalanffy H, Thron A, Gilsbach JM. Microsurgically produced bifurcation aneurysms in a rabbit model for endovascular coil embolization. *J Neurosurg*. 1996;85:488-495

428. Sherif C, Marbacher S, Fandino J. High-resolution three-dimensional 3 t magnetic resonance angiography for the evaluation of experimental aneurysm in the rabbit. *Neurol Res*. 2009;31:869-872

429. Kirse DJ, Flock S, Teo C, Rahman S, Mrak R. Construction of a vein-pouch aneurysm at a surgically created carotid bifurcation in the rat. *Microsurgery*. 1996;17:681-689

430. Turk AS, Aagaard-Kienitz B, Niemann D, Consigny D, Rappe A, Grinde J, et al. Natural history of the canine vein pouch aneurysm model. *AJNR. American journal of neuroradiology*. 2007;28:531-532

431. Kallmes DF, Altes TA, Vincent DA, Cloft HJ, Do HM, Jensen ME. Experimental side-wall aneurysms: A natural history study. *Neuroradiology*. 1999;41:338-341

432. Marbacher S, Erhardt S, Schlappi JA, Coluccia D, Remonda L, Fandino J, et al. Complex bilobular, bisaccular, and broad-neck microsurgical aneurysm formation in the rabbit bifurcation model for the study of upcoming endovascular techniques. *AJNR. American journal of neuroradiology*. 2011;32:772-777

433. Marjamaa J, Tulamo R, Abo-Ramadan U, Hakovirta H, Frosen J, Rahkonen O, et al. Mice with a deletion in the first intron of the col1a1 gene develop dissection and rupture of aorta in the absence of aneurysms: High-resolution magnetic resonance imaging, at 4.7 t, of the aorta and cerebral arteries. *Magn Reson Med*. 2006;55:592-597

434. Lowe HC, James B, Khachigian LM. A novel model of in-stent restenosis: Rat aortic stenting. *Heart*. 2005;91:393-395

435. Crapo PM, Gilbert TW, Badylak SF. An overview of tissue and whole organ decellularization processes. *Biomaterials*. 2011;32:3233-3243

436. Dahl SL, Koh J, Prabhakar V, Niklason LE. Decellularized native and engineered arterial scaffolds for transplantation. *Cell transplantation*. 2003;12:659-666

437. Lee D, Yuki I, Murayama Y, Chiang A, Nishimura I, Vinters HV, et al. Thrombus organization and healing in the swine experimental aneurysm model. Part i. A histological and molecular analysis. *J Neurosurg*. 2007;107:94-108

438. dos Santos ML, Spotti AR, dos Santos RM, Borges MA, Ferrari AF, Colli BO, et al. Giant intracranial aneurysms: Morphology and clinical presentation. *Neurosurg Rev*. 2013;36:117-122; discussion 122

439. Kuijper PH, Gallardo Torres HI, Lammers JW, Sixma JJ, Koenderman L, Zwaginga JJ. Platelet and fibrin deposition at the damaged vessel wall: Cooperative substrates for neutrophil adhesion under flow conditions. *Blood*. 1997;89:166-175

440. Houard X, Touat Z, Ollivier V, Louedec L, Philippe M, Sebbag U, et al. Mediators of neutrophil recruitment in human abdominal aortic aneurysms. *Cardiovascular research*. 2009;82:532-541

441. Koole D, Zandvoort HJ, Schoneveld A, Vink A, Vos JA, van den Hoogen LL, et al. Intraluminal abdominal aortic aneurysm thrombus is associated with disruption of wall integrity. *J Vasc Surg*. 2013;57:77-83

442. Mack CP. Signaling mechanisms that regulate smooth muscle cell differentiation. *Arteriosclerosis, thrombosis, and vascular biology*. 2011;31:1495-1505

443. Churchman AT, Anwar AA, Li FY, Sato H, Ishii T, Mann GE, et al. Transforming growth factor-beta1 elicits nrf2-mediated antioxidant responses in aortic smooth muscle cells. *Journal of cellular and molecular medicine*. 2009;13:2282-2292

444. Folkesson M, Silveira A, Eriksson P, Swedenborg J. Protease activity in the multi-layered intra-luminal thrombus of abdominal aortic aneurysms. *Atherosclerosis*. 2011;218:294-299

445. Juvela S, Porras M, Poussa K. Natural history of unruptured intracranial aneurysms: Probability of and risk factors for aneurysm rupture. *J Neurosurg*. 2008;108:1052-1060

446. Nahed BV, DiLuna ML, Morgan T, Ocal E, Hawkins AA, Ozduman K, et al. Hypertension, age, and location predict rupture of small intracranial aneurysms. *Neurosurgery*. 2005;57:676-683; discussion 676-683

447. Weir B, Disney L, Karrison T. Sizes of ruptured and unruptured aneurysms in relation to their sites and the ages of patients. *J Neurosurg*. 2002;96:64-70

448. Hasan D, Chalouhi N, Jabbour P, Dumont AS, Kung DK, Magnotta VA, et al. Early change in ferumoxytol-enhanced magnetic resonance imaging signal suggests unstable human cerebral aneurysm: A pilot study. *Stroke*. 2012;43:3258-3265

449. Krings T, Piske RL, Lasjaunias PL. Intracranial arterial aneurysm vasculopathies: Targeting the outer vessel wall. *Neuroradiology*. 2005;47:931-937

450. Krings T, Mandell DM, Kiehl TR, Geibprasert S, Tymianski M, Alvarez H, et al. Intracranial aneurysms: From vessel wall pathology to therapeutic approach. *Nature reviews. Neurology*. 2011;7:547-559

451. Valavanis A. Classification and treatment of intracranial aneurysms “lumen-oriented and incomplete. *NeuroNews*. 2012;10 Jul 2012

452. Hayakawa M, Katada K, Anno H, Imizu S, Hayashi J, Irie K, et al. Ct angiography with electrocardiographically gated reconstruction for visualizing pulsation of intracranial aneurysms: Identification of aneurysmal protuberance presumably associated with wall thinning. *AJNR Am J Neuroradiol*. 2005;26:1366-1369

453. Sherif C, Kleinpeter G, Mach G, Loyoddin M, Haider T, Plasenzotti R, et al. Evaluation of cerebral aneurysm wall thickness in experimental aneurysms: Comparison of 3t-mr imaging with direct microscopic measurements. *Acta Neurochir (Wien)*. 2014;156:27-34

454. Steinman DA, Antiga L, Wasserman BA. Overestimation of cerebral aneurysm wall thickness by black blood mri? *Journal of magnetic resonance imaging : JMRI*. 2010;31:766

455. Zacharatos H, Hassan AE, Qureshi AI. Intravascular ultrasound: Principles and cerebrovascular applications. *AJNR Am J Neuroradiol*. 2010;31:586-597

456. Majidi S, Grigoryan M, Tekle WG, Watanabe M, Qureshi AI. Feasibility of using intravascular ultrasonography for assessment of giant cavernous aneurysm after endovascular treatment: A technical report. *Journal of vascular and interventional neurology*. 2012;5:6-9

457. DeLeo MJ, 3rd, Gounis MJ, Hong B, Ford JC, Wakhloo AK, Bogdanov AA, Jr. Carotid artery brain aneurysm model: In vivo molecular enzyme-specific mr imaging of active inflammation in a pilot study. *Radiology*. 2009;252:696-703

458. Hasan DM, Mahaney KB, Magnotta VA, Kung DK, Lawton MT, Hashimoto T, et al. Macrophage imaging within human cerebral aneurysms wall using ferumoxytol-enhanced mri: A pilot study. *Arteriosclerosis, thrombosis, and vascular biology*. 2012;32:1032-1038

459. Hasan DM, Chalouhi N, Jabbour P, Dumont AS, Kung DK, Magnotta VA, et al. Evidence that acetylsalicylic acid attenuates inflammation in the walls

of human cerebral aneurysms: Preliminary results. *Journal of the American Heart Association*. 2013;2:e000019

460. Trivedi RA, JM UK-I, Graves MJ, Cross JJ, Horsley J, Goddard MJ, et al. In vivo detection of macrophages in human carotid atheroma: Temporal dependence of ultrasmall superparamagnetic particles of iron oxide-enhanced mri. *Stroke*. 2004;35:1631-1635

Appendix

1. Bifurcation rabbit complex microsurgical aneurysm model.
2. Long-term patency of complex microsurgical aneurysms.
3. The Helsinki rat microsurgical sidewall aneurysm model.
4. Loss of mural cells causes aneurysm growth and rupture.
5. Smooth muscle cells and thrombus in aneurysms.